

# Evaluating storage technologies for wind and solar energy

by

Joshua Michael Mueller

B.S., United States Naval Academy (2004)

B.A., University of Oxford (2006)

S.M., Massachusetts Institute of Technology (2015)

Submitted to the Institute for Data, Systems, and Society  
in partial fulfillment of the requirements for the degree of

Doctor of Philosophy in Engineering Systems

at the

MASSACHUSETTS INSTITUTE OF TECHNOLOGY

June 2018

© 2018 Massachusetts Institute of Technology. All rights reserved.

**Signature redacted**

Author.....

Institute for Data, Systems, and Society  
June 1, 2018

**Signature redacted**

Certified by.....

Jessika E. Trancik  
Associate Professor of Data, Systems, and Society  
Thesis Supervisor and ~~Doctoral~~ Committee Chair

**Signature redacted**

Certified by.....

John E. Parsons  
Senior Lecturer, Sloan School of Management  
Doctoral/Committee Member

**Signature redacted**

Certified by.....

Yet-Ming Chiang  
Kyocera Professor of Materials Science and Engineering  
Doctoral Committee Member

**Signature redacted**

Accepted by.....

Stephen C. Graves

Professor of Mechanical Engineering and Engineering Systems  
Abraham J. Siegel Professor of Management Science  
IDSS Graduate Officer





# Evaluating storage technologies for wind and solar energy

by

Joshua Michael Mueller

Submitted to the Institute for Data, Systems, and Society  
on June 1, 2018, in partial fulfillment of the  
requirements for the degree of  
Doctor of Philosophy in Engineering Systems

## Abstract

Rapidly falling wind and solar energy costs over the past four decades have led to exponential growth in installation of these technologies. However, these intermittent renewables do not reliably produce power on demand. One possible mitigation strategy is the addition of energy storage technologies, which are able to shift generation to later periods of higher demand or price. In competitive markets, storage adoption to facilitate renewables penetration will depend on how much value storage can bring to a wind or solar power plant. Which of the diverse energy storage technologies are best suited to profitably perform this function? How do price and resource variability determine the preferred technologies?

This thesis develops two novel methods of comparing storage technologies in hybrid wind-storage or solar-storage power plants. In the first, we evaluate technologies based on the increased value of a marginal hybrid plant under today's conditions. We further explain these results by finding the determinants of storage value under uncertainty. In the second, we find the least-cost hybrid plants able to meet pre-defined demand profiles. Through simulation, optimization, and statistical analysis, we address the following questions: 1) How can one compare candidate storage technologies? 2) What price and resource features determine storage value? 3) What are the cost targets for storage under different market conditions?

To address question 1, we optimize storage operation and size for grid-scale energy arbitrage, and study the value of hybrid plants using different storage technologies. The value of the hybrid plant is found by comparing benefits to costs, and is estimated across locations and technologies. We show that at today's wind and solar generation costs, some storage technologies can provide value, but further cost improvement is needed, especially for electrochemical technologies, to facilitate widespread adoption.

Finally, we determine both cost targets and the optimal direction of cost improvement for diverse storage technologies and locations.

In order to answer question 2, we identify features of the electricity market and the renewables resource availability that determine value. Through simulations of an artificial price time series in which features of electricity price spikes are varied, we find that storage value is driven by the frequency and amplitude of price spikes and the availability of the energy resource. The durations of price spikes determine the relative value of one storage technology to another, because of differing technology cost structures. We demonstrate these results in historical data and explain the differences in storage value across locations. We also explore how uncertainty in future prices impacts storage value. We determine a new heuristic for storage operation and sizing absent perfect foresight. This approach is able to capture at least 80% of the expected value under perfect foresight and improves upon existing heuristics.

In answering question 3, we determine the least-cost combination of wind and solar with storage that provides reliable, dispatchable, pre-determined outputs. This approach allows for the evaluation of storage technologies for a possible future with higher renewables penetration. Preferred technologies for this use context have very low energy capacity costs ( $< \$50/\text{kWh}$ ), enabling inexpensive installation of long duration storage. Long periods of low wind or solar availability determine storage requirements and can be mitigated by including both wind and solar in the generation portfolio. New cost targets are derived for storage development that would help enable higher levels of renewables adoption.

**Jessika E. Trancik**

Associate Professor of Data, Systems, and Society  
Thesis Supervisor and Doctoral Committee Chair

**John E. Parsons**

Senior Lecturer, Sloan School of Management  
Doctoral Committee Member

**Yet-Ming Chiang**

Kyocera Professor of Materials Science and Engineering  
Doctoral Committee Member

## Thesis Errata Sheet

Author Joshua Mueller  
Primary Dept. Institute for Data Systems and Society  
Degree Ph.D. Graduation date Jun 2018

### Thesis title

Evaluating storage technologies for wind and solar energy

### Brief description of errata sheet

Methods and results of Chapter 5 have been corrected in the citation provided in  
Errata - p.2. An updated chapter footnote is provided for the reference.

Number of pages 2 (11 maximum, including this page)

► **Author:** I request that the attached errata sheet be added to my thesis. I have attached two copies prepared as prescribed by the current *Specifications for Thesis Preparation*.

Signature of author Signature redacted Date 5/11/2021

► **Thesis Supervisor or Dept. Chair:** I approve the attached errata sheet and recommend its addition to the student's thesis.

Signature Signature redacted Date 5/11/2021  
Name Jessika E. Trancik  Thesis supervisor  Dept. Chair

► **Vice Chancellor or his/her designee:**

I approve the attached errata sheet and direct the Institute Archives to insert it into all copies of the student's thesis held by the MIT Libraries, both print and electronic.

Signature Signature redacted Date 12/3/21  
Name IAN A. WAITZ

This chapter's methods and results have been corrected in the following publication:

Ziegler, MS, Mueller, JM, Pereira, GD, Song, J, Ferrara, M, Chiang, YM and Trancik, JE, Storage requirements and costs of shaping renewable energy toward grid decarbonization, *Joule*, 2019, Vol. 3, pp.2134-2153.

Please refer to the above publication instead of this thesis chapter.

Additionally, the footnote on page 101, "A version of this chapter is in preparation for publication with co-authors Gonçalo D. Pereira, Marco Ferrara, Yet-Ming Chiang, and Jessika E. Trancik69: Joshua M. Mueller, Gonçalo D. Pereira, Marco Ferrara, Yet-Ming Chiang, and Jessika E. Trancik. Energy storage requirements for shaping renewable energy toward grid decarbonization. In preparation.", should be replaced with the text below:

"Please refer to the following publication in place of this thesis chapter for corrected methods and results: Ziegler, MS, Mueller, JM, Pereira, GD, Song, J, Ferrara, M, Chiang, YM and Trancik, JE, Storage requirements and costs of shaping renewable energy toward grid decarbonization, *Joule*, 2019, Vol. 3, pp.2134-2153."

## Acknowledgments

This thesis is the product of many people's effort, guidance, suggestions, and help over the past five years. I would like to extend my heartfelt thanks and appreciation for all their support and time. First, thank you Jessika Trancik for your guidance as my P.I., for your high standards as my Committee Chair, and for your mentorship as my advisor. Thanks also to my committee members John Parsons and Yet-Ming Chiang for your challenging questions and your insight.

Thanks to the members of the Trancik lab for your friendship, editing help, and research discussions: Wei Wei, Sankaran, Micah, Phillip, Morgan, James, Mandira, and Goksin. Thanks too to Gonçalo, my co-author and collaborator on storage modeling. Special thanks to Zach Needell who arrived when I did and has listened to me for five years. Finally, thanks to Marco and Magdalena whose friendship and conversation will be especially missed.

Thanks to Beth, Barb, Kim, Jeannille, Jennifer, Erica, Arlyn, Ed, and Laura. Without you there would be no IDSS, no TPP, no ESD. Thanks as well to my TPP and ESS cohort, especially Chris Saulnier, Josh Wolff, and Sarah Fletcher.

My graduate studies were supported by the John and Fannie Hertz Foundation and the Post-9/11 GI Bill; thank you for your financial support. I would like to extend special thanks to the Hertz Staff: Jay Davis and Robbee Kosak for their leadership, as well as to Kathy Young and Mandy O'Connor. Thanks too to the Hertz Community for your friendship, creativity, and passion: Dan, Max, Vyas, Kelly, Jim, Grant, Thomas, Mollie, Katie, Jesse, D.J., Ashvin, and Megan.

I acknowledge Lockheed Martin and the MIT Portugal Program as funding sources for this research. Thank you for your generous contribution to this work.

Lastly, thanks to my beautiful wife and perfect baby girl. You are my rock.



# Contents

<b>1</b>	<b>Introduction</b>	<b>13</b>
1.1	Research motivation . . . . .	13
1.2	Background . . . . .	14
1.3	Research contributions . . . . .	17
1.4	Thesis overview . . . . .	18
<b>2</b>	<b>Value of storage technologies for wind and solar energy</b>	<b>23</b>
2.1	Introduction . . . . .	24
2.2	Methods . . . . .	26
2.3	Results . . . . .	32
2.4	Conclusions . . . . .	45
<b>3</b>	<b>Determinants of the value of storage for wind and solar energy</b>	<b>49</b>
3.1	Introduction . . . . .	50
3.2	Methods . . . . .	51
3.3	Results . . . . .	56
3.4	Conclusions . . . . .	73
<b>4</b>	<b>Impact of forecasting uncertainty on the value of storage for renew-</b>	

<b>able energy arbitrage</b>	<b>75</b>
4.1 Introduction . . . . .	76
4.2 Methods . . . . .	77
4.3 Results . . . . .	90
4.4 Conclusions . . . . .	98
<b>5 Energy storage requirements for shaping renewable energy toward grid decarbonization</b>	<b>101</b>
5.1 Introduction . . . . .	102
5.2 Methods . . . . .	104
5.3 Results . . . . .	111
5.4 Conclusions . . . . .	122

# List of Figures

2-1	Schematic of model to determine $\chi_{\max}$ . . . . .	29
2-2	Storage shifts generation to periods of highest price . . . . .	33
2-3	Demonstration of $\chi$ vs. $\chi_{\max}$ in each season . . . . .	35
2-4	Selecting $\chi_{\max}$ for different cost intensities . . . . .	36
2-5	$\chi_{\max}$ for wind plus storage power plants . . . . .	37
2-6	$\chi_{\max}$ for solar plus storage power plants . . . . .	38
2-7	Storage technology cost comparison for wind in Texas . . . . .	41
2-8	Storage technology cost comparison for solar in Texas . . . . .	42
2-9	Robustness of storage value for wind energy to cost considerations . .	43
2-10	Robustness of storage value for solar energy to cost considerations . .	44
3-1	Resource availability and artificial price time series . . . . .	52
3-2	Storage threshold comparison across locations . . . . .	57
3-3	Impact of capacity factor on plant value . . . . .	60
3-4	Simulation of storage value with increased renewables penetration . .	62
3-5	Impact of varying price spike frequency and amplitude . . . . .	66
3-6	Elasticity of threshold costs to price spike frequency and amplitude .	67
3-7	Impact of price spike duration on preferred technology selection . . .	69

3-8	Electricity price dynamics . . . . .	71
4-1	Electricity price dynamics in CA, MA, PA, and TX . . . . .	79
4-2	Decision rule schematic . . . . .	84
4-3	Demonstration of process to determine $\rho_{\text{rule}}$ . . . . .	85
4-4	Impact of storage size on storage operation and average discharge price	87
4-5	Daily electricity price profiles and summary statistics . . . . .	91
4-6	Comparison of decision rules for a range of storage capacities . . . . .	93
4-7	Impact of forecasting error on plant value . . . . .	94
4-8	Impact of forecasting error on plant value - backcast . . . . .	95
4-9	Impact of forecasting error on plant value - hours of highest price . .	97
5-1	Predetermined output shapes modeled on traditional grid roles . . . . .	107
5-2	Model schematic for reliable, pre-determined output shapes . . . . .	110
5-3	Optimizing wind and solar resource mix . . . . .	113
5-4	Minimum levelized cost of shaped electricity . . . . .	114
5-5	Optimizing storage and renewables size for shaped outputs . . . . .	115
5-6	Demonstration of storage state of charge in low-resource years . . . . .	116
5-7	Reduced equivalent availability factor (EAF) analysis . . . . .	117
5-8	Wind levelized cost of shaped electricity . . . . .	118
5-9	Solar levelized cost of shaped electricity . . . . .	119

# List of Tables

- 2.1 Simulation parameter space . . . . . 30
  
- 3.1 Artificial price simulation parameter space . . . . . 53
- 3.2 Determinants of wind and solar value . . . . . 58
- 3.3 Determinants of wind and solar value under simulated renewables scaling 63
- 3.4 Correlation between resource availability and artificial price time series 64
- 3.5 Frequency of electricity price spikes per location . . . . . 72
  
- 4.1 Percent improvement for our new decision rule over previous heuristics 96
  
- 5.1 Wind and solar capacity factors . . . . . 106
- 5.2 Locations studied . . . . . 108
- 5.3 Reliable shapes input parameters . . . . . 109



# Chapter 1

## Introduction

### 1.1 Research motivation

Achieving climate change mitigation targets likely requires that the energy sector shift to low-carbon generation technologies. Two promising candidate technologies are wind and solar power, which have seen cost reductions of approximately 30% per year for the past four decades, leading to increased adoption<sup>60</sup>. Wind and solar are variable renewable resources, and their intermittency means that they do not reliably produce power at times of greatest price or highest demand<sup>30</sup>. However, with the addition of energy storage, wind and solar power plants can be made dispatchable<sup>101</sup>. Diverse storage technologies have been developed or proposed for the purpose of shifting generation to meet demand, and adoption of one or more technologies will depend on storage features. Storage performance is evaluated along a number of metrics including cost, round-trip efficiency (summed losses during both charge and discharge energy transformation), self-discharge (e.g., evaporation of a pumped hydro reservoir), environmental impact, and geographic deployability<sup>14</sup>.

A major impediment to the adoption of storage for renewables is the high upfront capital costs of storage<sup>68</sup>. For storage to facilitate renewables adoption in competitive markets, the addition of storage to a wind or solar power plant must be economically viable<sup>96</sup>. To be viable, the increased benefit of providing dispatchable wind or solar power should exceed the increased cost from storage. Determining what costs storage needs to achieve for adoption in dynamic electricity markets requires the development of new techniques for evaluating storage. Cost targets provide guidance for storage development, and we aim to determine cost targets for real and future hypothetical storage technologies across locations, resources, and timescales. What costs must storage achieve to add value to wind and solar? What determines these cost targets? Which technologies are promising candidates to meet these targets? Addressing these questions is the focus of this research.

## 1.2 Background

This thesis bridges the gap between two distinct bodies of research, which we define here as the storage technology literature and the storage operation literature. These bodies of research are classified by their different approaches to storage evaluation and encompass previous attempts to compare storage technologies. For example, research we classify as belonging to the storage technology literature evaluates technologies along one or more performance metrics. However, these studies tend to analyze technologies absent a formal, quantitative model of storage use context, and therefore have a limited ability to quantitatively compare technologies across locations, resource penetrations, and timescales. On the other hand, research we classify as belonging to the storage operation literature provides detailed operational models of storage for a use context. These operational models, however, are not designed

to analyze the impact of technology features on the model outcomes. Thus, a gap exists between these literatures. This gap limits our ability to understand how storage technology features determine storage performance in specific use contexts. This section presents an overview of the existing storage technology and operation literatures, highlighting the opportunity to inform storage development by bridging the gap between both bodies of research, e.g., understanding how storage technology features impact storage performance in a specific use context in order to provide guidance for storage improvement.

In the storage technology literature we identify two subsets of research, each of which employ storage performance criteria often absent a detailed evaluation of the storage use context. The subsets are grouped as either papers comparing existing technologies or studies focused on specific storage technology development. We provide an overview of the research in each subset below.

Research on specific storage technology development focuses on the performance metrics of a technology to suggest design improvements<sup>4</sup>. This body of work includes methods for designing and evaluating the heat transmission of a sodium sulfur battery<sup>58,77</sup>, analysis of different lithium ion chemistries to promote better ion transference<sup>20,93</sup>, or development of lower cost flow battery chemistries<sup>24,63</sup>. Examples of storage technology development research for mechanical systems include work on improved compressors, expanders, and turbines<sup>88</sup>, as well as studies of locations and techniques for locating underground storage caverns for compressed air energy storage<sup>66,78</sup>. By analyzing storage technologies absent their use context, these studies may not focus on the most pressing metrics for improvement nor do they have clear and informed targets for the storage technology features they aim to improve.

In the storage technology literature we also include research comparing diverse storage technologies across one or more performance metrics<sup>5,14,31,39,52,76,92</sup>. These

studies, including review papers, often score storage technology features according to multiple metrics without consideration of the possible tradeoffs between different dimensions of storage performance<sup>2,17,35,61,104</sup>. Two example performance metrics of importance for storage adoption are the high upfront capital costs for storage power and energy capacity. These high fixed costs are an impediment to widespread deployment and therefore are of interest when comparing technologies<sup>87</sup>. Those studies that try to reduce storage costs to a single leveled cost of storage arbitrarily constrain storage power and energy capacities without optimizing storage size<sup>76</sup>. Analyzing storage technologies for a given use context, such as energy arbitrage, constrains the tradeoffs between competing dimensions of storage performance. This enables determination of performance requirement targets for specific storage technology features. Without consideration of the storage use context, technology comparisons occur in a vacuum.

The other body of research, the storage operation literature, focuses on the storage use context, but often does so absent any consideration of actual technologies or their features. This literature is situated in the broader literature on commodity storage where technology considerations are not as relevant as they are in energy storage<sup>11,44,94</sup>. Research in this domain analyzes generic storage, or occasionally a single existing technology, operating within a use context. Examples of storage use contexts are energy arbitrage and renewables shaping, in addition to reserves, frequency regulation, and load following<sup>1,83</sup>. Energy arbitrage is the storing of electricity during periods of low price for later resale during periods of higher price, a function specifically important for non-dispatchable generation like wind and solar. We distinguish energy arbitrage from pure price arbitrage, the latter allowing for direct charging from the grid and therefore representing traditional commodity arbitrage. Renewables shaping is the transformation of intermittent, noisy, input generation into

reliable, predetermined, output shapes, for example providing baseload power<sup>26,40,45</sup>. These two use contexts represent primary value streams for bulk, grid-scale storage, though additional functions, such as power quality management, will likely also play a role in facilitating renewables integration<sup>49,91</sup>.

Examples of research comprising the storage operation literature span a range of storage use contexts. However, previous work is limited in that it too often uses a technology agnostic approach for storage absent consideration of important storage technology features. Much of this literature analyzes storage when used with renewables, with little agreement on the question of whether storage is profitable<sup>21,22,38,56,57</sup>. Storage operation includes modeling of the charge and discharge schedules of storage to determine whether it will be profitable for a specific technology such as pumped hydro<sup>22</sup>, whether it will reduce energy sector emissions<sup>26</sup>, or whether it will increase the revenue of wind farms<sup>97</sup>. For example, storage can be used in conjunction with natural gas to help smooth small fluctuations in wind power in order to regulate frequency<sup>49</sup>. Finally, we include detailed engineering cost analyses of existing and proposed storage facilities<sup>1,86</sup> in the storage operation literature.

### 1.3 Research contributions

This thesis asks how we can evaluate diverse storage technologies in order to inform their development, and through what mechanisms drivers of storage value explain these results. The modeling techniques and conceptual advancements made to address this challenge provide both applied and fundamental contributions to the fields of storage operation, technology evaluation, technology development, and electricity market analysis. We develop a mechanistic understanding of how features of the electricity prices and the resource availability determine storage value and affect the

comparison of different storage technologies.

The principal result of this thesis is the development and detailed exploration of a novel method for evaluating storage technologies. Additionally, we identify location-specific cost targets storage must achieve to provide value. By examining real storage technologies in a specific use context, we develop a quantitative method to evaluate storage that can be used to set storage cost targets and directions of improvement, thus guiding the development of future technologies. Cost targets are location and resource dependent, and can therefore inform state and regional subsidies and support for renewables deployment, helping tailor solutions to local conditions. We develop a new decision rule for storage operation, enabling determination of the cost of forecasting errors. Finally, cost targets for renewables with storage in a future high-renewables grid are also determined, thus enabling longer term development and guidance of storage technology research.

The results of this thesis also advance our understanding of storage value, operation, and electricity markets. Development of new statistical models focusing on the frequency, amplitude, and distribution of the duration of price spike events explain storage cost targets across locations and the direction of best improvement for storage technologies independent of location. We develop a new method of storage operation absent perfect foresight of future prices and resource availability. Finally, we develop new methods for exploring storage value in markets with high renewables penetration.

## 1.4 Thesis overview

This thesis is structured as four stand-alone chapters all aiming to address facets of the question “what is the value of storage for wind and solar energy.” The first three

chapters focus on the value of storage for renewables energy arbitrage under market conditions similar to those today, and they explore a new metric of storage value,  $\chi$ , or the annualized system revenue to cost ratio. The final chapter analyzes least-cost renewables and storage options in order to provide reliable and predictable output of a type that might be beneficial in a high renewables environment. Each chapter is a reproduction of a published paper<sup>12</sup> or a paper in preparation<sup>69,70,71</sup>.

**Chapter 2.** The second chapter asks how can one evaluate diverse storage technologies. To answer this question it is necessary to both choose a storage use context, in this case energy arbitrage for wind and solar energy, and a metric for comparison. Here we develop a new metric,  $\chi$ , the annual revenue over the annualized cost of a hybrid renewables with storage plant performing energy arbitrage. We present a model of storage operation that first maximizes the revenue of a wind or solar with storage power plant subject to storage power and energy capacity constraints and second selects the storage size which maximizes the  $\chi$  value. We find that storage adds value by shifting generation to periods of higher prices. Optimal storage value, power capacity, and energy capacity are presented as a function of the technology's separable power and energy capacity cost intensities. Storage provides different value depending on the location's solar and wind resource availability and electricity prices. However, the relative value of one technology to another (which technology is preferred) is the same across all locations and resources. At today's solar and wind costs, some storage technologies, at the lower end of cost estimates, can provide value through energy arbitrage, but improvement is needed, especially for electrochemical technology costs, in order to facilitate widespread adoption.

**Chapter 3.** The third chapter further explores features of electricity markets and resource availability to find determinants of storage value. In this chapter, we address “how and why” storage value differs across resource and location and yet the same technology cost structure is preferred. We use a set of artificial price time series with independent control of the frequency, amplitude, and duration of price spikes to show that increased frequency and amplitude of price spikes makes storage more valuable. We find that storage is more valuable when periods of high prices and resource availability do not coincide. Using both simulation and analytical methods we show that the tradeoff between power and energy capacity cost is equal to the optimal storage duration for a pair of cost intensities. We also show that the distribution of the duration of price spike events determines this tradeoff and these distributions are similar across locations in the U.S. The chapter concludes by showing how the features in historical electricity prices match the expectations developed based on the artificial price series simulation findings.

**Chapter 4.** The fourth chapter relaxes the assumption of perfect foresight in order to determine how uncertainty in resources and prices affect storage value. Through the process of determining a cost of forecasting errors, based on a simple price-based decision rule, we develop new insights into the operation and installation of storage of various sizes. The new decision rule developed here captures at least 80% of the expected value under perfect foresight and is compared with existing techniques in the literature for determining storage value absent perfect foresight. Our method improves upon the current estimates of the cost of forecasting errors for nearly every system size for wind and solar in all locations.

**Chapter 5.** The final chapter shifts focus to a high-renewables penetration environment to begin analyzing how storage technologies can help wind and solar meet demand at lowest cost. In this analysis, solar and wind generation capacity along with storage power and energy capacity are jointly optimized to find the least cost combination that can produce certain output shapes for a twenty year period. Four output shapes are examined which are modeled on the traditional grid roles of baseload, intermediate load, and two types of peaker power plants. Cost targets are found for renewables with storage to be competitive with conventional generation, such as coal, nuclear, and natural gas, for providing dispatchable power in four U.S. locations representing a range of wind and solar resource availability. Storage with low energy costs, below an estimated target of \$50/kWh, could be used to make renewables plants cost-competitive with other on-demand generation technology options in renewable resource abundant locations. Suitable technologies include pumped hydro, compressed air energy storage, and some flow battery chemistries, with the latter being feasibly deployable in all locations.



## Chapter 2

# Value of storage technologies for wind and solar energy

*Wind and solar industries have grown rapidly in recent years but they still supply only a small fraction of global electricity. The continued growth of these industries to levels that significantly contribute to climate change mitigation will depend on whether they can compete against alternatives that provide high-value energy on demand. Energy storage can transform intermittent renewables for this purpose but cost improvement is needed. Evaluating diverse storage technologies on a common scale has proved a major challenge, however, owing to their widely varying performance along the two dimensions of energy and power costs. Here we devise a method to compare storage technologies, and set cost improvement targets. Some storage technologies today are*

---

A version of this chapter is published in *Nature Climate Change* with co-authors William A. Braff and Jessika E. Trancik<sup>12</sup>: William A. Braff, Joshua M. Mueller, and Jessika E. Trancik. Value of storage technologies for wind and solar energy. *Nature Climate Change*, 6:964-969, 2016.

*shown to add value to solar and wind energy, but cost reduction is needed to reach widespread profitability. The optimal cost improvement trajectories, balancing energy and power costs to maximize value, are found to be relatively location invariant, and thus can inform broad industry and government technology development strategies.*

## 2.1 Introduction

Wind and solar energy technologies have attractive attributes including their zero direct carbon emissions (during operation)<sup>7,115</sup>, low water withdrawal and consumption requirements<sup>82</sup>, the speed with which they can be installed<sup>55</sup>, and the flexibility in the scale of their installations<sup>103,105</sup>. Innovation in these technologies has taken off in the past two decades<sup>9</sup>. Levelized electricity costs for both technologies have been dropping over the past few decades, with photovoltaics costs falling exceptionally quickly, by two orders of magnitude over the past 40 years<sup>73,106</sup>. The installed base of solar and wind has grown dramatically in recent decades, each at approximately 30% per year on average over the past 30 years, but together still supplies only 3% of global electricity<sup>106</sup>. Although the global solar and wind energy resources are large, these technologies do not measurably contribute to climate change mitigation at current installations levels.

A variety of government policy-based incentives have supported the growth in solar and wind energy technologies in recent decades<sup>42,108</sup>, but continued, rapid growth to levels that can help meet climate change mitigation goals will depend on whether the adoption of wind and solar can be made self-sustaining. Low-cost storage can play a pivotal role by converting intermittent wind and solar energy resources, which fluctuate over time with changes in weather, the diurnal cycle, and seasons<sup>19</sup>, to electricity on demand that can be sold when most profitable, thereby increasing the

value and attractiveness of these technologies to investors<sup>37,109</sup>. However, storage costs need to improve to achieve sizable adoption<sup>50,96</sup>. Quantifying the cost reduction needed has proven challenging and is the topic of this paper.

A range of stationary, large-scale energy storage technologies are currently in development<sup>35</sup>. These technologies have widely varying power and energy costs, with some storage technologies having more expensive power-related component costs (e.g. pumped hydro power generation equipment) and cheaper energy-related costs (e.g. pumped hydro natural reservoirs), and vice versa<sup>104</sup>. This paper aims to understand the value of storage for wind and solar energy at today's costs, and how technology costs need to improve, trading off energy and power costs, to reach profitability. This question can only be answered by examining the context in which storage technologies will be used, in particular the temporal variations in the energy price and intermittent energy resource. Here we investigate the potential for energy storage to increase the value of solar and wind energy in several U.S. locations—in Massachusetts, Pennsylvania, Texas, and California—with varying electricity price dynamics and solar and wind capacity factors.

As pointed out in earlier papers, comparing the costs of different storage technologies on a common scale is challenging because no single technology clearly dominates the others along the two dimensions of energy and power costs (e.g.<sup>35,104</sup>). Studies have quantified the benefits of particular storage technologies for given locations and contexts of use, including for frequency regulation, energy arbitrage, converting intermittent renewables into baseload power, and increasing the profits of intermittent renewable energy (e.g.<sup>15,45,56,65,80,96,103,113</sup>), but past research has not shown how the benefit depends on the costs of different storage technologies. In this paper we address this gap and present a comparison of a spectrum of storage technologies (current and future hypothetical), showing quantitatively and across locations how

the benefits of storage depend on storage technology costs. This approach allows for the quantification of technology cost performance targets for each given level of benefit. Specifically we focus on how the energy and power costs of storage affect the value added to wind and solar energy. This *ex ante* evaluation of storage options, based on salient features of the technologies and contexts in which they will be used, can inform and accelerate their development through directed innovation<sup>109,116</sup>.

The article is organized as follows. We first present the results of optimizing the discharge behavior of a solar or wind plant combined with storage, for a fixed storage size, to maximize the revenue of the plant. We then optimize the storage size in order to maximize the value of the plant, where value is defined as the ratio of the plant revenue to the plant cost. The analysis is performed for a wide spectrum of storage energy and power costs. Finally, we assess the value of current storage technologies, based on their energy and power costs, and discuss optimal cost improvement trajectories across locations.

## 2.2 Methods

The analysis involved three steps: (1) Hourly electricity pricing data and wind and solar energy resource availability data was compiled for each of the four U.S. locations studied. Results are presented for the year 2004, a conservative year in which the value of storage is lower than it is in the other years studied. All dollar values in the paper are presented in 2004 currency. (2) The charging and discharging behavior of a set of hypothetical hybrid renewable energy and storage plants with a range of fixed storage sizes was optimized in order to maximize revenue. (3) An optimal storage system size for each location and energy resource was determined in order to maximize the value (annual revenue divided by annualized cost) of the wind and

solar energy with storage plant, for a range of energy- and power-related costs of storage.

**Site selection.** Four geographic sites were examined as locations for hypothetical wind and solar with storage plants: McCamey, Texas, Palm Springs, CA, Altoona, PA, and Plymouth, MA. The Texas site was chosen as an example of a high performing wind site, with an average capacity factor of 32% over the period examined (where capacity factor is defined as the annual output of a hypothetical plant divided by the output if operated continuously at the rated power capacity). The California site was selected as a high performing solar site, with an average capacity factor of 23%. The Pennsylvania and Massachusetts sites were chosen as cases where neither wind nor solar was particularly high performing, with capacity factors of 25% and 15%, respectively for both locations. Data for zonal real-time (hourly) pricing was obtained for the year 2004 from the ISO New England<sup>54</sup>, ERCOT<sup>33</sup>, PJM<sup>84</sup>, and CAISO<sup>13</sup>. To simulate the performance of a hypothetical wind turbine or solar array, local windspeed and solar insolation data was obtained from the Eastern and Western National Wind Integration Datasets and the National Solar Radiation Database<sup>72</sup>, and then transformed to time dependent output per MW installed using published performance data for a Vestas V90 3 MW wind turbine which aligns to face the wind<sup>112</sup> and a static photovoltaic system that reaches its maximum output when exposed to an insolation of 1 kW/ m<sup>2</sup> (corresponding to standard test conditions (STC)).

**Optimization of charging and discharging to maximize revenue.** Per hour charging and discharging of the storage system, and the direct sale of solar and wind generated electricity were optimized to achieve maximum revenue for a hypothetical

hybrid storage and generation plant at each site, given the electricity price and energy resource availability over time and subject to system power and energy constraints. The optimization was performed in three week intervals over the course of a year, with one week overlap between each interval to prevent discontinuities. The charge rate was capped at the real-time output of the generation resource, and the energy available for discharge was adjusted by a roundtrip efficiency of 90%. In order to reduce the computational expense of the optimization, the simulation considered charging and discharging separately so that a linear solution technique could be employed. The ability of the simulation to find the global optimum was confirmed by comparison with an analytical solution in the case of arbitrage that is not constrained by the renewable energy resource.

The optimization routine for each three week segment ( $N = 504$  hours) can be expressed in terms of the real time price  $P(t)$ , the generation profile  $x_{generation}(t)$ , storage roundtrip efficiency  $\eta$ , peak power  $\dot{E}_{max}$ , and duration  $h$  as:

$$R_{total} = \max\left(\sum_{t=0}^N P(t)(x_{generation}(t) + x_{discharge}(t) - x_{charge}(t)/\eta)\right)$$

subject to:

$$0 \leq x_{discharge}(t) \leq \dot{E}_{max}$$

$$0 \leq x_{charge}(t) \leq \min(\eta x_{generation}(t), \eta \dot{E}_{max})$$

$$0 \leq \sum_{t=0}^N (x_{charge}(t) - x_{discharge}(t)) \leq h \dot{E}_{max}. \quad (2.1)$$

An offset is included in the energy constraint for each optimization period to account for the amount of energy stored in the system at the beginning of the optimization period. The optimization protocol serves to temporally shift the output of

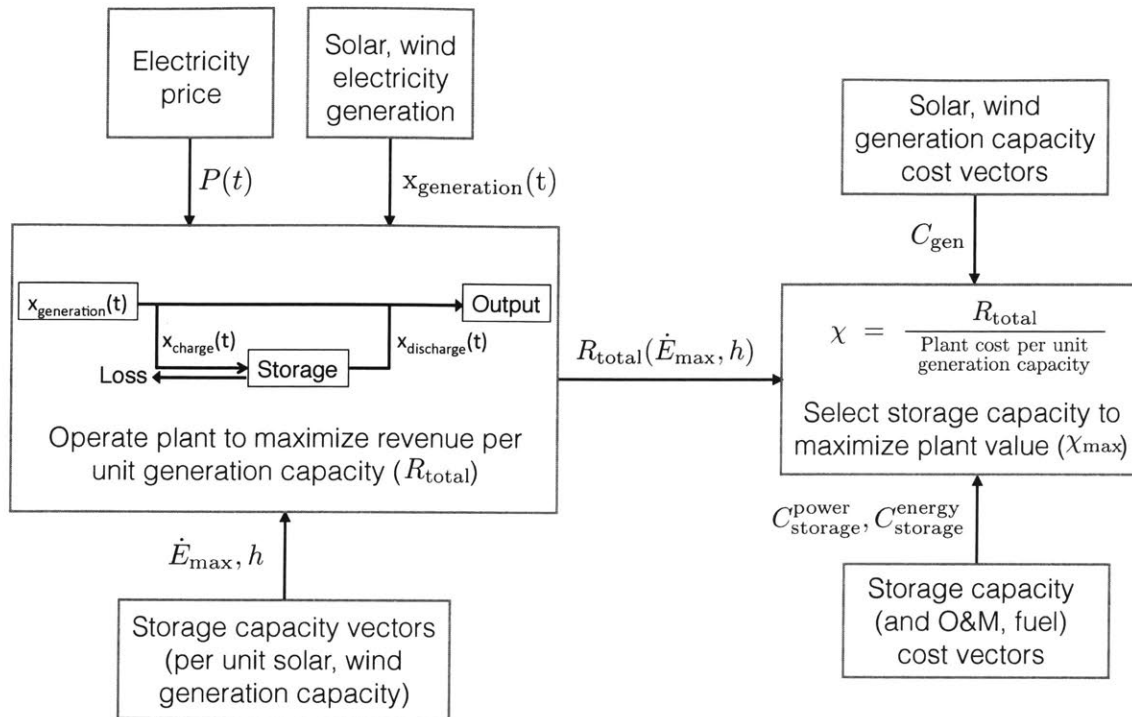


Figure 2-1: Diagram showing two major steps in the analysis: optimizing the operation of a wind or solar plant combined with storage for a range of storage sizes, and selecting the storage size per unit solar or wind generation capacity that maximizes the ratio of plant revenue to plant cost. A range of storage technology costs are investigated, including real and hypothetical storage technologies with costs spanning the range shown in Table 2.1.

the system to periods of high market pricing (often coinciding with times of peak demand), subject to the constraint that any energy to pass through the storage system pays an efficiency penalty.

We studied the case where hybrid renewables and storage systems are price takers in the spot market, which is an adequate approximation for small penetration levels. It is also assumed that the system operator has perfect information about future

Table 2.1: Experimental parameter space investigated

Parameter	Variable	Unit	Values
Location	-	-	TX, CA, MA, PA
Generation Technology	-	-	Wind, Solar
Peak Power (Storage Size)	$\dot{E}_{\max}$	MW storage/MW generation	0 - 5
Duration (Storage Size)	$h$	MWh storage/MW storage	0 - 4
Storage Roundtrip Efficiency	$\eta$	-	90%
Energy Related Storage Cost	$C_{\text{storage}}^{\text{energy}}$	\$/kWh (construction cost)	2 - 2000
Power Related Storage Cost	$C_{\text{storage}}^{\text{power}}$	\$/kW (construction cost)	2 - 3000
Wind, Solar Generation Cost	$C_{\text{gen}}$	\$/kW (construction cost)	500, 1000, 2000, 3000

three-week prices and resource availability. This approach employs the assumption supported by earlier work that the overestimate in revenue as a result of complete future knowledge is small<sup>34,36,41,44</sup>.

**Value of optimally-sized storage.** A dimensionless performance metric  $\chi$  was used to quantify the value of the energy generated, which is the ratio of the optimized annual revenue generated (Equation (2.1)) and the annualized plant cost (Equation (2.2)). Plant overnight construction costs are given as the sum of the storage and generation costs per unit rated power of installed solar or wind generation ( $C_{\text{gen}} + \dot{E}_{\max}(C_{\text{storage}}^{\text{power}} + hC_{\text{storage}}^{\text{energy}})$ ). To determine the annualized plant capital costs, the overnight construction costs are multiplied by a capital recovery factor,  $CRF(i, n)$ , defined as  $CRF(i, n) = \frac{i(1+i)^n}{(1+i)^n - 1}$ , with  $n = 20$  years and  $i = 5\%$ <sup>50</sup>. The capital recovery factor is the fraction of a loan that must be paid back annually, assuming a stream of equal payments over  $n$  years and an annual interest rate  $i$ . The plant costs are approximated in this framework by plant capital costs (e.g. for hypothetical storage technologies at various cost points in Figure 2-5). This approximation is reasonable given the dominance of the capital cost portion of total plant costs for most storage technologies, though we discuss below the effect of including estimated O&M costs for several currently available storage technologies. Plant

performance  $\chi$  was calculated using Equation (2.2) over a wide range of system configurations, technology costs, and locations, as summarized in Table 2.1.

The storage size, defined by the storage power and storage duration, was chosen to maximize  $\chi$  given the storage cost, where storage cost is defined by the power-related cost per kilowatt and energy-related cost per kilowatt-hour. Storage sizes were simulated in increments of 1/4 hours and  $1/2 W_{\text{storage}}/W_{\text{generation}}$ .

To compare the model results to the cost of candidate storage technologies today, the costs of energy and power of various storage technologies were taken from the literature, drawing inclusively on recent efforts to identify the modular power- and energy-related cost components of a storage system<sup>1,14,17,35,61,92,104</sup>. These wide-ranging costs are reported in the literature as rough estimates, mixing cost data and engineering estimates (as is common for technologies that have limited or no market adoption). These cost estimates are treated as 2004 real dollars (due to a lack of information otherwise) for the comparison to revenue in 2004 (an assumption that has a minor effect on the storage technology evaluation as compared to the wide range of reported storage costs for each technology). Technologies are modeled with a round trip efficiency of 90% as technology specific refinements to this estimate (which are themselves uncertain) have little effect compared to the wide range of storage costs reported. Replacement costs for storage technologies with estimated lifetimes of less than 20 years (based on the following references:<sup>1,14,17,35,61,92,104</sup>) are included in the storage overnight construction costs, assuming a constant power-related cost per kilowatt and energy-related cost per kilowatt-hour (in nominal dollars) in future years and discounting (with a 5% nominal discount rate, though the conclusions are robust to a reasonable range of assumed rates) the cost of future replacement to determine its present value at the start of plant operation.

In Figures 2-9 and 2-10 we explore the sensitivity of the storage technology costs

shown in Figures 2-7 and 2-8 to estimated O&M costs, reported efficiencies, extended construction lead times, and fuel costs for compressed air energy storage. Despite uncertainty in estimates of these additional costs<sup>1</sup>, the sensitivity analysis provides some insight. The general technology comparisons (i.e. the relative positions of ellipses shown in Figures 2-7 and 2-8) are found to be robust to the inclusion of these additional costs. Furthermore the uncertainty in storage technology cost estimates arises mainly from uncertainty in the capital costs.

## 2.3 Results

**Optimizing electricity output of a hybrid plant to maximize revenue.** Here we optimize the discharging behavior of a hybrid plant, combining wind and solar generation with energy storage, to shift output from periods of low demand and low prices to periods of high demand and high prices (Equation (2.1) in 'Methods'). Both the energy generation resource and the electricity price, which vary over time and whose distribution over time is location dependent, determine the optimal charging and discharging behavior of the system.

This effect is illustrated for the representative case of a storage system with a fixed size defined by a normalized power rating  $\dot{E}_{\max}$  of one MW/MW<sub>gen</sub> (storage power per unit rated power of solar or wind generation) and a duration  $h$  of four hours, coupled with a solar or wind plant in Texas and operated over the course of three days in the spring, summer, fall, and winter (Figure 2-2). Across both energy resources (wind, solar) and across locations, (Texas, California, Massachusetts) incorporating storage results in a reduction of output during periods of low prices, and an increase in output during periods of high prices. The ability to output energy to the grid at peak power during periods of high price is limited, however, by the availability of

sufficient renewable generation to charge the storage system in advance. Although the pricing in each of the three locations examined differ, the effect of storage in each case is to output electricity during periods of high pricing.

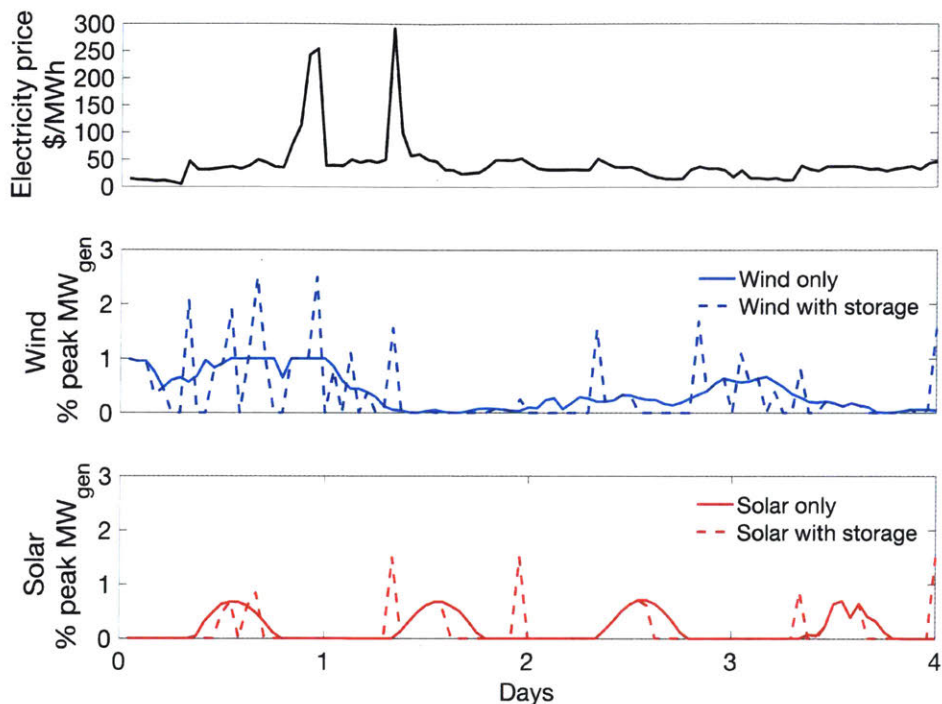


Figure 2-2: Electricity output to maximize revenue from a hypothetical hybrid storage and renewable energy plant located in McCamey, TX with a storage power capacity  $\dot{E}_{\max}$  of 2 MW/MW<sub>gen</sub>, a duration  $h$  of 1 hour, and a roundtrip efficiency of 90%. Data is shown here for a sample of 4 days, though the analysis considers all days of the year. Storage allows plant output to shift from the natural generation profile (solid lines, middle and bottom rows) to periods of high prices (top row: electricity price). Solar is unable to capture both price spikes because there is no resource availability between the spikes enabling the system to recharge. Total hybrid wind system generation is higher during the first smaller price spike because it is the sum of direct to grid wind generation and storage discharge, while only storage is available to generate during the second price spike.

For a given plant, increasing the storage system size in terms of power and duration raises its average electricity selling price. The average selling price without storage is lower for wind than solar, but as the energy storage increases in size (per

unit rated power of solar or wind generation), the pricing distribution and mean selling price become increasingly similar across the two energy resources. However, the addition of storage power and duration comes at a cost, as explored in the next section.

**Balancing revenue against cost to optimize the size and value of storage.**

Storage can increase the revenue generated by a solar or wind plant, but it also increases the capital costs of the plant. Here we optimize both the discharging behavior, as done above, but also the storage system size, in order to maximize the value of the electricity generation.

We quantify value using the dimensionless ratio  $\chi$ , the ratio of the annual revenue to the annualized cost of the hybrid plant.

$$\chi = \frac{R_{\text{total}}}{CRF(C_{\text{gen}} + \dot{E}_{\text{max}}(C_{\text{storage}}^{\text{power}} + hC_{\text{storage}}^{\text{energy}}))}. \quad (2.2)$$

$\chi$  is determined by the revenue  $R_{\text{total}}$ , which is maximized through optimal discharging (Equation (2.1)) at each storage size, and the costs of the hybrid plant. The plant cost is determined by the power capacity-related overnight construction cost of storage  $C_{\text{storage}}^{\text{power}}$ , the energy capacity-related overnight construction cost of storage  $C_{\text{storage}}^{\text{energy}}$ , the solar or wind generation cost  $C_{\text{gen}}$ , the capital recovery factor  $CRF$  (to annualize costs), and the storage size defined by peak power  $\dot{E}_{\text{max}}$  and duration  $h$  (which are given per unit rated power of solar or wind generation). (See Table 2.1 for a description of the parameter space considered.)

Figure 2-4 shows how  $\chi$  varies as a function of the storage system power and duration, and the power and energy-related costs, for the case of a hybrid wind plant sited in Texas with a generation cost of \$1/W. The contour plots in Figure 2-4

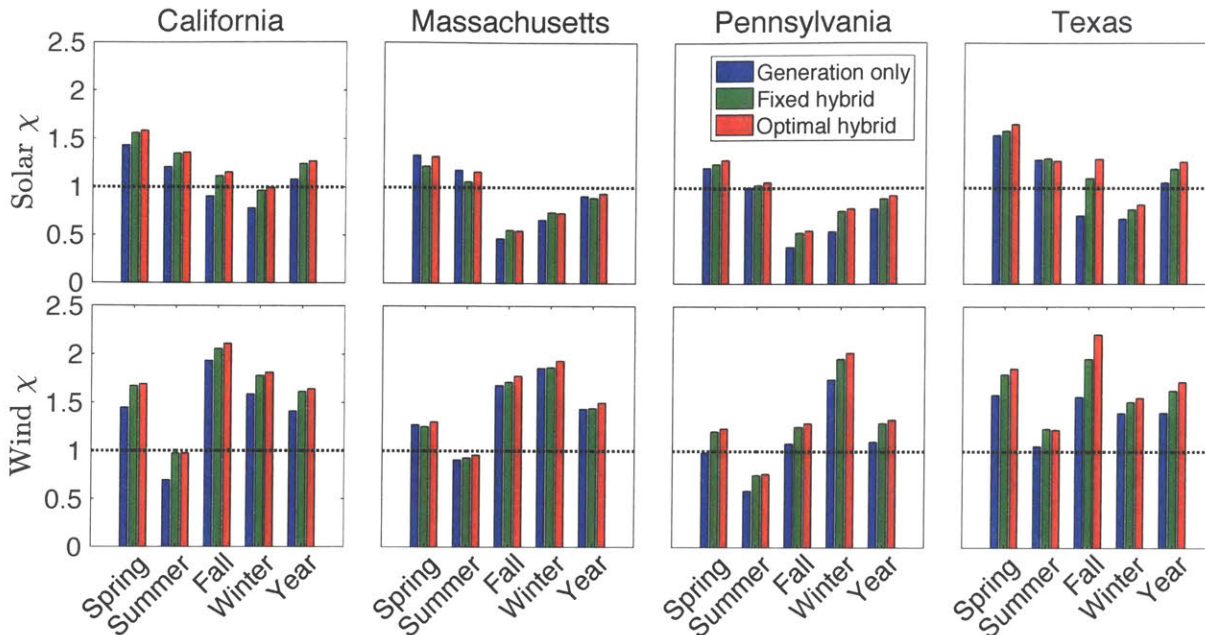


Figure 2-3: Comparison of  $\chi$  values without storage (*generation only*) and with storage for: a fixed storage size of  $\dot{E}_{\max} = 1 \text{ MW/MW}_{\text{gen}}$  and  $h = 4$  hours of storage (*fixed hybrid*), and a storage system whose power and hours of storage ( $\dot{E}_{\max}, h$ ) have been optimized to match the energy resource and the location for a full year (*optimal hybrid*). Results are shown for a wind or solar generation cost of  $\$1/\text{W}$  and power- and energy- related costs of storage of  $\$50/\text{kW}$  and  $\$50/\text{kWh}$ , respectively. Results show the benefits of size-optimized storage across energy resources (solar and wind) and locations (CA, MA, PA, TX). Because storage systems are sized to maximize the ratio of annual revenue to cost,  $\chi$ , they can therefore lead to sub-optimally sized storage in a particular season.

illustrate that if a sufficiently inexpensive storage technology is used (e.g.  $C_{\text{storage}}^{\text{power}} \leq \$130/\text{kW}$  and  $C_{\text{storage}}^{\text{energy}} \leq \$130/\text{kWh}$  for  $\$1/\text{W}$  Texas wind), the additional revenue generated by the storage system can outweigh its cost, thereby increasing the value,  $\chi$ , of the system. The plots also show how the optimal system size (to achieve  $\chi_{\max}$ ) depends on the energy and power-specific storage costs. As might be expected, storage systems with higher power-related costs performed better when specified

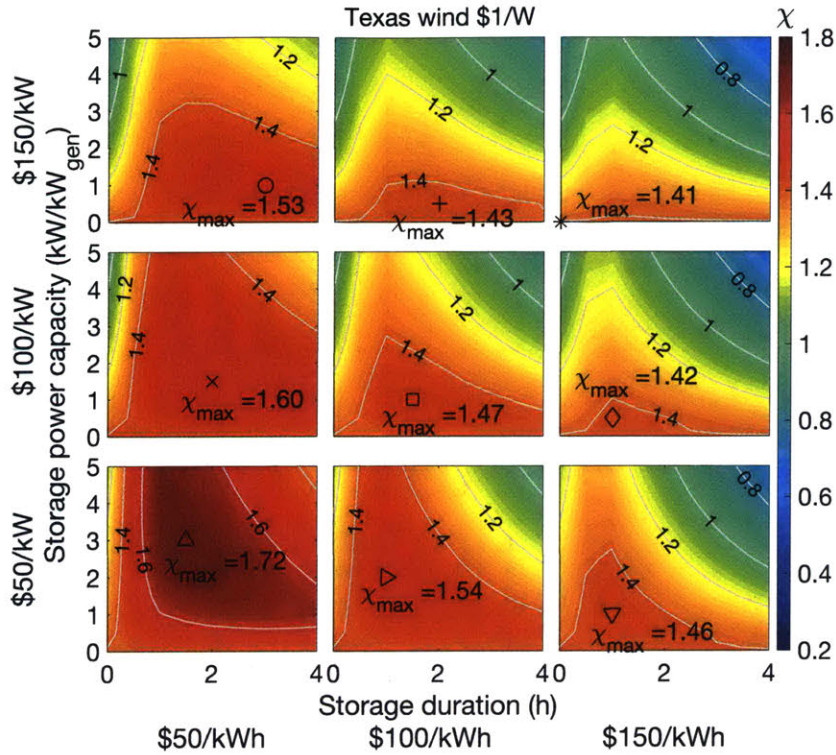


Figure 2-4: Value  $\chi$  of a wind hybrid plant in Texas versus storage size, power  $\dot{E}_{\max}$  (MW storage/MW generation) and duration  $h$  (hrs), for a wind generation cost  $C_{\text{gen}}$  of \$1/W and energy and power-related costs of storage ( $C_{\text{storage}}^{\text{energy}}$ ,  $C_{\text{storage}}^{\text{power}}$ ) ranging from \$50/kWh-\$150/kWh and \$50/kW-\$150/kW respectively. The optimal storage system size is found for each storage energy and power-related cost pair to maximize the value of the hybrid plant ( $\chi_{\max}$ ).

with lower power, and storage systems with higher energy-related costs perform better when specified with lower energy (power  $\dot{E}_{\max}$  times duration  $h$ ).

Figure 2-3 summarizes the change in  $\chi$  with optimally sized storage across the four locations examined. Storage is more valuable for wind than solar in three out of the four locations studied (TX, MA, PA), but across all locations the benefit from storage is roughly similar across the two energy resources, in terms of the percent increase in value due to the incorporation of optimally sized storage. However, the benefit of storage differs more significantly across locations, with a much higher

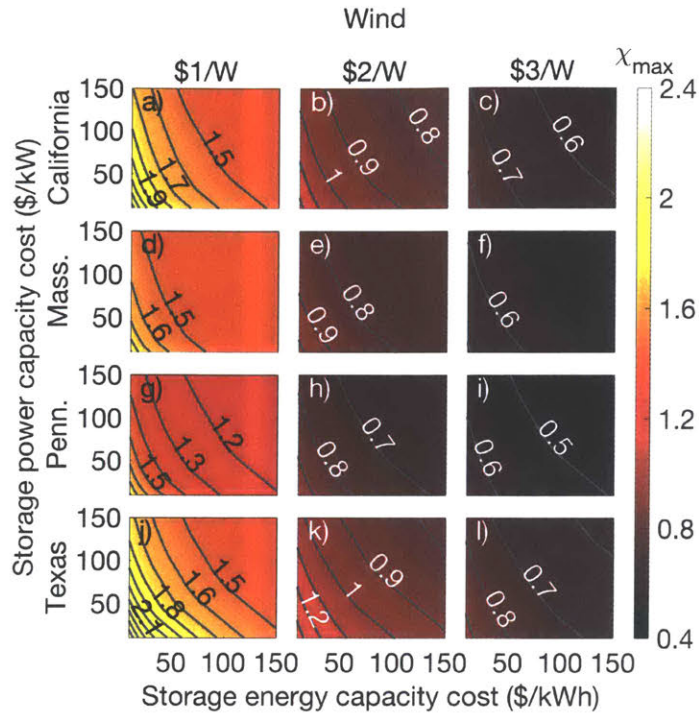


Figure 2-5: Value of a hybrid wind with storage plant as a function of location, generation costs (top row labels), and storage power and energy capacity costs. The size of storage ( $\dot{E}_{\max}, h$ ) has been optimized at all points on the plot to maximize  $\chi$ . (The bottom left panel shows the  $\chi_{\max}$  data from Figure 2-4.) For each contour of constant  $\chi$ , the slopes were found to be roughly consistent across locations and to be determined by the duration of electricity price spikes.

percent increase in value from storage occurring (across both energy resources) in Texas and California than in Pennsylvania and Massachusetts.

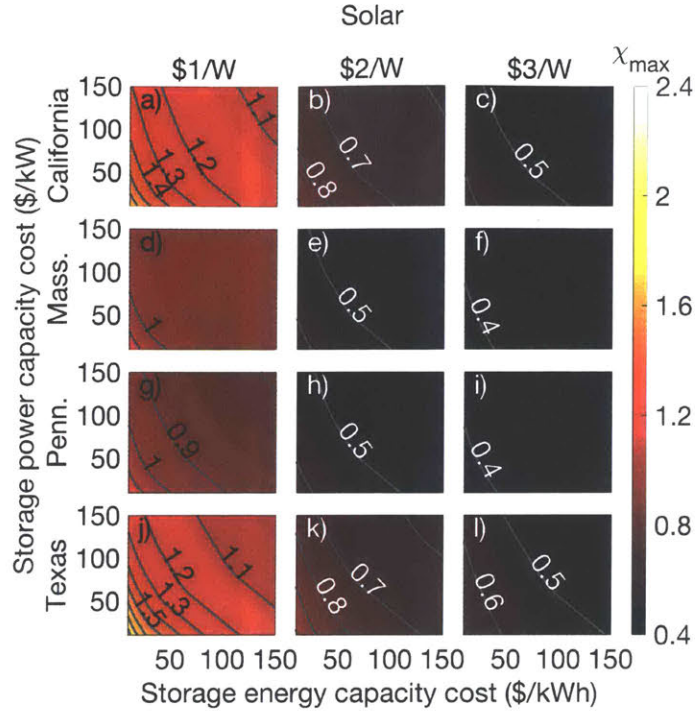


Figure 2-6: Value of a hybrid solar with storage plant as a function of location, generation costs (top row labels), and storage power and energy capacity costs. The size of storage ( $\dot{E}_{\max}, h$ ) has been optimized at all points on the plot to maximize  $\chi$ . For each contour of constant  $\chi$ , the slopes were found to be roughly consistent across locations and to be determined by the duration of electricity price spikes.

**Assessing the cost performance of storage technologies.** The value of diverse storage technology options can be related to their energy-related costs  $C_{\text{storage}}^{\text{energy}}$  and power-related costs  $C_{\text{storage}}^{\text{power}}$ . Here we compare storage technologies that have been optimally sized to maximize  $\chi$  for a given set of storage and generation costs, and energy resource and price dynamics in each location. The relationship between the dimensionless performance parameter  $\chi$  and energy and power costs of storage is shown in Figures 2-5 and 2-6 across the four locations studied.

The results obtained can be compared to existing and future hypothetical energy

storage technologies. Several papers have estimated the power- and energy-related costs of a number of energy storage technologies<sup>1,14,17,35,61,92,104</sup>, finding that these costs can be treated as roughly modular because adding to power generation requires one set of components while adding to energy capacity requires another set of components (with caveats for batteries for which this distinction does not fully apply, see ‘Conclusions’). Widely ranging cost estimates have been reported in the literature<sup>1,14,17,35,61,92,104</sup> and are compared to our results in Figures 2-7 and 2-8. We observe that some technologies available today<sup>29</sup>, based on the lower end of the range of reported cost estimates (Figures 2-7 and 2-8), would add value to wind and solar energy. Included in this group of technologies are compressed air energy storage and pumped hydro storage for Texas wind or solar generation at \$1.5/W (or greater) (Figures 2-7 and 2-8). This analysis allows for a quantitative comparison of disparate technologies. For example, despite power cost estimates that are several times larger for pumped hydro storage than lead acid batteries, we find that pumped hydro storage technologies can significantly outperform lead-acid batteries for this application.

The results are further illuminated through specific examples. For the case of \$3/W solar generation and \$450/kW and \$10/kWh storage, roughly comparable to recently reported photovoltaics system costs<sup>10,90</sup> and the lower end of estimated costs of compressed air energy storage not utilizing natural gas (Figures 2-7 and 2-8), the addition of optimally sized storage provides an approximately 25% increase in the plant value in Texas. (For lower photovoltaics systems costs of \$2/W, comparable to several recent utility-scale cost estimates<sup>53,90</sup>, compressed air energy storage also adds value.) However, at these generation and storage costs the system does not reach a  $\chi$  value of 1, where revenue equals cost and the system becomes profitable. At these costs, it is advantageous to incorporate storage but subsidies are still required for

the overall system to be profitable. For the case of \$450/kW and \$10/kWh storage and \$1.5/W wind generation (roughly comparable to recently reported costs<sup>53,117</sup>) storage adds approximately 11% additional value in Texas and  $\chi$  just reaches 1, the profitability threshold. In comparison, for the case of \$50/kW and \$50/kWh and \$1/W solar or wind generation, which are aspirational costs,  $\chi$  significantly exceeds 1, the profitability threshold, and storage adds roughly 20% to the value of the system  $\chi$  as shown in Figure 2-3.

As the cost of the solar and wind generation technology drops, the cost of storage must also drop in order to continue to add value (Figures 2-7 and 2-8). This is because if generation costs are low enough relative to storage costs, it is more valuable to add generation capacity than storage capacity, even though this means that discharging cannot be optimized to increase revenue. As storage costs decrease relative to generation costs, the ability to increase revenue more than compensates for the additional cost of storage (Equation (2.2)).

Although  $\chi$  values change across locations, the slopes of the contour lines of constant  $\chi$  (iso- $\chi$  lines) are relatively location independent, suggesting a power to energy cost trade-off that is roughly consistent across locations (Figures 2-5 and 2-6). The power to energy cost trade-off of storage technologies is also similar across the two energy resources. This means that the direction of optimal improvement in energy and power costs is similar across the three locations and two energy resources for any given storage technology. This is important because it means that the results reported here can be used to inform industry and policy performance targets and to guide research and development of storage technologies, which once developed could be used for both intermittent energy resources and across various locations. Further study is required to determine how widely this applies across locations, see ‘Conclusions’.

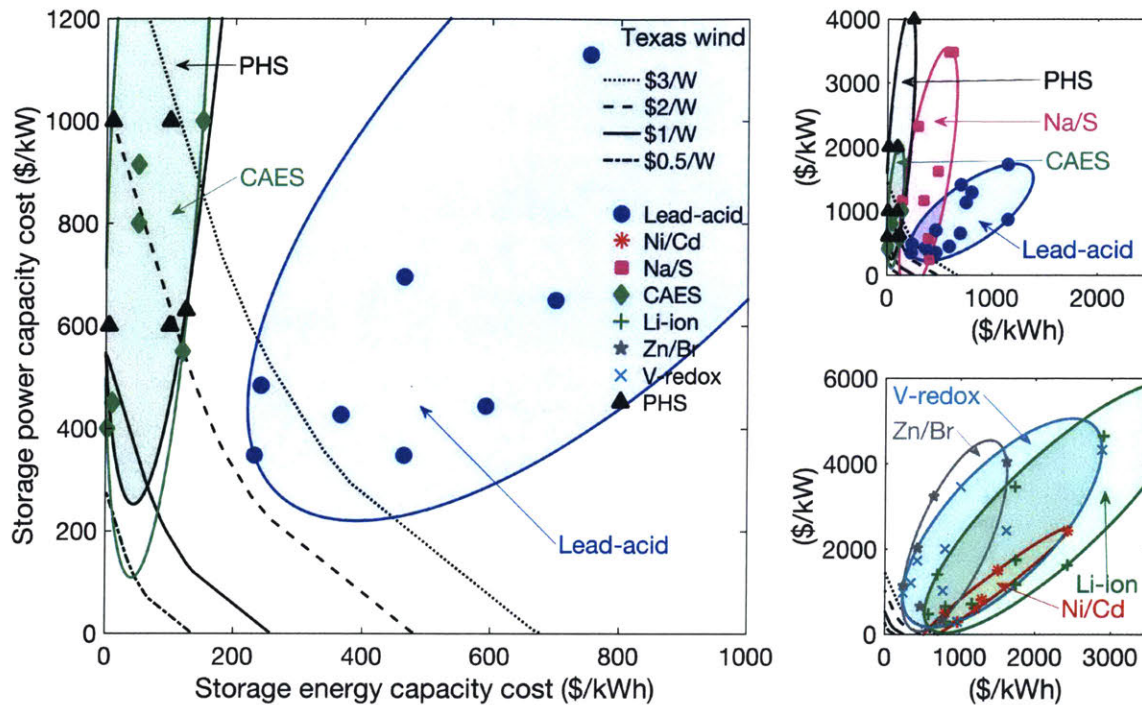


Figure 2-7: Cost intensities of a range of energy storage technologies<sup>1,14,17,35,61,92,104</sup> overlaid on lines, for a given wind generation cost, which show the threshold storage cost intensities at which it becomes valuable to incorporate storage into a Texas wind farm. CAES: compressed air energy storage; PHS: pumped hydro storage; Lead-acid, Ni/Cd, Na/S, Li-ion: batteries; Zn/Br, V-redox: flow batteries. Results for solar are shown in Figure 2-8. The sensitivity of storage cost estimates to additional operations and maintenance (O&M) costs, expanded capacity to account for lower round-trip efficiency, and extended construction times, as well as fuel costs (for CAES utilizing natural gas), are shown in Figure 2-9. Ellipses are plotted to encapsulate the range of cost estimates for each storage technology, while minimizing the shaded area. The ellipses are visual guides and do not represent joint probability distributions; all results discussed in the paper refer to the data points themselves, and not the shaded regions.

The similarity across locations and energy resources in the slopes of the iso- $\chi$  lines can be attributed to commonalities in the electricity price dynamics across locations. The distribution of the duration of price spikes was found to be similar across the locations studied and to define the slopes of the iso- $\chi$  lines.

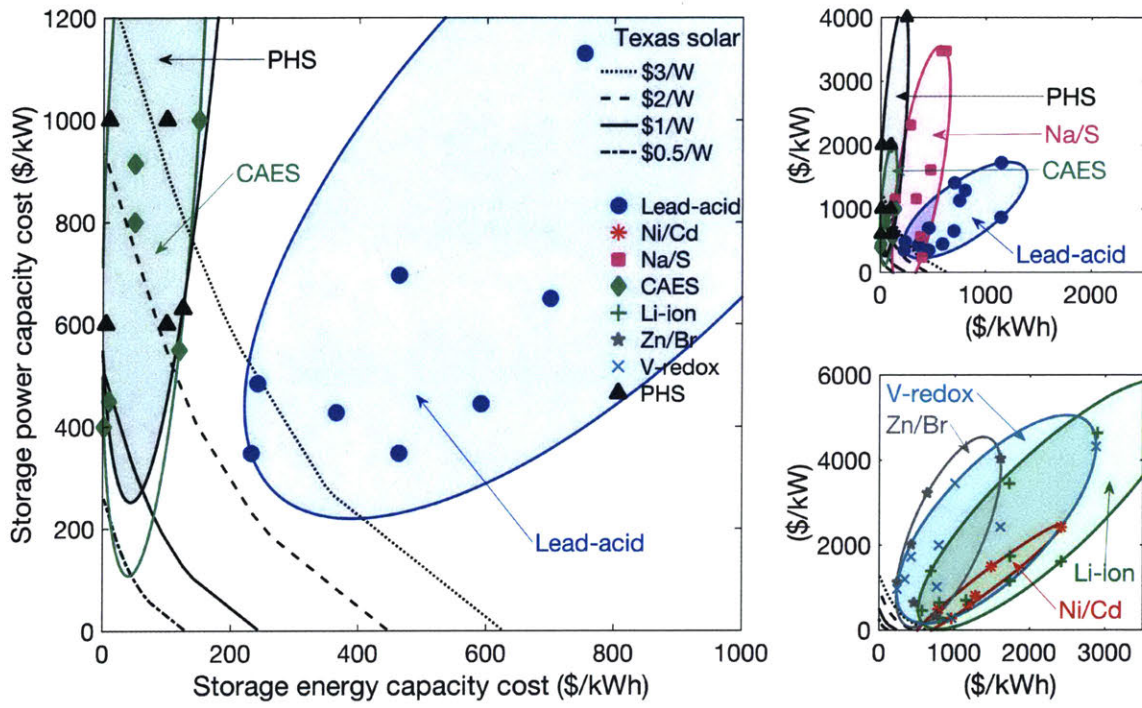


Figure 2-8: Cost intensities of a range of energy storage technologies<sup>1,14,17,35,61,92,104</sup> overlaid on lines, for a given solar generation cost, which show the threshold storage cost intensities at which it becomes valuable to incorporate storage into a Texas solar farm. CAES: compressed air energy storage; PHS: pumped hydro storage; Lead-acid, Ni/Cd, Na/S, Li-ion: batteries; Zn/Br, V-redox: flow batteries. The sensitivity of storage cost estimates to additional operations and maintenance (O&M) costs, expanded capacity to account for lower round-trip efficiency, and extended construction times, as well as fuel costs (for CAES utilizing natural gas), are shown in Figure 2-10. Ellipses are plotted to encapsulate the range of cost estimates for each storage technology, while minimizing the shaded area. The ellipses are visual guides and do not represent joint probability distributions; all results discussed in the paper refer to the data points themselves, and not the shaded regions.

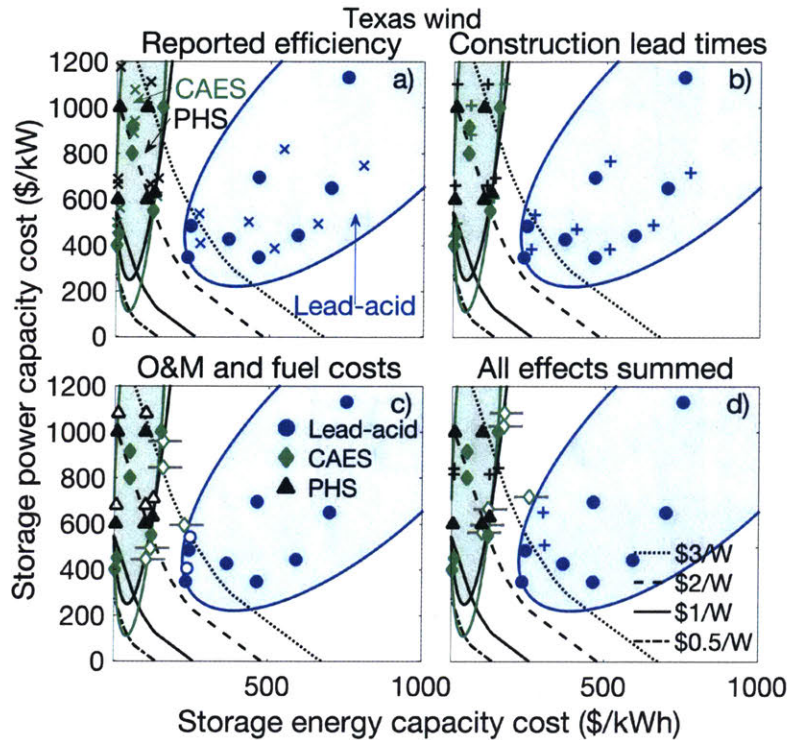


Figure 2-9: Sensitivity analysis of the capital cost intensities to inclusion of: reported efficiency values (a); construction lead times of three years (b); reported operations, maintenance, and CAES fuel costs (c); and all three effects summed (d). Storage costs are shown relative to value thresholds for wind in Texas, and operational costs are based on optimal operation for wind energy arbitrage for each cost structure. Costs for fuel and operations and maintenance are dependent on the energy discharged from storage, and so only those cost estimates where installation of storage is valuable are considered for these additional costs. CAES fuel costs, panels c) and d), assuming non-advanced adiabatic expansion, are based on the average Henry Hub natural gas price during period 1997-2015 with error bars demonstrating the maximum and minimum yearly cost. As storage cost estimates shift to higher values, the installed optimal storage size is smaller, this sensitivity analysis demonstrates the outer limit for reported costs, actual values will fall between the original markers and the new markers for each panel. For panels b) and d), shorter construction times will result in cost estimates closer to the original reported values. This analysis shows that the findings are robust to inclusion of these operational costs, as the largest component of storage costs is the high upfront capital cost. Ellipses are plotted as a visual guide for the original reported cost estimates.

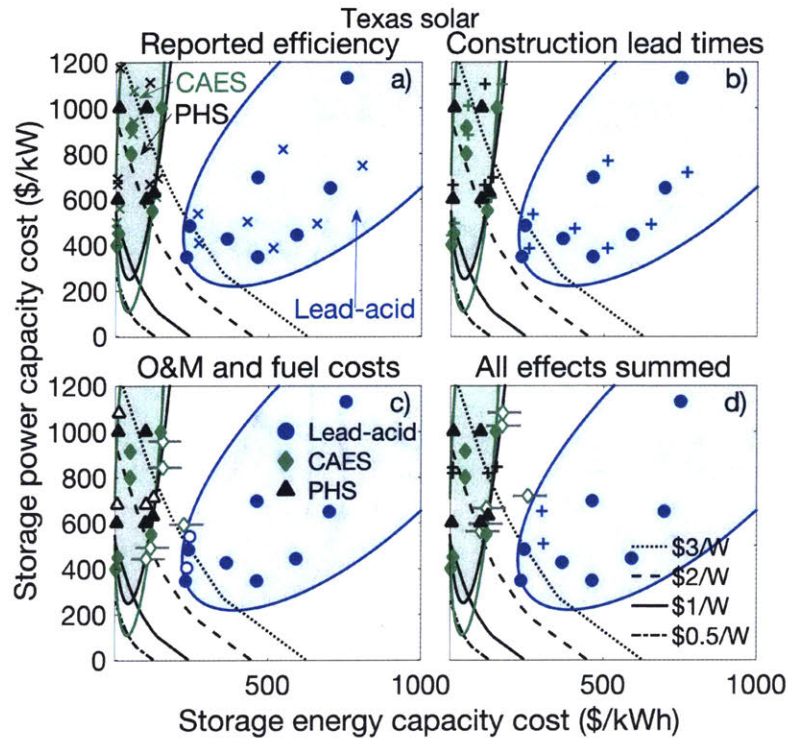


Figure 2-10: Sensitivity analysis of the capital cost intensities to inclusion of: reported efficiency values (a); construction lead times of three years (b); reported operations, maintenance, and CAES fuel costs (c); and all three effects summed (d). Storage costs are shown relative to value thresholds for solar in Texas, and operational costs are based on optimal operation for solar energy arbitrage for each cost structure. Costs for fuel and operations and maintenance are dependent on the energy discharged from storage, and so only those cost estimates where installation of storage is valuable are considered for these additional costs. CAES fuel costs, panels c) and d), assuming non-advanced adiabatic expansion, are based on the average Henry Hub natural gas price during period 1997-2015 with error bars demonstrating the maximum and minimum yearly cost. As storage cost estimates shift to higher values, the installed optimal storage size is smaller, this sensitivity analysis demonstrates the outer limit for reported costs, actual values will fall between the original markers and the new markers for each panel. For panels b) and d), shorter construction times will result in cost estimates closer to the original reported values. This analysis shows that the findings are robust to inclusion of these operational costs, as the largest component of storage costs is the high upfront capital cost. Ellipses are plotted as a visual guide for the original reported cost estimates.

## 2.4 Conclusions

Our results suggest that storage technologies can substantially increase the value of wind and solar energy. For example, we find that storage at costs comparable to several published estimates for compressed air energy storage and pumped hydro storage can add value to wind and solar energy in TX and CA at current costs. However, to reach profitability without subsidies across the locations studied, further cost improvement is needed in wind and solar generation costs and storage costs. Furthermore, as renewable generation costs decrease over time, storage costs must also decrease in order to add value.

Importantly, the results presented here point to cost performance targets for storage technologies to add value and for the renewable energy and storage hybrid plant to reach profitability. For example, researchers and research and development (R&D) managers in the public and private sectors might use the results to assess the potential benefit of pursuing one technology design over another, or one class of storage technology over another, based on its distance from a cost threshold and potential for cost improvement along energy and power cost dimensions. Despite differences across the locations studied in the benefits of adding storage, the direction of optimal storage cost improvement, balancing decreases in the energy and power-related costs of storage, is similar across locations. Thus the results can inform a roadmap for cost improvement to guide broad government and industry technology development strategies.

Additional research is needed to assess the costs of storage technologies today, as current estimates span a large range (Figures 2-7 and 2-8). The assumption of modular power and energy costs<sup>1,14,17,35,61,92,104</sup> may be more appropriate for some technologies (e.g. compressed air energy) and less for others (e.g. batteries) and

deserves further investigation. For batteries, many studies nonetheless used the approximation of modular costs<sup>14,35,61,104</sup> and assign shared component costs to the energy cost estimate. As energy is often the limiting factor for a given total investment in a stationary battery<sup>24</sup>, this treatment is a reasonable approximation. Additionally, the cycling behavior of storage will affect the lifetime capacities of technologies differently<sup>16,59</sup>. This effect is currently not represented in our model but will have a significantly smaller effect on storage capacity costs than the span of costs reported in the literature. These refinements can be incorporated in the future as cost estimates for storage technologies are further resolved.

We have focused here on increasing revenue from the sale of renewable energy but note that storage technologies installed for this purpose might generate additional revenue streams from other services which we do not consider, including frequency regulation, meeting installed power capacity requirements, and arbitrage that is not constrained by the renewable energy resource. This additional revenue could increase the added value of storage relative to the results presented in this paper. Assessing the scale of this added value, and the degree to which it is predictable and can be used to distinguish between candidate storage technologies, is a subject for future investigation.

Furthermore, the analysis performed here is for a low-penetration case in which the solar and wind plants are price takers, and do not measurably influence the electricity price over time. If renewables grow sufficiently to significantly influence the price time series of electricity in the locations studied, the results would change. The changing cost of electricity from other sources with which renewables are competing, or changing demand patterns and market structure, could also affect the results presented. Further study of the changes in electricity price dynamics over time and space is the subject for future research.

Deploying hybrid systems today could support the near-term growth in solar and wind, in contexts where storage technologies add value, as well as the investment and improvement in storage technologies that are needed to eventually allow greater intermittent renewables market share without very long-distance electricity transmission or carbon-emitting back-up generation. Understanding and maximizing the value of storage in today's low market share context is therefore critical to eventually achieving the large-scale adoption of very low carbon- and other air pollutant-intensity intermittent renewables.



## Chapter 3

# Determinants of the value of storage for wind and solar energy

*The value of a wind or solar power plant is a function of the electricity price during periods of resource availability. Moreover, intermittent renewables energy sources, such as wind and solar energy, are not reliably available at times of high prices, limiting their value and adoption. However, energy storage can shift the output of electricity from periods of low prices to periods of higher prices, thereby increasing plant revenue. Previous work has shown that in some locations, energy storage can add to the profitability of wind and solar power plants through energy arbitrage. The added value of storage has also been shown to differ across locations and resources (wind versus solar), and also across different storage technologies with different ratios of energy to power cost. However, questions remain about the determinants of storage value. Why does storage add more value in some locations than others, and what*

---

A version of this chapter is in preparation for publication with co-author Jessika E. Trancik<sup>70</sup>: Joshua M. Mueller and Jessika E. Trancik. Determinants of the value of storage for wind and solar energy. *In preparation.*

*determines which storage technology cost structures are preferred? These are the questions addressed here. Specifically, we examine features of the electricity price dynamics and resource profiles that determine the value of storage for wind and solar energy, and the preferred storage technology. We explore how storage value depends on the frequency and amplitude of price spikes relative to the availability of the solar or wind energy resource over time. We also find that the preferred storage technology cost structure is based on the duration of electricity price spikes.*

### **3.1 Introduction**

Wind and solar energy are generated from intermittent resources and do not reliably produce power at times of highest price or greatest demand. The value of wind and solar is therefore dependent on the local resource profiles over time, as well as the electricity demand and price profiles. Through the addition of energy storage, solar and wind power plants can shift their generation to periods of high demand or price<sup>96</sup>. Despite these benefits, storage has yet to be widely adopted.<sup>29</sup>.

Storage adoption is often limited by the high upfront capital costs of these technologies<sup>68</sup>. Earlier research has shown that the value of storage for renewable energy arbitrage depends on the location and renewable resource considered, but the reasons haven't been systematically studied.<sup>12</sup> For example, it is not known how resource availability and electricity price dynamics influence storage value. Here we seek to understand these determinants.

Electricity market features likely influence storage value across locations because of their impact on electricity prices, which influence the operation of storage<sup>51</sup>. Both the demand profile and supply mix are expected to have an influence on prices and therefore storage value. For example, renewables penetration can impact prices, with

higher penetration leading to lower prices during periods of resource availability<sup>48</sup>, and higher prices when the resource isn't available<sup>49</sup>, particularly in systems without energy storage (or extensive transmission infrastructure and/or demand-side management). By understanding how different electricity markets and prices impact the value of storage for wind and solar energy, it may be possible to better assess the prospects for storage development and adoption, and to guide research on storage technologies that may be particularly useful.

## 3.2 Methods

**Site selection and data sources.** Historical electricity prices, wind speeds, and solar insolation data were collected for four U.S. locations: Palm Springs, CA; Plymouth, MA; Altoona, PA; and McCamey, TX. Wind speed data was taken from Western and Eastern National Wind Integration Datasets and solar insolation data was taken from the National Solar Radiation Database<sup>72</sup>. Wind speed was transformed to hourly output per megawatt installed nameplate capacity using published performance data for a Vestas V90 3 MW wind turbine that aligns to face the wind<sup>112</sup>. For panel i) of Figure 3-3, wind generation data is similarly transformed using the published performance data for a Vestas V112 3 MW wind turbine<sup>112</sup>. Solar generation profiles were modeled as a static photovoltaic system that reaches peak output when exposed to 1 kW/m<sup>2</sup> insolation. Wind and solar generation profiles for a random selection of five consecutive days are shown in panel a) of Figure 3-1. Electricity prices are presented in real 2004 USD, and were collected from CAISO<sup>13</sup>, ISO New England<sup>54</sup>, PJM<sup>84</sup>, and ERCOT<sup>33</sup>.

For Denmark, historical electricity prices, wind generation, and solar generation were collected from Energinet<sup>32</sup>. Electricity prices and wind generation data were

collected for 2008, and converted to 2004 USD using the average exchange rate for 2008<sup>120</sup> and the US GDP deflator<sup>119</sup>. Wind generation was collected as total hourly wind production for each region, East and West, and normalized assuming that the maximum production during this period was the installed nameplate capacity. Solar generation data and prices were similarly calculated based on 2014 values.

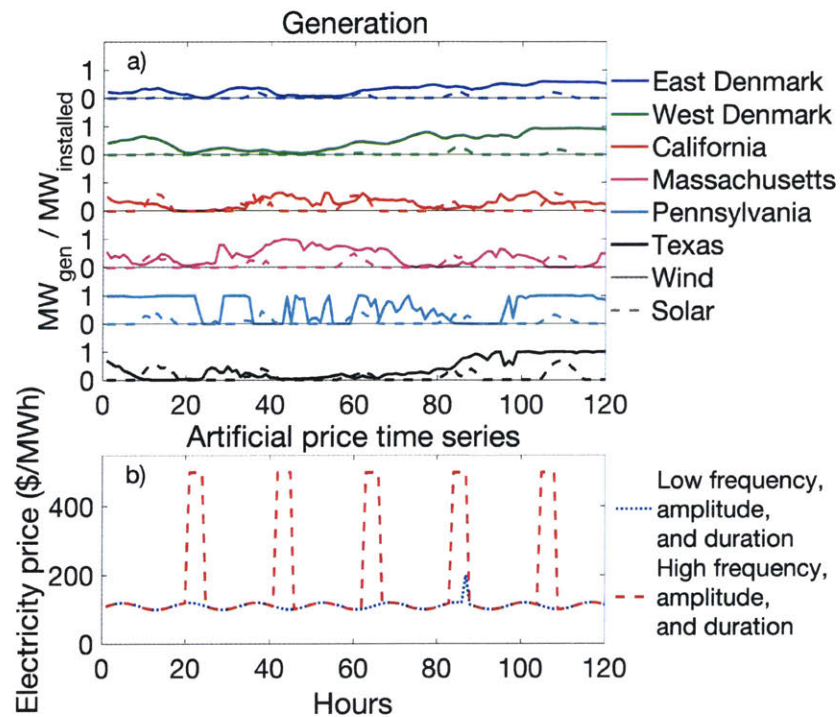


Figure 3-1: Generation data (a) presented for wind and solar power in the locations shown in Figure 3-2. Renewables generation is shown as a fraction of actual generation over the installed nameplate capacity with wind depicted as a solid line and solar as a dashed line. Generation profiles vary with changing location and resource. Two examples of artificial price series (b): 400 spikes per year of height \$500 and duration 4 hours (red), 100 spikes per year of height \$200 and duration 1 hour (blue). Artificial price series were created varying frequency from 100 to 400 spikes per year in 50 spike per year increments, amplitude from \$200/MWh to \$500/MWh in \$50/MWh increments, and duration from 1 to 5 hours, changing to also allow longer duration spikes every other or every third spike with the remaining spikes being 1 hour in duration.

**Artificial price time series simulation.** Hourly price time series were generated to allow independent control of the frequency, amplitude, and duration of price spikes. A base price time series of sinusoidally varying prices from \$100/MWh to \$120/MWh was used. Price spikes were added at consistent intervals, as determined by the selected frequency, replacing the hourly base prices value with the desired amplitude for the selected duration. The distribution of the duration of price spikes was varied, alternating the duration of price spike events in a deterministic fashion. The parameter space explored in developing the artificial price series for simulation is provided in Table 3.1.

Table 3.1: Experimental parameter space investigated

Parameter	Unit	Values
Frequency	Spikes/year	100 - 400
Frequency increments	Spikes/year	50
Amplitude	\$/MWh	200 - 500
Amplitude increments	\$/MWh	50
Duration	h	1 - 5
Duration increments	h	1
Event duration distribution	Spike events	All, every other, every third

Increased renewables penetration levels were simulated using artificial price time series in which prices are depressed when wind and solar generation peak. Hours of resource availability peaks were selected as the highest 200 (low), 365 (moderate), and 500 (high) hours of resource availability. Prices during these time periods were set to \$0/MWh. The prices were then normalized to have the same mean as prior to the simulated renewables penetration (i.e., adjusted upwards). Sensitivity to this normalization was performed showing that it has less than a 1% impact in the resulting values. This method was selected as a means of testing how storage value might increase due to the temporal mismatch of generation and prices with all other

factors held constant.

**Optimization model to determine storage value.** Maximum storage value is determined through a two-step optimization process as first developed by Braff *et al.* (2016)<sup>12</sup>. In the first phase, storage operation is optimized to maximize total plant revenue as constrained by the power and energy capacity of storage, Equation (3.1). Hourly charging and discharging of the storage system, and the direct sale of solar and wind generated electricity were optimized to achieve maximum revenue for a hypothetical hybrid storage and generation plant at each site, given the historical or artificial electricity price and energy resource availability over time and subject to system power and energy capacity constraints. Artificial price time series were evaluated against the wind and solar resource availabilities for twelve total combinations of the two generation technologies with six locations (California, Massachusetts, Pennsylvania, Texas, East Denmark, and West Denmark).

The optimization was performed in three week intervals over the course of a year, with one week overlap between each interval to prevent discontinuities, and an offset included in the energy constraint for each optimization period to account for the amount of energy stored in the system at the beginning of the period. The charge rate was capped at the lower of the real-time output of the generation resource and the storage power capacity. Additionally, the energy available for discharge was adjusted by a roundtrip efficiency of 90% applied to the charged energy. In order to reduce the computational expense of the optimization, the simulation considered charging and discharging separately so that a linear solution technique could be employed.

The optimization routine for each three week segment ( $N = 504$  hours) can be expressed in terms of the real time price  $P(t)$ , the generation profile  $x_{generation}(t)$ ,

storage roundtrip efficiency  $\eta$ , peak power  $\dot{E}_{max}$ , and duration  $h$  as:

$$\begin{aligned}
R_{total} &= \max\left(\sum_{t=0}^N P(t)(x_{generation}(t) + x_{discharge}(t) - x_{charge}(t)/\eta)\right) \\
&\text{subject to:} \\
0 &\leq x_{discharge}(t) \leq \dot{E}_{max} \\
0 &\leq x_{charge}(t) \leq \min(\eta x_{generation}(t), \eta \dot{E}_{max}) \\
0 &\leq \sum_{t=0}^N (x_{charge}(t) - x_{discharge}(t)) \leq h \dot{E}_{max}. \quad (3.1)
\end{aligned}$$

In the second step of the optimization, the value of the plant,  $\chi$ , is determined as the annual revenue divided by the annualized costs for all combinations of power ( $C_{storage}^{power}$ ) and energy ( $C_{storage}^{energy}$ ) capacity cost intensity, Equation (3.2). Plant overnight construction costs are given as the sum of the storage and generation costs ( $C_{gen}$ ) per unit rated power of installed solar or wind generation ( $C_{gen} + \dot{E}_{max}(C_{storage}^{power} + hC_{storage}^{energy})$ ). To determine the annualized plant capital costs, the overnight construction costs are multiplied by a capital recovery factor,  $CRF(i, n)$ , defined as  $CRF(i, n) = \frac{i(1+i)^n}{(1+i)^n - 1}$ , with  $n = 20$  years and  $i = 5\%$ <sup>50</sup>. Generation costs of \$500, \$1000, \$2000, and \$3000/kW were evaluated.

For each pair of storage power capacity and energy capacity costs, between \$2-3000/kW and \$2-3000/kWh, the storage power capacity and duration which maximize  $\chi$  are selected. The maximum  $\chi$  results are plotted on the z-axis as a function of the separable power and energy capacity costs. Further detail on this model can be found in Braff *et al.* 2016<sup>12</sup>.

$$\chi = \frac{R_{total}}{CRF(C_{gen} + \dot{E}_{max}(C_{storage}^{power} + hC_{storage}^{energy}))} \quad (3.2)$$

$R_{\text{total}}$  is the total annual revenue of optimally operated storage with power capacity,  $\dot{E}_{\text{max}}$ , duration,  $h$ , and at 90% roundtrip efficiency.  $CRF$  is the capital recovery factor. Storage sizes were simulated in increments of 1/2 hours and 1/2  $W_{\text{storage}}/W_{\text{generation}}$ .

### 3.3 Results

**Wind and solar value differs across locations.** The value of wind and solar energy at a given location is dependent on the amount of electricity available to sell, the price at which it can be sold, and how much it costs to produce that electricity. When total costs of ownership for wind and solar are held constant across locations the amount of energy available, in terms of resource availability, and the costs to produce electricity are inversely related. In this section we look at how the capacity factor, defined here as the mean output in terms of  $\text{MW}/\text{MW}_{\text{peak}}$ , and the prices at times of resource availability determine the value of wind and solar.

Correlations between the amount of energy available and the price at which it can be sold determine the revenue available in a given location. The more positively correlated the resources and prices are, the more revenue any given kWh can capture. We find that in the historical data, solar availability is positively correlated with prices in all U.S. locations, see Table 3.2. However, recent work has shown this may be changing with increased solar penetration<sup>43,48,51</sup>. Wind energy production was negatively correlated with prices in California, Pennsylvania, and Texas, where California and Texas are the locations with the highest wind production levels (Table 3.2). Pennsylvania's near-zero negative correlation may be due to the matching of wind availability with early morning hours of low demand.

The cost of wind and solar electricity production is largely dependent on the

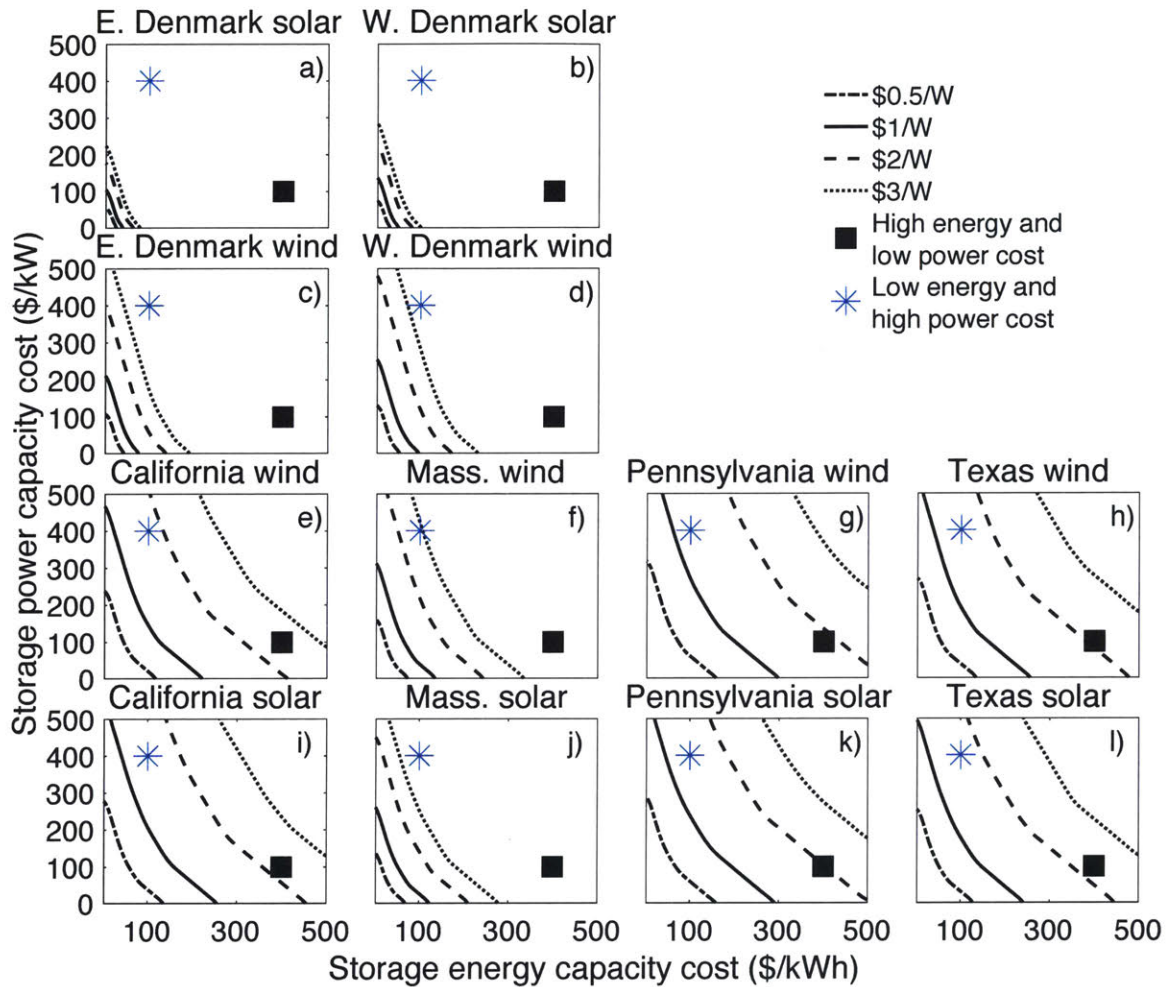


Figure 3-2: For different locations and resources, storage value thresholds are plotted against example storage technology cost structures to show how these thresholds can be used to evaluate storage technologies. Storage energy capacity costs are presented on the horizontal axis and power capacity costs on the vertical axis. A high power and low energy capacity cost technology (asterisk) and a low power and high energy capacity cost technology (square) are plotted to roughly represent the cost structures of mechanical systems and flow batteries (former) and sealed batteries (latter). While the thresholds are in different positions for each U.S. location, the slopes of the lines are similar for both resources and U.S. locations. The slopes of the lines for both Denmark locations are steeper for any given pair of storage costs, meaning that in these locations storage with lower energy to power capacity cost ratios are more valuable.

Table 3.2: Determinants of wind and solar value. Higher capacity factor leads to a higher  $\chi_{\max}$  value for renewables only. Here we see weak to no correlation between resource availability, or generation amount, and prices. Locations with lower capacity factor and more negative correlation between prices and resource availability have higher value thresholds, though these results are also impacted by the electricity price dynamics discussed later. Storage costs are provided where the value threshold intersects a 45° ray from the origin along which the \$/kWh equals the \$/kW costs of storage.

Location	Resource	Capacity factor	Correlation generation and prices	$\chi_{\max}$ wind or solar only	Storage cost at threshold (\$/kW & \$/kWh)
California	Solar	23.3%	0.088	0.54	271
	Wind	33.9%	-0.051	0.71	238
Massachusetts	Solar	15.4%	0.090	0.46	147
	Wind	25.5%	0.036	0.72	155
Pennsylvania	Solar	15.3%	0.173	0.39	304
	Wind	24.4%	-0.007	0.55	305
Texas	Solar	21.6%	0.088	0.53	264
	Wind	33.0%	-0.104	0.70	270

upfront fixed capital costs and the availability of the resource. Resource availability in this study is represented by the capacity factor of generation. Increasing the amount of electricity generated, i.e., increasing the capacity factor, both raises revenues and lowers energy costs. Capacity factors differ across resource and location, but also are partially determined by the choice of wind turbine or solar photovoltaics orientation and operation. The capacity factors in Figure 3-3 were changed by switching among the resource availability profiles for each U.S. location and for panel i) the Texas wind speed data is transformed based on the published performance data for a Vestas V112 turbine as opposed to the V90 used in panels a) through h)<sup>112</sup>. The same artificial price series is used for each panel. The value of wind or solar without storage is the  $\chi_{\max}$  value above the value threshold (bold line).

As would be expected, wind and solar value are highest in locations with higher resource capacity factors (Table 3.2). Locations with high correlations in the timing of wind and solar availability and prices will also have higher  $\chi$  values. However, as renewables penetration increases, we expect this correlation to decrease. In Table 3.3 we show similar results as in Table 3.2 for simulations of modified historical prices and resources under conditions of increasing simulated renewables penetration. We see that as the simulated renewables penetration increases, this leads to an increasingly negative correlation between prices and generation as well as a decrease in the  $\chi$  values for wind or solar without storage. In these scenarios, the ability of storage to shift output to times of high prices becomes increasingly valuable. In the next sections we explore the determinants of this increased value of storage and explore the similarities in the drivers of storage value across the locations.

**Resource availability over time impacts storage value.** When performing energy arbitrage, storage derives value by shifting generation to later periods with higher prices. Thus, storage is valuable when there is revenue to be gained by selling electricity at later periods. Storage value is also dependent on the generation costs. We see in Figure 3-2 that storage value thresholds are lower as the generation cost declines<sup>12</sup>. Here we explore how resource variations impact storage value through timing of resource availability and reductions in the overall cost of energy.

We find that increasing the capacity factor of the resource decreases the costs at which storage begins to provide value, because additional generation units are now more valuable. Figure 3-3 demonstrates how as capacity factor increases, and therefore levelized energy costs fall, storage value thresholds occur at lower costs. As wind and solar become more valuable, storage costs must decline to continue to provide value.

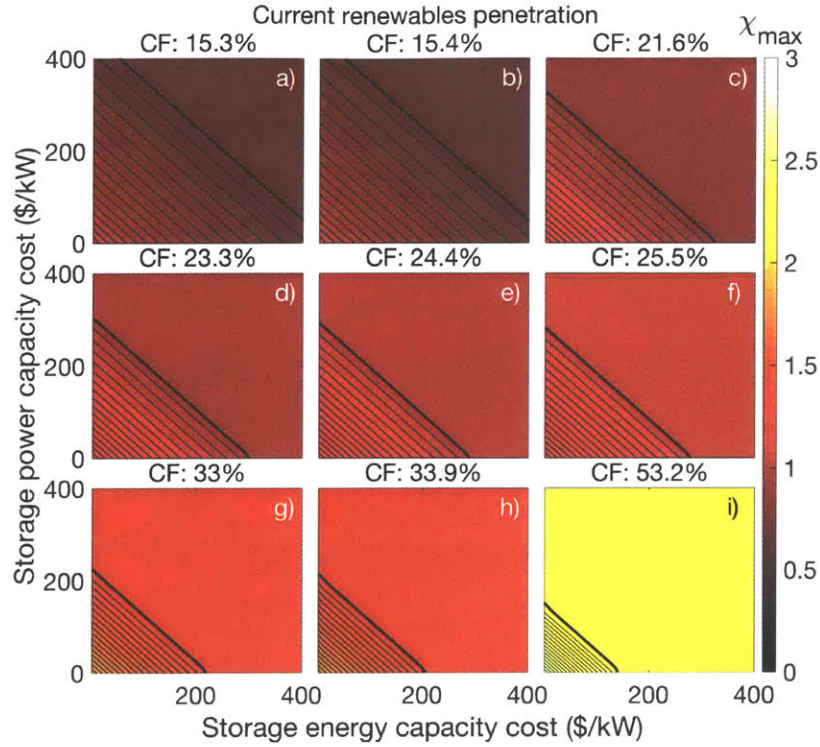


Figure 3-3: Effects of increasing capacity factor on the costs at which storage provides value. Hybrid renewables and storage value,  $\chi_{\max}$ , is shown as a heat map plotted as a function of separable storage energy capacity (horizontal) and power capacity (vertical) costs for a single artificial price series of 100 spikes per year, at \$350/MWh per spike, with a duration of one hour. Panels a) through d) show solar in Pennsylvania, Massachusetts, Texas and California respectively. Panels e) through h) show wind profiles for a Vestas V90 in Pennsylvania, Massachusetts, Texas and California respectively. Panel i) shows the wind generation of a Vestas V112 high capacity turbine for the same input wind speed as in panel g) (Texas). For high storage costs, it may be more optimal to install more wind turbines or photovoltaic panels, even if they cannot be optimally operated, due to the lower energy costs. Thus, high capacity factors result in a reduction in storage value cost thresholds. It should be noted that increased capacity factor increases the overall system value, as seen by the higher  $\chi$  values.

The added value of storage is impacted by resource timing and is increased when wind and solar generate at times of low prices and are unavailable during periods of higher prices. For a constant capacity factor, when prices are low at times of resource availability, i.e., negatively correlated, storage value thresholds occur at

higher costs. Under these conditions there is a greater benefit in the ability for storage to shift generation times. We show in Table 3.3 how value thresholds increase as the correlation between prices and resources becomes more negative. These results are derived from a simulation of renewables penetration where increased penetration leads to increasingly negative correlations between prices and resource availability. We see these results in both artificial price series (Table 3.4), where the original artificial price time series show no correlation between resource availability and prices, and in the historical data (Table 3.3).

More expensive storage may become valuable as renewables adoption leads to increasingly mismatched periods of resource availability and high prices. As wind and solar adoption increases, these technologies may lower the locational marginal price of electricity when they generate, since they have near-zero variable costs<sup>43,48</sup>. Using the same approach as in Table 3.3, we model this price collapse by lowering prices in an artificial price time series when resource availability peaks, thus simulating new price series capturing the increase in value for storage when shifting generation in dynamic markets. We find that as modeled renewables penetration increases, storage value thresholds move to higher costs, Figure 3-4. Simulating increased renewables penetration leads to increased storage value across all capacity factors in both the artificial price series (Figure 3-4), and the historical data (Table 3.3). We have shown the importance of electricity prices during periods of resource availability, and we now turn to analyzing the features of electricity price dynamics.

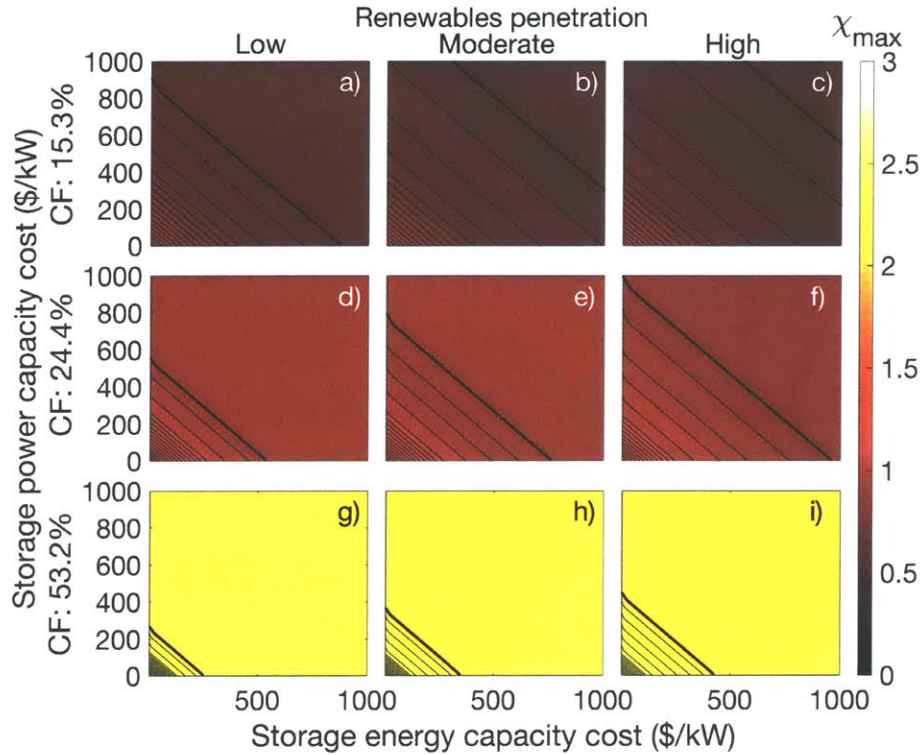


Figure 3-4: Storage thresholds determined across three capacity factors for low (left column), moderate (center column,) and high (right column) modeled renewables penetration. The top row corresponds to panel a) (CF: 15.3%), in Figure 3-3, the middle row to panel e) (CF: 24.4%), and the bottom row to panel i) (CF: 53.2%). At low levels of renewables, we expect there to be infrequent periods ( $<1$  per day) of low prices caused by high renewables resource availability, simulated here as 200 zero price events in a year. At moderate levels of renewables, we expect there to be infrequent periods ( $=1$  per day) of low prices caused by high renewables resource availability, simulated here as 365 zero price events in a year. At high levels of renewables, we expect there to be frequent periods ( $>1$  per day) of low prices caused by high renewables resource availability, simulated here as 500 zero price events in a year. We see that for all capacity factors the storage value thresholds occur at higher storage costs with increasing simulated renewables penetration.

Table 3.3: Determinants of wind and solar value as a function of simulated renewables penetration. There is a steady decline in renewables only value with simulated increased penetration, with an increase in the costs at which storage can provide value to the hybrid power plant. There is also an increasingly negative correlation, as forced by the simulations, between the generation and price time series. Here, low renewables is simulated as 200 zero-price hours per year, moderate renewables is simulated as 365 zero-price hours per year, and high renewables is simulated as 500 zero-price hours per year. Storage costs are provided where the value threshold intersects a 45° ray from the origin along which the \$/kWh equals the \$/kW costs of storage.

Location	Resource	Correlation generation and prices	$\chi_{\max}$ wind or solar only	Storage cost at threshold (\$/kW & \$/kWh)
<b>Low renewables</b>				
California	Solar	-0.008	0.50	366
	Wind	-0.107	0.68	296
Massachusetts	Solar	-0.057	0.41	305
	Wind	-0.091	0.68	236
Pennsylvania	Solar	0.015	0.35	478
	Wind	-0.122	0.52	395
Texas	Solar	-0.009	0.49	384
	Wind	-0.171	0.67	331
<b>Mod. renewables</b>				
California	Solar	-0.065	0.48	454
	Wind	-0.147	0.65	346
Massachusetts	Solar	-0.110	0.39	432
	Wind	-0.152	0.66	309
Pennsylvania	Solar	-0.054	0.33	616
	Wind	-0.179	0.50	472
Texas	Solar	-0.055	0.47	472
	Wind	-0.218	0.65	377
<b>High renewables</b>				
California	Solar	-0.085	0.47	517
	Wind	-0.178	0.64	392
Massachusetts	Solar	-0.126	0.39	499
	Wind	-0.184	0.65	371
Pennsylvania	Solar	-0.082	0.32	699
	Wind	-0.204	0.49	533
Texas	Solar	-0.069	0.46	517
	Wind	-0.245	0.64	392

Table 3.4: Correlation coefficients between an artificial price time series and resource availability from 2004 for simulated increases in renewables penetration. The frequency, amplitude, and duration of price spikes in the artificial price times series used here were: 100 spike per year, amplitude \$350/MWh per spike, and 1 hour duration. We see that there is no correlation between prices and resource availability for the original artificial prices, but as we simulate increasing renewable penetration there is an increasingly negative correlation between prices and resource availability. Here, low renewables is simulated as 200 zero-price hours per year, moderate renewables is simulated as 365 zero-price hours per year, and high renewables is simulated as 500 zero-price hours per year.

Location	Resource	Original	Low renewables	Moderate renewables	High renewables
California	Solar	0.00	-0.20	-0.27	-0.29
	Wind	-0.01	-0.14	-0.22	-0.27
Massachusetts	Solar	-0.01	-0.23	-0.29	-0.30
	Wind	0.00	-0.21	-0.29	-0.32
Pennsylvania	Solar	0.00	-0.23	-0.31	-0.34
	Wind	0.01	-0.22	-0.31	-0.34
Texas	Solar	0.00	-0.20	-0.27	-0.28
	Wind	0.00	-0.18	-0.27	-0.31

**Electricity price dynamics drive storage value.** Storage value is higher when price spikes occur more frequently. The change in storage value thresholds under increasingly frequent price spike events is shown in panels a) and b) of Figure 3-5. In these panels we also see that for low storage costs, the value of storage,  $\chi$ , is higher when price spikes are more frequent. This is because additional storage capacity is installed at lower cost estimates enabling the plant operator to capture more periods of high prices. We also see that the costs at which storage becomes valuable also increase. Figure 3-6 panel a) summarizes these results, showing that for a 1% increase in price spike frequency there is a roughly 0.9% increase in the storage costs at the value threshold, holding all other price dynamics constant. With frequent price spikes, higher cost storage may be able to generate enough additional revenue to outweigh the increased capital costs. Finally, there is no change in the slopes of the iso- $\chi$  lines when price spike frequency is increased.

Storage is more valuable when price spike amplitudes are higher. In panels c) and d) of Figure 3-5 we see that increasing the amplitude of the price spikes means that storage of higher costs are now valuable. In Figure 3-6 panel b) we see that for a 1% increase in price spike amplitude there is a roughly 1.55% increase in the storage costs at the value threshold, holding all other price dynamics constant.

The effects of amplitude and frequency on storage value are expected findings validated through these simulations. More unexpectedly, however, raising the amplitude of price spikes has no impact on the slope of the iso- $\chi$  lines. Changing the slopes of the iso- $\chi$  lines is important for determining the preferred technology cost structures in a given location (as described in the next section).

**Price spike duration determines the preferred storage technology.** When price spike duration increases we see a corresponding increase in the relative value

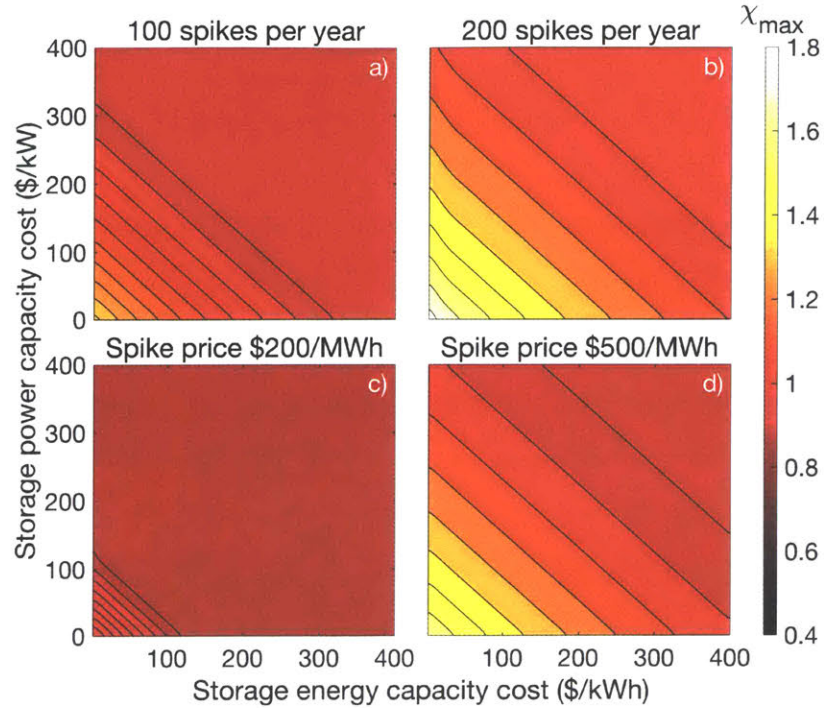


Figure 3-5: Effects of increasing price spike frequency and amplitude on storage value thresholds. Hybrid renewables and storage value,  $\chi_{\max}$ , is shown as a heat map plotted as a function of separable storage energy capacity (horizontal) and power capacity (vertical) costs for simulations of artificial price series with varying price spike frequency and amplitude. Increasing the frequency of price spikes raises the cost threshold at which storage becomes valuable, panels a) and b), shown for price spike amplitude of \$350/MWh. Increasing the amplitude of the price spikes, panels c) and d), shown for a price spike frequency of 100 spikes per year, similarly raises the cost threshold at which storage becomes valuable. All four plots are evaluated for price spikes of one hour duration, and we find that neither varying the frequency nor the amplitude of price spikes has an impact on the slopes of the iso- $\chi$  lines.

of low energy to power cost technologies (as compared to other technology cost structures). This effect is shown in Figure 3-7 where increasing the duration of the price spikes in the artificial price time series leads to steeper iso- $\chi$  lines and storage value thresholds. Adjusting the distribution of the duration of price spike events leads to a changing slope in the iso- $\chi$  line, panel d) of Figure 3-7, similar to the

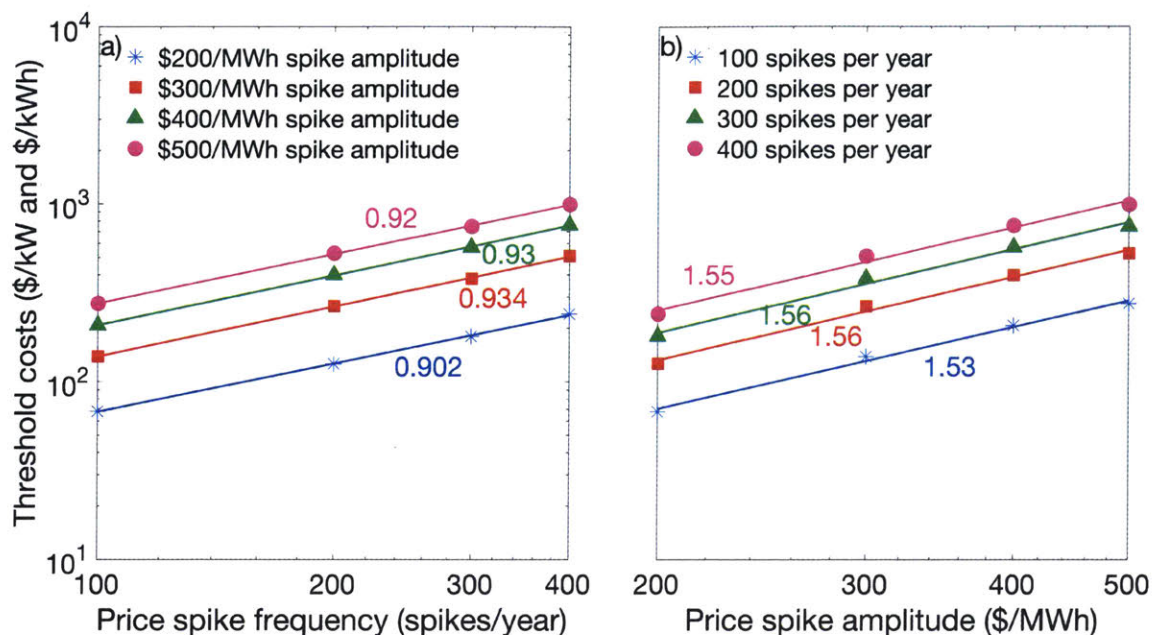


Figure 3-6: Storage costs at which the value threshold intersects a  $45^\circ$  ray from the origin along which the  $\$/\text{kWh}$  equals the  $\$/\text{kW}$  costs of storage. This cost structure represents the closest distance to the origin of the storage cost thresholds for 16 combinations of price spike frequency and amplitude, all with a 1 hour duration. Numbered values give the slope of the line in a log-log plot. Both panels show the same data points for a different horizontal axis. Increasing the frequency of price spikes (a) by 1% leads to a roughly 0.9% increase in the costs at which the value threshold occurs for a constant price spike amplitude. Increasing the amplitude of price spikes (b) by 1% leads to a roughly 1.55% increase in the costs at which the value threshold occurs for a constant price spike frequency.

curved and decreasing slopes in Figure 3-2. In panel d) price spikes of 3 hours in duration occur every third spike with all other price spikes being 1 hour in duration. This implies that the similarity in iso- $\chi$  slopes seen throughout the US locations may be a result of similar distributions in the duration of price spike events across locations.

The importance of price spike duration is further supported by analytical methods

exploring the meaning of the slope of the iso- $\chi$  lines. As presented fully below, the slope of the iso- $\chi$  lines, when storage capacities are held constant with respect to storage costs, is equal to the optimal installed duration of storage. Longer duration price spikes likely lead to optimal installation of longer duration storage, since there is not time to recharge storage between two consecutive hours of high prices. If the optimal storage duration is longer, the corresponding iso- $\chi$  slope at that storage cost is steeper. Steeper iso- $\chi$  slopes indicate that technologies with low energy capacity costs are more valuable.

The slopes of the iso- $\chi$  lines can be determined by taking the ratio of the partial derivatives of  $\chi$  with respect to the capacity cost intensities,  $C_{\text{storage}}^{\text{energy}}$  and  $C_{\text{storage}}^{\text{power}}$ :

$$\left. \frac{dC_{\text{storage}}^{\text{power}}}{dC_{\text{storage}}^{\text{energy}}} \right|_{\chi} = \frac{\partial \chi / \partial C_{\text{storage}}^{\text{energy}}}{\partial \chi / \partial C_{\text{storage}}^{\text{power}}} \quad (3.3)$$

The partial derivatives of  $\chi$  are (note: the symbol  $\gamma$  is used to in place of the capital recovery factor to ease the notation):

$$\begin{aligned} \frac{\partial \chi}{\partial C_{\text{storage}}^{\text{energy}}} &= \frac{\frac{\partial R_{\text{total}}}{\partial \dot{E}_{\text{max}}} \cdot \frac{d\dot{E}_{\text{max}}}{dC_{\text{storage}}^{\text{energy}}} + \frac{\partial R_{\text{total}}}{\partial h} \cdot \frac{dh}{dC_{\text{storage}}^{\text{energy}}}}{\gamma(C_{\text{gen}} + \dot{E}_{\text{max}}(C_{\text{storage}}^{\text{power}} + hC_{\text{storage}}^{\text{energy}}))} \\ &= \frac{R_{\text{total}} \left( \gamma \left( \frac{d\dot{E}_{\text{max}}}{dC_{\text{storage}}^{\text{energy}}} C_{\text{storage}}^{\text{power}} + \left( \frac{d\dot{E}_{\text{max}}}{dC_{\text{storage}}^{\text{energy}}} h + \frac{dh}{dC_{\text{storage}}^{\text{energy}}} \dot{E}_{\text{max}} \right) C_{\text{storage}}^{\text{energy}} + \dot{E}_{\text{max}} h \right) \right)}{\left( \gamma(C_{\text{gen}} + \dot{E}_{\text{max}}(C_{\text{storage}}^{\text{power}} + hC_{\text{storage}}^{\text{energy}})) \right)^2} \end{aligned} \quad (3.4)$$

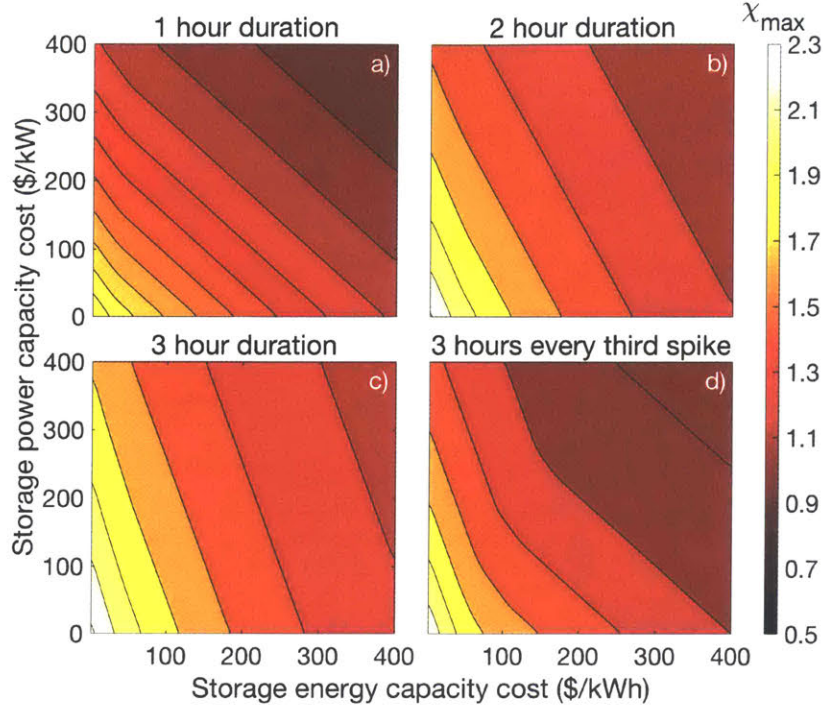


Figure 3-7: Effects of changing price spike duration on the slope of iso- $\chi$  lines. Hybrid renewables and storage value,  $\chi_{\max}$ , is shown as a heat map plotted as a function of separable storage energy capacity (horizontal) and power capacity (vertical) costs for simulated artificial price series with varying price spike durations. Increasing the duration of price spikes in an artificial price series increases the absolute value of the slope (steepness) of the iso- $\chi$  lines, or lines of constant value for a wind or solar with storage power plant. Steeper iso- $\chi$  slopes indicate that technologies with lower energy capacity to power capacity cost ratios will be more valuable. In panel d), the duration of price spikes was varied within the time series simulated with a 3 hour duration price spike occurring every third spike and all other spikes being 1 hour in duration.

and

$$\frac{\partial \chi}{\partial C_{\text{storage}}^{\text{power}}} = \frac{\frac{\partial R_{\text{total}}}{\partial \dot{E}_{\text{max}}} \cdot \frac{d\dot{E}_{\text{max}}}{dC_{\text{storage}}^{\text{power}}} + \frac{\partial R_{\text{total}}}{\partial h} \cdot \frac{dh}{dC_{\text{storage}}^{\text{power}}}}{\gamma(C_{\text{gen}} + \dot{E}_{\text{max}}(C_{\text{storage}}^{\text{power}} + hC_{\text{storage}}^{\text{energy}}))} \cdot \frac{R_{\text{total}} \left( \gamma \left( \frac{d\dot{E}_{\text{max}}}{dC_{\text{storage}}^{\text{power}}} C_{\text{storage}}^{\text{power}} + \left( \frac{d\dot{E}_{\text{max}}}{dC_{\text{storage}}^{\text{power}}} h + \frac{dh}{dC_{\text{storage}}^{\text{power}}} \dot{E}_{\text{max}} \right) C_{\text{storage}}^{\text{energy}} + \dot{E}_{\text{max}} \right)}{\left( \gamma(C_{\text{gen}} + \dot{E}_{\text{max}}(C_{\text{storage}}^{\text{power}} + hC_{\text{storage}}^{\text{energy}})) \right)^2}. \quad (3.5)$$

For large regions of the cost space, where the optimal size of storage is constant for a range of storage power and energy capacity cost intensities, we make the following simplifying assumptions:

$$\frac{dh}{dC_{\text{storage}}^{\text{energy}}} = 0 \qquad \frac{d\dot{E}_{\text{max}}}{dC_{\text{storage}}^{\text{energy}}} = 0 \qquad (3.6a)$$

$$\frac{dh}{dC_{\text{storage}}^{\text{power}}} = 0 \qquad \frac{d\dot{E}_{\text{max}}}{dC_{\text{storage}}^{\text{power}}} = 0. \qquad (3.6b)$$

Under these conditions, the partial derivatives of  $\chi$  simplify to:

$$\frac{\partial \chi}{\partial C_{\text{storage}}^{\text{energy}}} = \frac{-R_{\text{total}} \gamma \dot{E}_{\text{max}} h}{\left( \gamma (C_{\text{gen}} + \dot{E}_{\text{max}} (C_{\text{storage}}^{\text{power}} + h C_{\text{storage}}^{\text{energy}})) \right)^2} \qquad (3.7)$$

and

$$\frac{\partial \chi}{\partial C_{\text{storage}}^{\text{power}}} = \frac{-R_{\text{total}} \gamma \dot{E}_{\text{max}}}{\left( \gamma (C_{\text{gen}} + \dot{E}_{\text{max}} (C_{\text{storage}}^{\text{power}} + h C_{\text{storage}}^{\text{energy}})) \right)^2}. \qquad (3.8)$$

The ratio of which reduces simply to  $h$ , the optimal duration of storage for  $\chi_{\text{max}}$  at any given pair of cost intensities. This finding matches a simple unit analysis of the slopes of the iso- $\chi$  lines that shows the slopes have units of hours.

### **Comparing storage value determinants across locations and resources.**

Here we use the determinants we uncovered previously to explain the differences in storage value seen in Figure 3-2. Storage value differs across location, but the relative value of one optimal cost structure to another is similar across locations. We demonstrate why storage value thresholds occur at lower costs in Massachusetts and Denmark than in California and Texas. We demonstrate similarities in the distribution of the duration of price spike events that explain the slopes of the iso- $\chi$  lines in the U.S., panels e) through l) of Figure 3-2. We further explain why in panels

a) through d) we see that for East and West Denmark, the iso- $\chi$  slopes are slightly steeper.

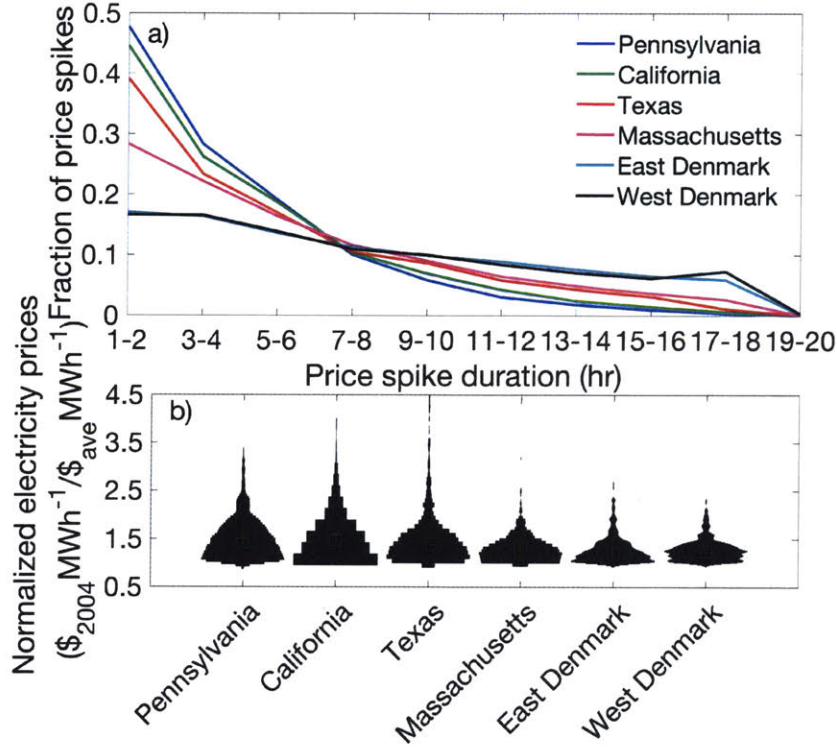


Figure 3-8: Distributions of the duration of price spike events (a) and price spike amplitudes (b) supporting the explanation of storage value. In panel a), the distribution of duration of price spike events shows that the shape of the distribution is similar across the four U.S. locations but flatter in Denmark, which has a much higher relative percentage of longer duration price spike events. Violin plots for the price spike amplitudes (b) show that price spikes are lower in Denmark and Massachusetts than in the other U.S. locations. Price spike amplitudes are shown normalized to the mean of the day in which the price spike occurred. Additionally, price spikes occur less frequently in Denmark, with roughly 590 price spikes per year, as opposed to an average of 940 per year in the U.S., see Table 3.5. Both features further explain the location of the storage cost thresholds in Figure 3-2.

Price spike frequency, amplitude, and resource capacity factor differ across locations, leading to differences in the location of the value thresholds. Real prices vary more freely than we allowed in our artificial price time series simulations, but we can

Table 3.5: Number of price spikes in 2004 for each location.

Location	Number of price spikes in 2004
East Denmark	583
West Denmark	596
California	1050
Massachusetts	763
Pennsylvania	1098
Texas	847

still see relevant features which drive the value of storage. In Figure 3-8 panel b) we show the distributions of the amplitudes of price spikes for each location. Price spike amplitudes are shown normalized to the mean price of the day in which the price spike occurred. In Table 3.5 and Figure 3-8, we find that Massachusetts has the lowest amplitude of price spikes for U.S. locations and that Texas has both high amplitude and frequent price spikes. Danish price spikes are lower than in the U.S. on average and there are 30% fewer price spikes in Denmark. Both the lower amplitude and lower frequency of price spikes in Denmark may help explain the lower value of storage in this location.

Distributions of the durations of price spike events are similar across the four U.S. locations. We see in Figure 3-8 panel a) that the fraction of price spikes of a given duration fall consistently as duration increases for each of the U.S. locations. Furthermore, we see that for both East and West Denmark the distribution of the duration of price spike events is much flatter. The fraction of price spike events with durations longer than 1-2 hours is much higher in Denmark than in the U.S. locations. This helps explain why the optimal duration of storage is longer for any pair of storage and energy capacity cost intensities in West and East Denmark,

i.e., why the iso- $\chi$  slope is steeper. Steeper iso- $\chi$  contours indicate higher value for low energy cost storage technologies. Example technologies with this cost structure are pumped hydro storage, compressed air energy storage, and most flow battery chemistries<sup>61</sup>.

### 3.4 Conclusions

Storage can add value to a wind or solar power plant through energy arbitrage, or charging during periods of low price for later resale at times of higher price. The value that storage can provide differs across location and generation technology. However, in the U.S. it was found that the preferred technology cost structure in one location was also preferred in other locations. Here we analyzed features of the electricity price dynamics and resource availability to explain these results.

We find that storage adds more value in locations with more frequent and higher amplitude price spikes, and it is natural to ask how these determinants might change over time. Furthermore, storage is more valuable when there is a mismatch between times of resource availability and periods of high prices. Some studies have suggested that increased renewables penetration may lead to negatively correlated prices and resources<sup>43,48</sup>, and we have presented a simplified model of this phenomenon here. However, additional research on how increased renewables penetration and storage adoption will endogenously impact future prices would help us understand how storage value may change under different conditions.

The selection of one preferred technology over another depends on the value each provides, and as the duration of price spike events increases, low energy cost technologies are increasingly preferred relative to other technologies. Locations with more long duration price spike events favor technologies like pumped hydro, compressed

air, and flow batteries, all of which have cost structures with very low energy to power capacity cost ratios<sup>12,14,17,61</sup>. Price spike duration may be a function of wind penetration, where long unforeseen resource shortages can be common. Denmark has a higher wind penetration than any of the locations studied in the U.S., supporting this hypothesis<sup>118</sup>. More evidence is necessary to pin down these effects. Market features and how they change the determinants found here is a subject of ongoing research.

Storage can add value to renewables through other use contexts in addition to the energy arbitrage function analyzed here. Revenue stacking from other value streams, such as frequency regulation and forward capacity markets, may be possible for grid-scale storage<sup>1,47</sup>. For example, PJM and ISONE have forward capacity markets where renewables with storage may be expected to earn additional revenue<sup>54,84</sup>. Determining features that impact storage value for these other use contexts and how they complement the determinants found here are subjects for future research.

The results presented here highlight features of the electricity prices and resource availability that drive storage value for wind and solar energy arbitrage. The results can be used to inform expectations of storage value in other locations, based on the electricity price and resource profiles. Furthermore, storage value can be estimated for future scenarios with changes to the determinants found here. By informing future storage value estimates, we can guide research and investment decisions to efficiently develop these technologies, thereby helping to facilitate further adoption of wind and solar. Increasing wind and solar adoption would allow these technologies to play a significant role in climate change mitigation.

## Chapter 4

# Impact of forecasting uncertainty on the value of storage for renewable energy arbitrage

*Energy storage can increase the revenue of wind and solar power plants through energy arbitrage. If storage costs are sufficiently low, this added revenue can outweigh the additional cost of adding storage, thereby increasing the value of the power plant. The conditions under which storage can add value to solar and wind have been studied in earlier research under the assumption of perfect foresight, where the optimal storage size and operation is solved for with knowledge of the future prices and renewable energy resource availability. But how does uncertainty about the future affect the value of storage for wind and solar energy arbitrage? In this work, we develop a new decision rule for operation when future prices and resource availability are unknown.*

---

A version of this chapter is in preparation for publication with co-author Jessika E. Trancik<sup>71</sup>: Joshua M. Mueller and Jessika E. Trancik. Impact of forecasting uncertainty on the value of storage for renewable energy arbitrage. *In preparation.*

*The rule takes into account how storage would be operated under perfect foresight for some period of time in the past, for which data is available. The simple rule we develop for storage operation is able to capture at least 80% of the value that would be expected under perfect foresight, and improves upon several existing heuristics.*

## 4.1 Introduction

Rapidly falling capital costs<sup>60,106</sup>, zero direct carbon emissions<sup>7</sup>, and flexibility in installation scale all contribute to the increasing penetration of wind and solar energy in the U.S. electricity mix<sup>107</sup>. Further contributing to wind and solar growth are U.S. government policies supporting renewables adoption. These policies occur at both the state and federal level, with the investment tax credit for wind and solar being an example of a federal incentive<sup>42,51</sup>. Despite the many government incentives supporting renewables adoption, continued, self-sustained, rapid growth in these technologies is required to reach levels that can help meet climate change mitigation goals<sup>12,106</sup>. Low-cost storage can play a pivotal role in converting intermittent renewables into dispatchable power plants able to provide electricity on demand<sup>1</sup>. The ability to sell electricity when most profitable increases the attractiveness of these technologies.

Storage with renewables may be profitable for some technologies and locations, but there is little consensus on how much value is reasonably achievable<sup>21,64,98,99,113</sup>. For example, optimally sized and operated storage has been shown to provide value to wind and solar power plants in some locations today, by increasing their profitability through shifting generation to periods of high prices<sup>12,70</sup>. However, these analyses often assume perfect foresight of electricity prices and resource availability. How much does uncertainty about the future affect the value of using storage for renewable energy arbitrage? We begin to address this question here by examining

the effectiveness of various forecasting approaches.

Several heuristics have been proposed for determining the operation of storage when future prices and wind or solar resource availability are unknown. These heuristics include methods based on previous optimal operation and those that schedule operation based on time of day<sup>21,44,64,99</sup>. We examine these approaches and also develop our own decision rule.

In addition to decisions about the operation of storage, one must also decide how to size storage. Appropriate sizing of storage, in terms of power and energy capacities, depends on the use context and the location being studied<sup>8,18,25,62,121</sup>. We examine simple rules for this as well, focusing on a use case where storage is constrained to discharging electricity from solar or wind plants, as might be expected under carbon-emissions-constraining policies.

## 4.2 Methods

We investigate the impact of uncertainty on the value of storage for renewable energy arbitrage in order to quantify the value lost due to forecasting errors. We quantify the cost, or lost value, of forecasting errors by developing a rule that determines how a storage system should operate based on current and historical prices. We compare the results of our decision rule to other heuristics for storage operation absent perfect foresight. Finally, we develop two new methods for sizing storage facilities for renewable energy arbitrage.

**Site selection.** Historical electricity prices and wind and solar resource availability were obtained for four U.S. locations: Palm Springs, CA; Plymouth, MA; Altoona, PA; and McCamey, TX. Data for real-time (hourly) locational marginal pricing was

obtained for the years 2004-2005 as available from the CAISO<sup>13</sup>, ISO New England<sup>54</sup>, PJM<sup>84</sup>, and ERCOT<sup>33</sup>. These prices were converted to 2004 USD using the GDP deflator<sup>119</sup>. Price dynamics are depicted in Figure 4-1. Training data sets use 2004 data, while the test data set uses the remainder of the time series (2005). We use 2004 prices and resource data as previous studies have found these to give conservative (low) estimates for the value of storage<sup>12</sup>. To simulate the performance of a hypothetical wind turbine or solar array, local windspeed and solar insolation data was obtained from the Eastern and Western National Wind Integration Datasets and the National Solar Radiation Database<sup>72</sup>. We then computed the time dependent output per MW installed using published performance data for a Vestas V90 3 MW wind turbine which aligns to face the wind<sup>112</sup> and a static photovoltaic system that reaches its maximum output when exposed to an insolation of 1 kW/ m<sup>2</sup> (corresponding to standard test conditions (STC)).

**Heuristics from the literature.** Here we describe how we developed alternative decision rules from heuristics published in the literature. For all methods, storage is only charged from renewables. Each method is applied to 40 combinations of storage power capacity and duration constraints for each of the 4 locations and 2 resources, equaling 1280 total analyses.

We note that the methods discussed below were not originally designed for renewable energy arbitrage<sup>64,99</sup> nor was storage constrained in either model to charge only from intermittent renewables. Studies constraining storage charging from renewables have focused on other use contexts and have not considered storage power capacities larger than the generation capacity of wind or solar nor have they optimized storage operation to maximize value<sup>26,40</sup>. To our knowledge, this is the first paper to compare methods of maximizing storage value when storage charging is constrained to

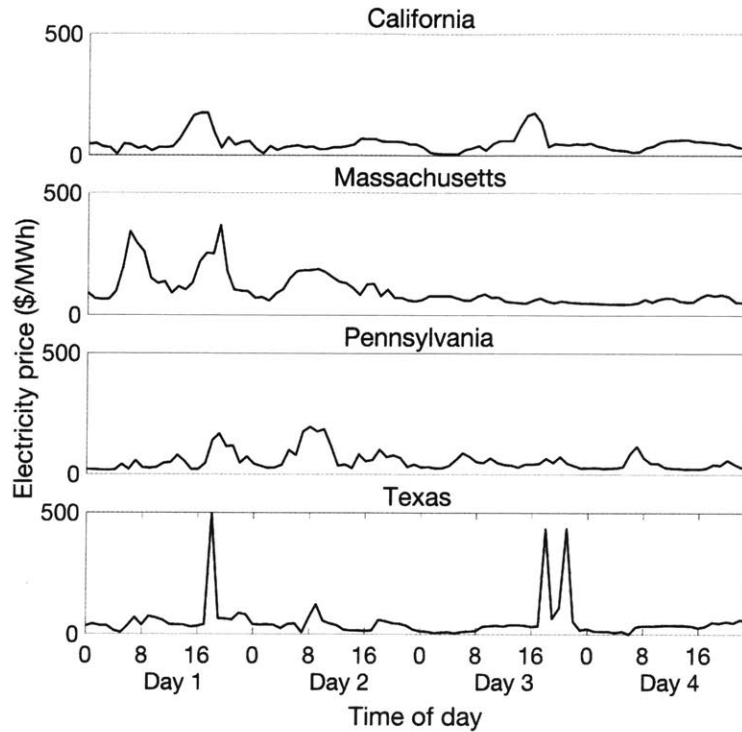


Figure 4-1: Hourly electricity prices for a selection of four days in 2004 for each location studied. Nodal locational marginal prices are used in California, Massachusetts, and Pennsylvania, while zonal locational marginal prices are used in Texas. Different days are used for each location. The days selected were chosen to demonstrate similarities in price spike occurrence, e.g., price spikes in the afternoon of Day 1, and price spike dynamics, e.g. price spikes of varying duration occurring at any hour of the day.

times of wind or solar generation.

*Time-based heuristics.* Time-based heuristics charge storage during all hours except those four during which storage is set to discharge. We compare three time-based heuristics discharging during the periods 14:00-18:00, 16:00-20:00, and during the four hours which had the highest average price over the course of a year. The method using the four hours with the highest average price for a location is based on 2004 prices and the four hours are not a consecutive window. If renewables are

generating, storage is not full, and the time is outside the discharging window, then storage is charged. If storage is full, any renewables generation is sold directly to the grid.

*Sioshansi's backcast.* The backcast method, as proposed by Sioshansi *et al.* (2009)<sup>99</sup> uses a previous optimal storage operation schedule based on perfect foresight to direct the current operation of storage. We determine the optimal operation of storage based on Equations (4.2). We then use this schedule to charge and discharge storage each hour for the subsequent two week period, subject to energy and power capacity constraints. For example, storage operation at 3 p.m. on the 17th of the month is determined based on the optimal operation of storage at 3 p.m. on the 3rd of the month.

**Developing the decision rule.** This section lays out the steps in developing the decision rule. First, we develop a normalization of electricity prices which allows us to present the hourly price as a ratio of the current price to a moving average of the previous peak prices. Next, storage operation is modeled with perfect foresight and non-normalized prices to determine the optimal charge and discharge times for each storage system size for the full year of training data. We then analyze the optimal hourly operation of storage as a function of the normalized price in that hour. Finally, we select a normalized price,  $\rho_{\text{rule}}$ , which will serve as the threshold above which our decision rule directs storage to discharge. We seek a value of  $\rho_{\text{rule}}$  that maximizes expected revenue of the combined renewables and storage system.

*Normalizing electricity prices.* We compare normalized prices as a means of incorporating recent historical price information. Prices are normalized by taking

the ratio of the current hourly price to the ten-day moving average of the daily peak electricity price, where the daily peak electricity price is itself an average over four hours (two hours before the peak hourly price and one hour after):

$$\rho_{nd} = \frac{P_{nd}}{\sum_{j=-10}^{-1} \sum_{i=\max-2}^{\max+1} P_{ij} / 40} \quad (4.1)$$

The subscript notation  $n$  indicates the hour of the day and the subscript  $d$  the day. The ‘max’ used in the internal summation indicates that the selected hour of each day is the hour of highest price for that day. We denote prices normalized in this manner as  $\rho$  and hourly prices in \$/MWh as  $P$ . The two summations have a total count of 40 hourly values, hence the division by 40 to find the ten-day moving average.

Normalization parameters of ten days and four hours (two hours before and one hour after) were selected to produce the highest revenue and are supported by analysis of electricity prices and optimal storage operation. The four hour peak period is selected based on the maximum storage duration investigated. Previous work has shown that storage duration of four hours or less generates the most value today<sup>12</sup>. Comparisons of current price to historical prices were performed for moving average windows sized from three to fourteen days. Ten days was selected as the window which maximized the expected revenue when testing the decision rule. Additionally, an analysis of the time between price spikes showed that across all locations, 80% of spikes occurred within ten days of a previous spike. This is true for all spikes where the price during the spike is three times the daily mean or less. (Here we define a price spike as a price greater than the daily mean.) Because storage discharges during times of high prices, this serves as an indication that storage is cycling within this ten day window and thus older price information would not be indicative of the value of the energy currently in storage.

*Optimal storage operation and capacity.* Hourly charging and discharging of the storage system, and the direct sale of solar and wind generated electricity were optimized to achieve maximum revenue. This is performed for a hypothetical hybrid storage and generation plant at each site, given the 2004 electricity price and energy resource availability, subject to system power and energy constraints. We use a model of storage operation for renewable energy arbitrage first developed by Braff *et al.* (2016)<sup>12</sup>. The optimization was performed in three week intervals over the course of a year, with one week overlap between each interval to prevent discontinuities. An offset is included in the energy constraint for each optimization period to account for the amount of energy stored in the system at the beginning of the optimization period. The charge rate was constrained by either the real-time output of the generation resource or the power capacity, and the energy available for discharge was adjusted by a roundtrip efficiency of 90%. In order to reduce the computational expense of the optimization, the simulation considered charging and discharging separately so that a linear solution technique could be employed.

The optimization routine for each three week segment ( $N = 504$  hours) can be expressed in terms of the real time price  $P(t) = P_{nd}$ , the generation profile  $x_{generation}(t)$ , storage roundtrip efficiency  $\eta$ , peak power  $\dot{E}_{max}$ , and duration  $h$  as:

$$\begin{aligned}
R_{\text{total}} = \max\left(\sum_{t=0}^N P(t)(x_{\text{generation}}(t) + x_{\text{discharge}}(t) - x_{\text{charge}}(t)/\eta)\right) \\
\text{subject to:} \\
0 \leq x_{\text{discharge}}(t) \leq \dot{E}_{\text{max}} \\
0 \leq x_{\text{charge}}(t) \leq \min(\eta x_{\text{generation}}(t), \eta \dot{E}_{\text{max}}) \\
0 \leq \sum_{t=0}^N (x_{\text{charge}}(t) - x_{\text{discharge}}(t)) \leq h \dot{E}_{\text{max}} \quad (4.2)
\end{aligned}$$

*Analysis of perfect foresight operation.* Our decision rule is informed by the optimal operation of storage under perfect foresight. The decision to charge, discharge, or generate directly to the grid, under perfect foresight, is a function of both past and future electricity prices and resource availability. With no foresight, signals for storage operation can only include real-time and historical data. To inform our decision rule we frame the hourly optimal operation of storage behavior as though it is solely a function of the normalized price,  $\rho_{nd}$ , thereby including both real-time and historical information.

Optimal storage operation presented as a function of normalized prices provides some insight into the challenges being addressed by our decision rule. Panel A) of Figure 4-3 shows probability distributions of the operation (charging, discharging, or generating straight to the grid) of storage,  $2 \text{ kW}/\text{kW}_{\text{gen}}$  for 1 hour of duration, with wind in Texas based on the training data. Storage power capacities are reported in units relative to the installed generation capacity of wind or solar. We see that the general location of each distribution matches expectations, with the charging occurring at lower prices and the discharging occurring at higher prices. However,

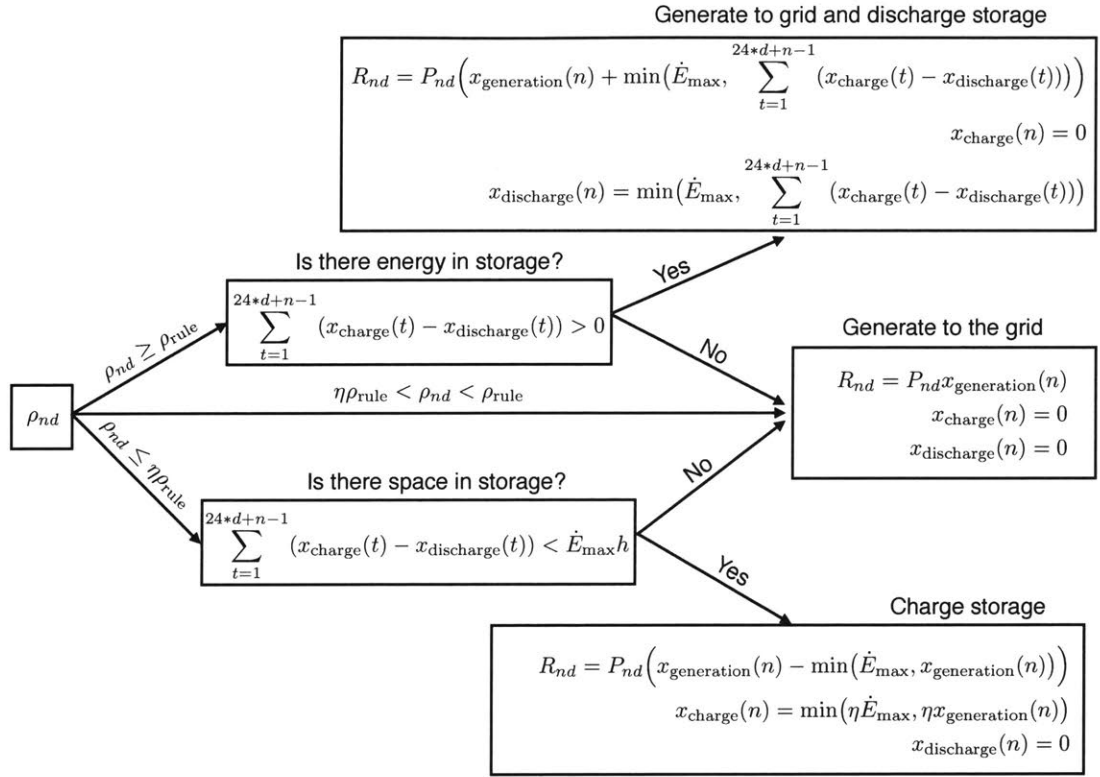


Figure 4-2: Model diagram of storage operation using our new decision rule. The normalized hourly price,  $\rho_{nd}$ , is compared to the price rule,  $\rho_{\text{rule}}$ , the development of which is shown in Figure 4-3. If the price is greater than the decision rule (upper path), the wind or solar plant generates straight to the grid and if there is energy in storage, storage discharges. If the price is less than the efficiency,  $\eta$ , times the  $\rho_{\text{rule}}$  (lower path), then storage charges, unless it is already at full energy capacity in which case any excess is generated to straight to the grid. For all other prices (center path), the wind or solar plant generates straight to the grid and storage neither charges nor discharges. The other two decision rule sets, the time based rules and the backcast method, use the same analysis of whether there is energy or space in storage, only changing the rules for choosing the initial path directing storage operation.

there is also significant overlap in the three distributions, indicating that the normalized price in any given hour is only one driver in determining optimal storage operation. Because of these overlapping distributions, we expect the decision rule to generate less revenue than the optimally operated storage system for all storage

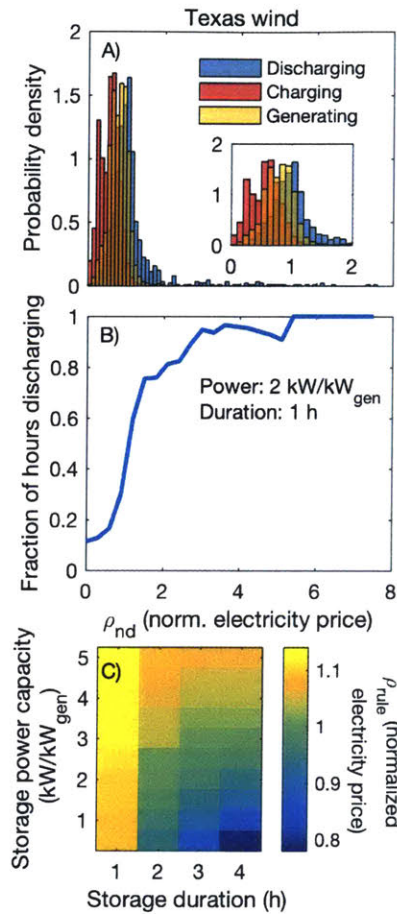


Figure 4-3: Depiction of the method of deriving  $\rho_{rule}$  using results for wind in Texas. Hourly prices,  $\rho_{nd}$ , are normalized based on a ten-day moving average of the daily peak price and surrounding four hours. Panel A) shows the probability distribution histograms for each type of storage and renewables hourly operation (discharging, charging, and generating only) as a function of the normalized price. Panel B) shows, as a function of normalized price, the percent of time storage was discharging. Panel B) depicts the relative size of the discharging histogram at each normalized price to the other histograms in panel A). Panels A) and B) are shown for a specific storage size, of 2 kW/kW<sub>gen</sub> and 1 hour. Panel C) shows  $\rho_{rule}$  for each storage size studied for wind in Texas.  $\rho_{rule}$  is the normalized price above which optimally operated storage discharged at least 50% of the time.

capacities. Each combination of storage power capacity and duration has different discharging, charging, and generating-only distributions, supporting the modeling

choice that the optimal and the price-directed behavior of storage are functions of the storage capacities.

*Selecting a  $\rho_{rule}$ .* There is a different threshold normalized price,  $\rho_{rule}$ , for each storage capacity combination, location, and renewables resource. This is because there is a different operating behavior of storage for each storage size, resource, and location. (For example, differences in storage operation in Texas for all studied sizes and both resources are shown in Figure 4-4.) However, we develop a simple and consistent method to determine the  $\rho_{rule}$  based on the fraction of hours the optimally operated storage system discharged over a year for a given  $\rho_{nd}$ , based on the training data set. Figure 4-3 panel B) shows the fraction of time storage is discharging as a function of normalized price. Each storage system size, system location, and renewables resource produce different curves for panel B). To have a consistent method of determining  $\rho_{rule}$  we select the  $\rho_{rule}$  based on the same fraction of hours discharging (vertical axis value). We analyzed a range of discharge probabilities and selected each associated price as a candidate  $\rho_{rule}$  for each storage size, generation technology, and location.

The  $\rho_{rule}$  and above at which storage discharges when operated under our decision rule is chosen to increase the expected revenue,  $R_{expected}$ . The  $R_{expected}$  is not the theoretical maximum as we consider only a small set of possible decision parameters. The  $R_{expected}$  is the sum of hourly revenue,  $R_{nd}$ , for one year when storage is operated according to the decision rule. (See Figure 4-2, with 2005 electricity price and resource availability input data.) We use price data from a different year as test data to evaluate our rule. For our rule, storage will discharge when the current normalized price is equal to or greater than the normalized price at which storage, when optimally operated under perfect foresight for 2004 prices and resource availability

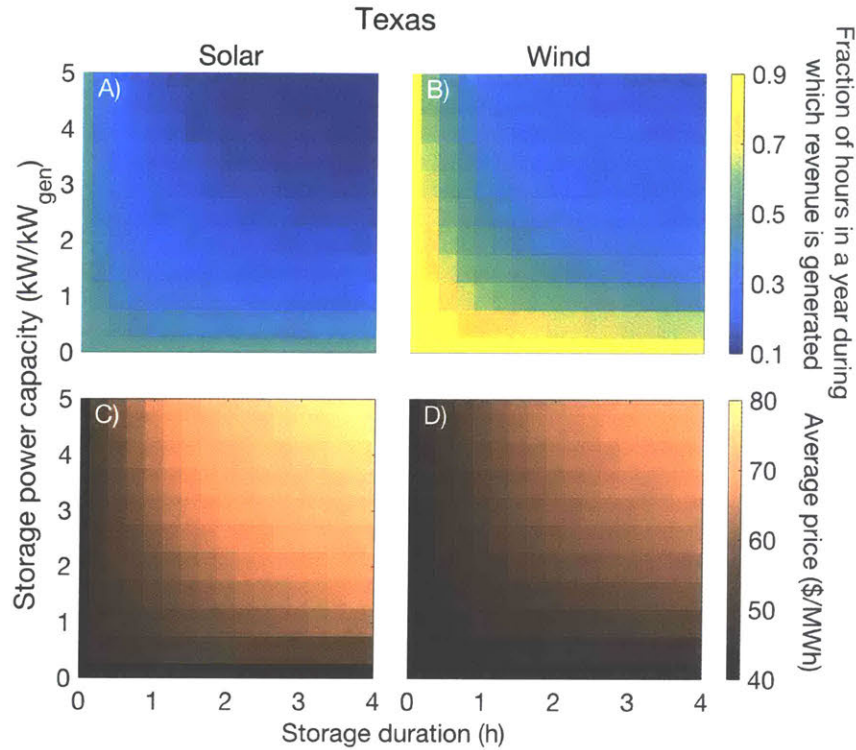


Figure 4-4: Impact of initial storage capacity decisions on storage operation and average price of generation and discharge for wind and solar in Texas. Storage duration is presented on the horizontal axis and storage power capacity, relative to the generation capacity, is presented on the vertical axis for each panel. Each cell depicts a single storage capacity combination. Panels A) and B) show the fraction of the year in which wind or solar with storage is generating or discharging as a function of the storage system capacity. As the storage size increases, the number of hours in which the hybrid system is generating decrease, i.e., more energy is sold during fewer hours. Panels C) and D) show that as storage size increases, the average price at which electricity is sold increases. In order to provide value, storage of larger system sizes must be able to capture the highest price spikes, generating for more revenue during fewer hours of the year. California, Massachusetts, and Pennsylvania show similar behaviors.

data, discharged 50% of the time (over the year and not necessarily in each ten day period). We show the  $\rho_{\text{rule}}$  at which we discharge in panel C) of Figure 4-3 for all combinations of storage power and energy capacity examined. The values in panel C) show along the z-axis the normalized price at which storage discharged 50% of the time.

$\rho_{\text{rule}} = \rho|_{\text{normalized price at which storage discharged 50\% of the time}}$

Discharge:  $\rho_{nd} \geq \rho_{\text{rule}}$  AND there is energy in storage

Charge:  $\rho_{nd} \leq \eta\rho_{\text{rule}}$  AND there is space in storage

Generate to grid: Otherwise

$\eta$  is the round-trip efficiency and  $\rho_{nd}$  is the hourly price (normalized). The value of  $\rho_{\text{rule}}$  is reduced by the roundtrip efficiency to determine the charge threshold. This accounts for the value lost in energy conversion.

**Selecting a storage size.** We optimize the power and energy capacity of storage by selecting those sizes of storage which maximize  $\chi$ , the annual revenue over the annualized cost for all combinations of storage power capacity costs ( $C_{\text{storage}}^{\text{power}}$ ) and energy capacity costs ( $C_{\text{storage}}^{\text{energy}}$ ), Equation (4.3). This technique was first developed by Braff *et al.* (2016)<sup>12</sup>. Plant overnight construction costs are given as the sum of the storage and generation costs per unit rated power of installed solar or wind generation ( $C_{\text{gen}} + \dot{E}_{\text{max}}(C_{\text{storage}}^{\text{power}} + hC_{\text{storage}}^{\text{energy}})$ ). To determine the annualized plant capital costs, the overnight construction costs are multiplied by a capital recovery factor,  $CRF(i, y)$ , defined as  $CRF(i, y) = \frac{i(1+i)^y}{(1+i)^y - 1}$ , with  $y = 20$  years and  $i = 5\%$ <sup>50</sup>.

We select storage capacities that maximize  $\chi$  for  $R_{\text{total}}$ , which is the annual revenue when storage is operated under perfect foresight based on the training dataset. We denote the ‘perfect foresight sized’ storage power capacity as  $\dot{E}_{\text{max}}^{\text{opt}}$  and the ‘perfect foresight sized’ storage duration as  $h^{\text{opt}}$ . Storage power capacity and duration

were simulated in increments of 1/2 hours and 1/2  $W_{\text{storage}}/W_{\text{generation}}$ .

$$\chi_{\text{max}} = \frac{R_{\text{total}}}{CRF(C_{\text{gen}} + \dot{E}_{\text{max}}^{\text{opt}}(C_{\text{storage}}^{\text{power}} + h^{\text{opt}}C_{\text{storage}}^{\text{energy}}))}. \quad (4.3)$$

We then analyze two methods of storage sizing. In the ‘perfect foresight sized’, storage capacities are selected as  $\dot{E}_{\text{max}}^{\text{opt}}$ , the optimal storage power capacity, and  $h^{\text{opt}}$ , the optimal storage duration. Storage is therefore sized based on the revenue expected under perfect foresight. We then determine  $\chi_{\text{new}}$  by taking the expected annual revenue operating the decision rule,  $R_{\text{expected}}$ , on the test data set, 2005 prices and resource availability data, and dividing this by the annualized cost of storage, using the previously determined storage capacities, Equation (4.4).  $R_{\text{expected}}$  is a variable which is a function of  $\dot{E}_{\text{max}}^{\text{opt}}$  and  $h^{\text{opt}}$  in Equation (4.4).

$$\text{Perfect foresight sized: } \chi_{\text{new}} = \frac{R_{\text{expected}}}{CRF(C_{\text{gen}} + \dot{E}_{\text{max}}^{\text{opt}}(C_{\text{storage}}^{\text{power}} + h^{\text{opt}}C_{\text{storage}}^{\text{energy}}))}. \quad (4.4)$$

$$\text{Decision rule sized: } \chi_{\text{new}} = \frac{R_{\text{expected}}}{CRF(C_{\text{gen}} + \dot{E}_{\text{max}}(C_{\text{storage}}^{\text{power}} + hC_{\text{storage}}^{\text{energy}}))}. \quad (4.5)$$

In the second method of determining storage size, ‘decision rule sized’, the storage capacity is sized to maximize system value based on the expected revenue as determined by a decision rule operating heuristic, Equation (4.5). This new revenue will be lower than the  $R_{\text{total}}$  because it includes the cost of forecasting errors. This is similar to the original  $\chi_{\text{max}}$  formulation, Equation (4.3), but instead first replacing

$R_{\text{total}}$  with  $R_{\text{expected}}$  and then selecting storage power and energy capacities which maximize this new benefit cost ratio. Here,  $R_{\text{expected}}$  is a variable determined by the new smaller sizes of storage selected. Storage sizes under this second, decision-rule sized, formulation tend to be smaller than under perfect foresight as they are based on maximizing a ratio with a smaller numerator.

### 4.3 Results

**Current techniques.** We first recreate several standard techniques in the literature for operating storage under limited foresight<sup>21,64,99</sup>. One such technique is a backcasting method in which the operational schedule for a two-week period is based on the optimal perfect foresight operation during the previous two-week period<sup>99</sup>. A benefit of this backcasting method is that it captures changes throughout the year, for example due to seasons, by basing the operational schedule on only recent optimal behavior. (This technique can be easily incorporated our model of optimal storage operation<sup>12</sup>. In our perfect foresight model, we use an overlapping three-week interval. The operation in the first two weeks is determined with consideration of the final week, to ensure storage is not emptied at the end of each two-week period.)

Another class of heuristics bases operational schedules on predetermining certain hours of the day during which storage always discharges<sup>64</sup>. Liu *et al.* (2017)<sup>64</sup> propose a time-based heuristic in which storage discharges from 14:00-18:00 to match expected peak demand and price periods. In addition to this period, we consider two other time-based heuristics. In the first, we discharge between 16:00-20:00 to better match new peak-demand periods<sup>81</sup>. In the second, we consider a time-based heuristic in which the four hours with the highest average historical prices are determined for each location, as seen in Figure 4-5. Storage is then scheduled to discharge only

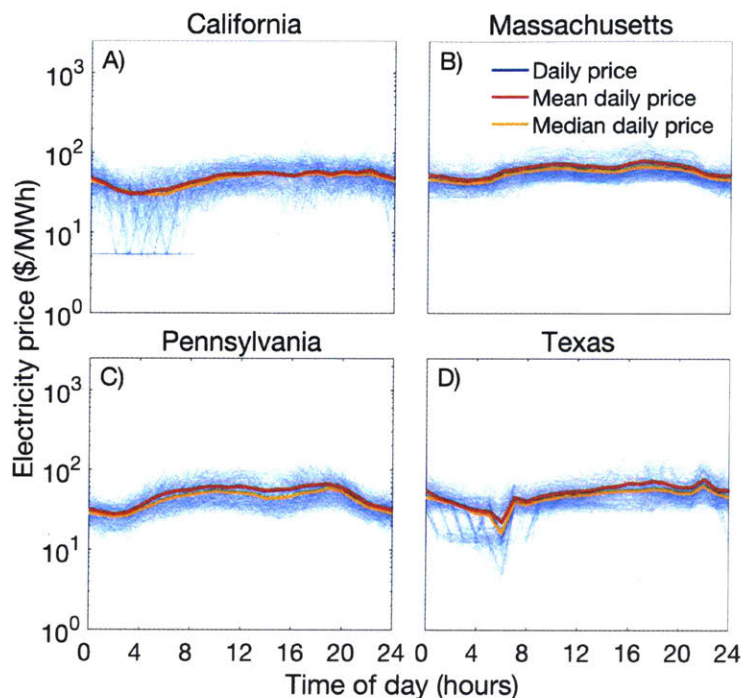


Figure 4-5: Hourly electricity price plotted daily showing the distribution in spot prices across time and location. Each panel shows 8784 data points, plotted as daily hourly prices for 2004. Data is nodal locational marginal price for California, Massachusetts, and Pennsylvania, and zonal locational marginal price for Texas. The horizontal axis shows the hour of the day for each spot market price, while the vertical axis presents the wholesale market price on a logarithmic scale. The red line shows the mean hourly price over the time period. Key features of importance are the highly stochastic nature of price spikes - occurring at all hours of the day in all locations, and the hours with highest average prices. The peak mean times shown here are used in the analysis of storage operation based on hours of highest price. Median daily price is shown in orange, and is always lower than the mean daily price, a feature of the long-tailed electricity price distributions.

during this period.

Out of these existing techniques, we find that the backcasting method routinely outperforms the time-based methods. Of the time-based heuristics, the method based on discharging during the four hours with the highest average prices captures the most revenue. These two methods incorporate the most information about the loca-

tion in which they are applied. For all four methods described, i.e., three time-based methods and the backcasting method, the capacities of storage should be considered in determining the operational strategy. The two best-performing heuristics of those studied above take this information into account, which also explains their better performance. For the time-based methods, storage commences discharging at the beginning of the period and does not commence charging until the end of the period. In practice this means that a storage system with one hour of duration will discharge only during the first hour of the period and the hybrid wind or solar with storage facility will generate directly to the grid for the remainder of the period. For the method based on the highest average historical hourly price, the installed duration of storage determines how many hours are considered for discharging, i.e., a one hour storage facility will only discharge during the hour with the highest average price and will charge during the remaining time. For the backcasting method, the storage system capacity is already included as a constraint in determining the optimal operation during the previous period.

**New decision rule and comparison to others.** Here we present results for a new, price-based decision rule, which uses somewhat different information from past data on optimally operated storage than the rules reviewed above. In the new rule, we select a time period from which historical data is examined and solve for a price threshold above which storage is told to discharge. The details are described above in Methods. The new rule generates more revenue than the other decision rules examined for nearly all storage sizes and locations.

All decision rules examined lead to a loss of power plant revenue due to forecasting errors. In Figure 4-6, we show the percent improvement of the new rule relative to the others examined<sup>64,99</sup>. The price-based decision rule presented here shows a 2-40%

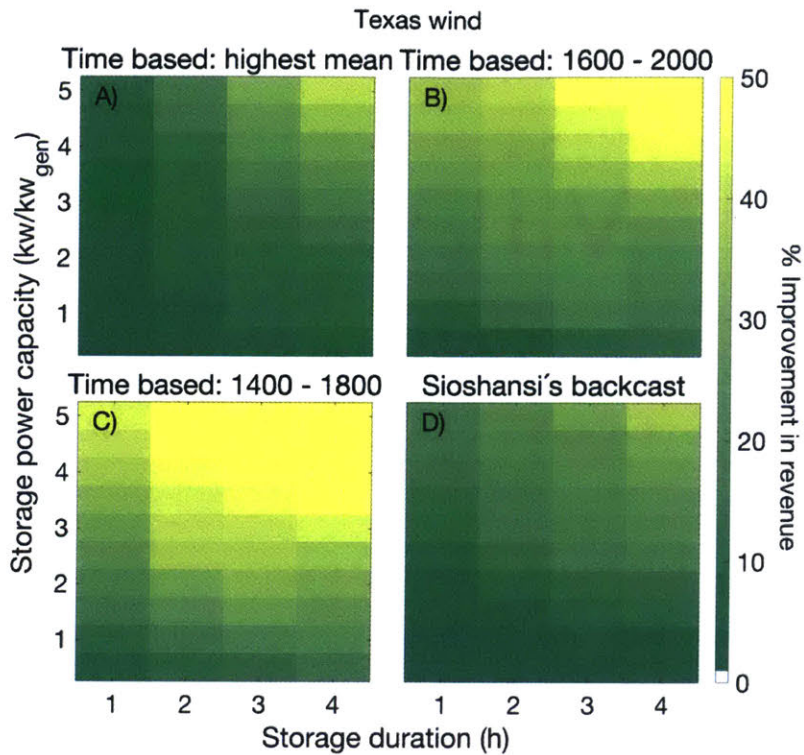


Figure 4-6: Percent improvement of our decision rule over other heuristics presented in the literature<sup>64,99</sup> for wind in Texas. Storage duration is shown on the horizontal axis and power capacity, relative to generation capacity, on the vertical axis, for each panel. Each cell depicts a single storage size (power and energy capacity combination). For each storage size, the percent improvement in revenue of our decision rule over a previously published heuristic is shaded according to the color axis. Panels A), B), and C) present variations of time-based heuristics in which: in A) storage is discharged during the one to four hours (depending on installed storage duration) with the highest average prices (Figure 4-5); in B) storage is discharged between the hours 16:00-20:00 and charged until at capacity otherwise; and in C) storage is discharged between the hours 14:00-18:00 and charged until at capacity otherwise. Panel D) shows the backcast method. Ranges for the percent improvement for other locations are shown in Table 4.1.

improvement over the backcasting method and the method based on the previous day's four hours of highest average price for all storage system sizes for Texas wind. Even greater improvement is seen over the other heuristics from the literature. For almost all 1280 comparisons of storage power capacity, duration, location, renewable resource, the new decision rule improves on the other heuristics, often substantially

(Table 4.1). In the case of 7 storage sizes for Massachusetts wind, other heuristics improve on the revenue generated by the new rule by less than 1%.

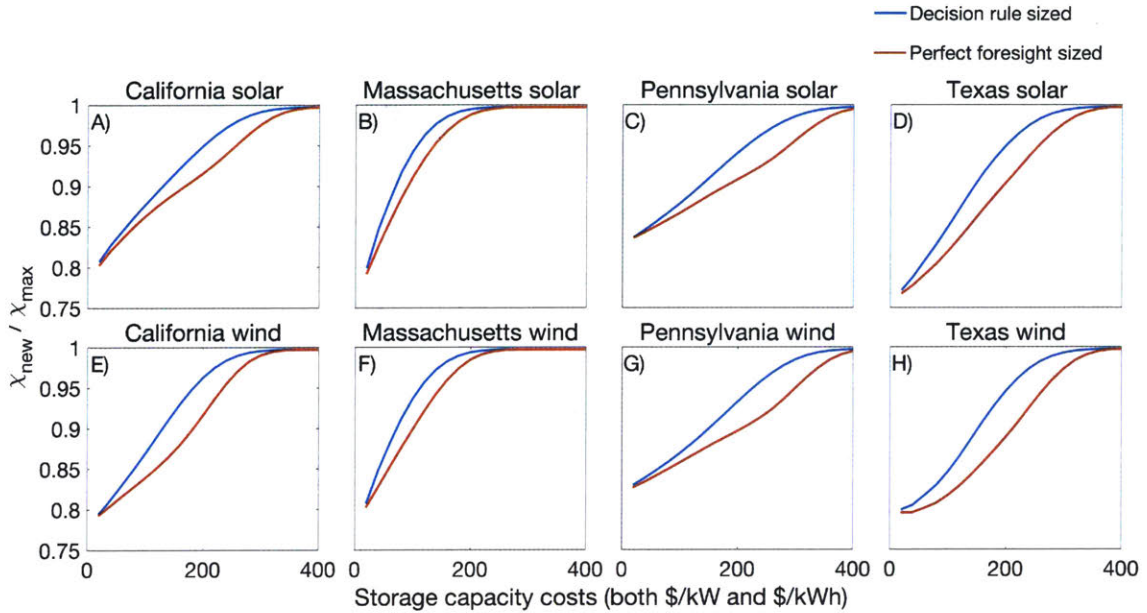


Figure 4-7: Decision rule sized storage captures more value than perfect foresight sized storage. For each location, the blue line compares storage value when sized based on the decision rule to the optimal storage value while the red line shows storage value when sized under perfect foresight relative to the optimal storage value. Both comparisons of value are plotted as a function of the storage power and energy capacity costs along a 45° ray from the origin along which the \$/kW and \$/kWh of storage are equal. Optimal storage value is the  $\chi_{\text{max}}$  under perfect foresight<sup>12</sup>. In both cases, storage revenue is determined through operation based on our decision rule for 2005 price and resource data. Decision rule sized storage captures at least 80% of the value expected under perfect foresight.

Storage of larger capacity captures more revenue by discharging during fewer hours of the year. The price-based decision rule shows the greatest improvement over the other heuristics for these larger storage system sizes, because it delays discharge to be able to take advantage of periods of highest price, though the forecasting errors are greater for larger storage system sizes across all heuristics. Storage of smaller capacities tend to cycle more frequently, and therefore discharge at lower prices (see

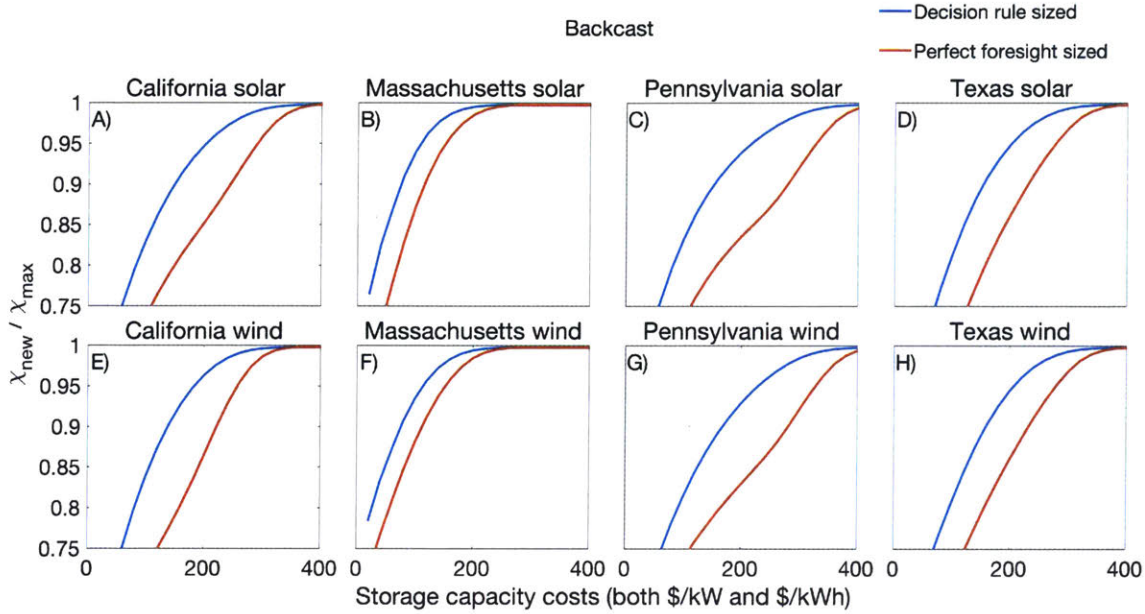


Figure 4-8: Storage value is lower under the backcast method than under the new price-based decision rule developed here. For each location, the blue line compares storage value when sized based on the decision rule (with  $R_{\text{expected}}$  now equal to the annual revenue under the backcast method) to the optimal storage value while the red line shows storage value when sized under perfect foresight relative to the optimal storage value. Both comparisons of value are plotted as a function of the storage power and energy capacity costs along a  $45^\circ$  ray from the origin along which the  $\$/\text{kW}$  and  $\$/\text{kWh}$  of storage are equal. Optimal storage value is the  $\chi_{\text{max}}$  under perfect foresight<sup>12</sup>. In both cases, storage revenue is determined through operation based on Sioshansi’s backcast method (panel D) in Figure 4-6) for 2005 price and resource data. Storage value is lower for all storage costs when compared with Figure 4-7.

panel C) of Figure 4-3).

In addition to a decision about how to operate storage, a decision must be made about how to size storage. This decision can be made based on either the expected revenue under operation of a decision rule, Equation (4.5), or on the optimal revenue under perfect foresight, Equation (4.3). When using the expected revenue under the decision rule, the installed capacities of storage are lower than they would be under perfect foresight. In Figure 4-7 we compare the ratio of  $\chi_{\text{new}}$  (using the expected

Table 4.1: Ranges for percentage improvement in annual revenue (2005 electricity price and resource availability data) for our decision rule over previously suggested heuristics in the literature, presented for each combination of location and resource. Lower values of percent improvement are for smaller storage capacities while the most improvement is for the larger storage sizes. This table presents numerical data for all locations similar to that which can be seen in Figure 4-6 for wind in Texas.

Locaion	Resource	Time-based: highest mean	Time-based: 16:00 - 20:00	Time-based: 14:00 - 18:00	Sioshansi's backcast
California	Solar	2 - 46%	6 - 47%	7 - 43%	4 - 42%
	Wind	3-30%	4 - 50%	4 - 41%	3 - 36%
Massachusetts	Solar	0.3 - 29%	4 - 35%	4 - 30%	1 - 21%
	Wind	-0.9 - 11%	3 - 24%	2 - 32%	-0.2 - 18%
Pennsylvania	Solar	6 - 68%	10 - 68%	9 - 61%	6 - 42%
	Wind	6 - 46%	7 - 77%	7 - 83%	4 - 36%
Texas	Solar	2 - 49%	9 - 56%	8 - 64%	3 - 38%
	Wind	3 - 40%	6 - 55%	6 - 67%	2 - 39%

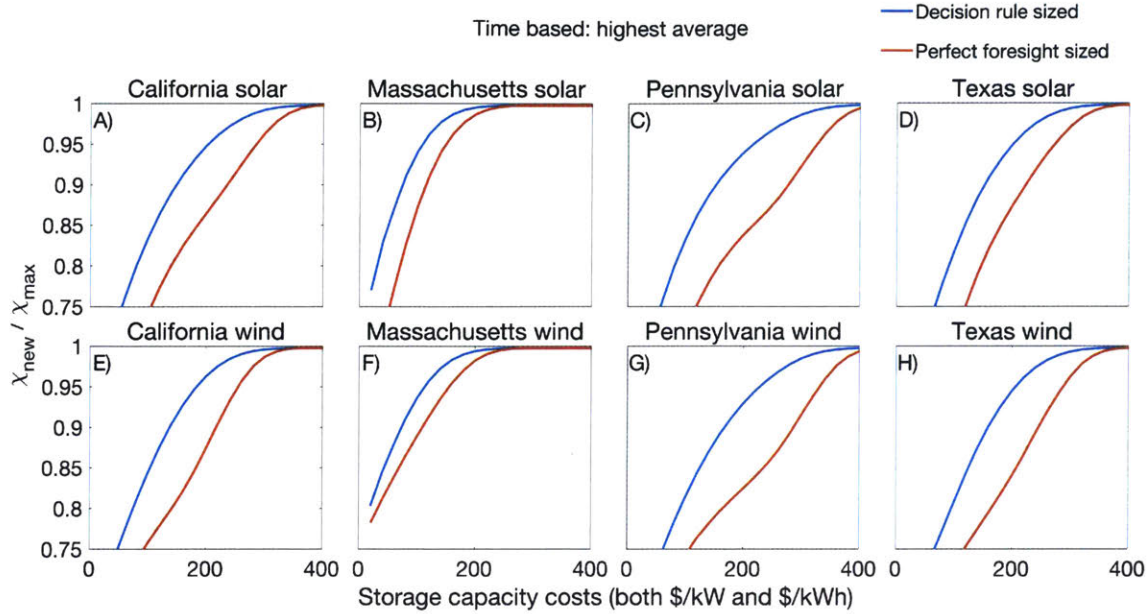


Figure 4-9: Storage value is lower under the time-based methods (shown here is the best performing heuristic, discharging during the hours with the highest average price) than under our new price-based decision rule. For each location, the blue line compares storage value when sized based on the decision rule (with  $R_{\text{expected}}$  now equal to the annual revenue under the time based heuristic with discharging during the hours with the highest average price) to the optimal storage value while the red line shows storage value when sized under perfect foresight relative to the optimal storage value. Both comparisons of value are plotted as a function of the storage power and energy capacity costs along a  $45^\circ$  ray from the origin along which the  $\$/\text{kW}$  and  $\$/\text{kWh}$  of storage are equal. Optimal storage value is the  $\chi_{\text{max}}$  under perfect foresight<sup>12</sup>. In both cases, storage revenue is determined through operation based on time-based method using the hours of highest price (panel A) in Figure 4-6) for 2005 price and resource data. Storage value is lower for all storage costs when compared with Figure 4-7.

revenue for storage sizing) with  $\chi_{\text{max}}$  under perfect foresight. We find that the power plant value is higher when the storage capacity is based on the expected revenue under the decision rule, rather than on the optimal size under perfect foresight. When using the expected revenue under the new decision rule to determine storage sizing, the power plant value ( $\chi_{\text{new}}$ ) captures 80% or more of the value under perfect foresight ( $\chi_{\text{max}}$ ). Finally, storage value is higher under our decision rule than under

the previous heuristics. The  $\chi_{\text{new}}$  is higher because the revenue is higher for almost all storage sizes. This difference in  $\chi_{\text{new}}$  can be seen by comparing similar panels between Figures 4-8 and 4-9 with those in Figure 4-7.

## 4.4 Conclusions

Storage can increase the value of a wind or solar power plant, even when future prices and resource availability are unknown. Previous research on storage value has typically been based on models that assume perfect foresight of future electricity prices and resource availability. Here we ask how much we might expect this value to change given uncertainty about the future. We develop and deploy a new approach to storage operation absent perfect foresight to quantify the cost of forecasting errors. We find that storage can capture 80% or more of the value that would have been expected under perfect foresight.

Our new decision rule is a simple rule incorporating limited information on price and resource availability dynamics, and we might expect storage operation under models with more information incorporated to have greater predictive power than that presented here. In the class of models with more predictive power, we might expect to include those incorporating future weather predictions impacting solar and wind generation and other information relating to future prices and generation. Storage value under these models, for example where the impact of renewables resource availability and existing storage operation are endogenously included in models of future prices, is a subject of further research that can build upon the insights developed here.

The results presented here can be tailored to inform research efforts and government incentives supporting the deployment of wind and solar with storage. The  $\chi_{\text{new}}$

we develop can be used to calculate the storage costs expected to be necessary for wind or solar to be profitable. These updated cost targets can guide research efforts aimed at reducing storage costs. Additionally, government subsidies for storage can be designed around estimates of storage value which include the costs of forecasting errors.

Finally, we note that the estimates of storage value presented here are for the specific use context of energy arbitrage and that other value streams could generate additional revenue. Grid-scale storage can generate revenue by participating in multiple markets, such as frequency regulation markets and forward capacity markets<sup>1,47</sup>. Additional revenue from other value streams would increase the estimates of storage value presented here. Storage operation strategies that maximize value from different revenue streams under uncertainty is the subject of ongoing research.



## Chapter 5

# Energy storage requirements for shaping renewable energy toward grid decarbonization

*Decarbonizing electricity will likely require that low-carbon sources meet energy demand throughout the day and year. Wind and solar are possible low-carbon technology options, but resource variability can limit their effectiveness in meeting demand. Storage can help address this challenge by shaping renewables into desired output profiles. But can storage technologies cost-effectively fulfill this role? Given the diversity of storage technologies, how does one choose among different options? Here, we analyze wind and solar energy with storage to address these questions. We find that storage with low energy capacity costs below an estimated target of \$50/kWh*

---

A version of this chapter is in preparation for publication with co-authors Gonalo D. Pereira, Marco Ferrara, Yet-Ming Chiang, and Jessika E. Trancik<sup>69</sup>: Joshua M. Mueller, Gonalo D. Pereira, Marco Ferrara, Yet-Ming Chiang, and Jessika E. Trancik. Energy storage requirements for shaping renewable energy toward grid decarbonization. *In preparation.*

*could be used to make renewables plants cost-competitive with other on-demand generation technology options in resource abundant locations. Finally, we review storage technology options that could potentially reach the cost targets estimated here, and we highlight how these insights might be used to guide technology development.*

## 5.1 Introduction

Wind and solar energy technologies are two options for generating low-carbon electricity, and the costs of these technologies have dropped in recent decades while their market shares have grown<sup>46,89,107</sup>. In some prospective analyses, these costs continue to fall to levels where the levelized cost of wind and solar electricity (LCOE) drops well below higher-carbon alternatives<sup>67</sup>. However, to allow intermittent generation to meet demand, back-up generation, energy storage, expanded transmission infrastructure, demand-side management, and energy curtailment may be required, which can increase the total costs of electricity<sup>3,27,48,100</sup>.

Among different options for addressing renewables' intermittency, energy storage has certain advantages. Storage can require less coordination among decision-makers than transmission infrastructure expansion. It may allow for greater quantities of electricity to be time-shifted than demand-side management, and could achieve greater carbon emissions reductions than using back-up generators such as natural gas turbines<sup>26</sup>.

However, despite cost declines in recent decades<sup>91</sup>, storage costs remain relatively high. For example, even in a state such as Texas, which has one of the highest wind capacity factors in the U.S., a wind power plant combined with compressed air energy storage (CAES), which has relatively low costs among storage technologies, was found to be economically uncompetitive with combined cycle natural gas plants<sup>40</sup>.

Determining cost targets at which energy storage becomes cost-competitive requires a consideration of storage context of use. In past work, for example, cost targets have been determined for storage performing renewable energy arbitrage, i.e., charging wind or solar at times of low prices for later resale when demand and prices are higher<sup>12</sup>, for today’s electricity supply system. In this work, we focus instead on a potential future supply system that is further dominated by renewables. We estimate the costs of using storage together with wind and solar energy to supply various output profiles, and investigate the features of storage technologies that would be most beneficial. To our knowledge, this is the first paper to address these questions.

We consider output shapes for solar and wind energy power plants that match those observed in current electricity supply systems, based on a premise that guaranteeing these output shapes may allow for low-risk and easy integration of renewables into the generation mix. In current systems, a combination of price signals and generation costs results in a division of generation into distinct grid roles: baseload, intermediate, and peaker power plants<sup>6</sup>. These grid roles are defined by the relationship between fixed and variable costs for dispatchable technologies such that the lowest cost generators meet demand. Technologies with lower variable and higher fixed costs typically operate as baseload plants, amortizing their investment over longer periods of operation, while generation sources with higher variable and low fixed costs operate as peaker plants.

Our analysis accounts for inter- and intra-year variation in the solar and wind resource, and covers several locations with different levels of resource availability. This work builds on studies using data on a single year or a typical year<sup>40,45</sup> by capturing the variations that may occur over a lifetime of a power plant<sup>95,114,118</sup>. Moreover, we consider the effect of combining solar and wind energy in a portfolio

to take advantage of complementarity in the resource availability over time.

We design our study to reflect key differences among energy storage technologies, in order to gain new insight on the cost features of storage that can be most beneficial. We solve for the optimal renewable energy capacity, and energy and power capacities of storage installed for a particular use context by accounting for differences across storage technologies in the capital cost intensities of the power capacity (or rated power, e.g. in \$/kW), and the energy capacity (e.g. in \$/kWh). This approach was adapted from our earlier work on energy arbitrage for profit maximization<sup>12</sup>, to instead model the objective of meeting specified electricity output profiles.

## 5.2 Methods

We analyze the costs of wind and solar power plants coupled with storage. Our methodology relies on industry-accepted meteorological data and models<sup>85</sup>. After selecting appropriate wind and solar technology models to convert wind speeds and solar radiation to expected hourly electricity generation, we simulate the operation of renewable resources with energy storage for a set of locations, roles, and resource mixes. A summarized list of input parameters is presented in Table 5.3. The objective is to analyze the features of storage technologies that could enable wind and solar energy to provide deterministic output shapes at competitive prices while being resilient enough to operate in renewable resource scarce years.

**Resource availability and location selection.** Historical 100m wind speeds and solar irradiation data were obtained for a 20 year period from 1997-2016 from AWS True Power<sup>85</sup> for locations in Arizona, Iowa, Massachusetts, and Texas. These locations were selected based on their average solar irradiance and wind speeds reported

by the National Renewable Energy Laboratory<sup>75</sup>. Locations were selected to provide a mix of high and low resource availability for both wind and solar generation as shown in Table 5.1. Within each region, co-located wind and solar datasets falling between the 70th and 80th percentile for resource availability in that state were selected. This was done under the assumption that ideal locations have already been developed for other renewables functions and that long-term grid decarbonization will require development of less-than-perfect resource sites.

Wind generation was calculated for 16 popular on-shore turbine models, by power-curve interpolation, at each location<sup>102</sup>. The turbine model with the highest capacity factor based on location specific wind speeds was selected. As a result of the wide range of wind speeds across which it maintains rated power, the Vestas 112 model turbine with a 94m hub height was the best performing turbine for each location<sup>111</sup>. Total cost of ownership for the wind plant is estimated at \$1500/kW<sup>118</sup>.

Solar generation was calculated using NREL's solar simulator PVWatts, which is a simplified version of the System Advisory Model (SAM)<sup>75</sup>. Photovoltaic plants were built using the default options for crystalline silicon modules, single-axis tracking configuration tilted at local latitude with default azimuth (180 degree). The remaining simulation inputs are summarized in Table 5.3. Global, direct and diffused radiation, surface pressure, and temperature were directly read from WRF simulations. Wind speed at module height,  $w_2$ , was calculated using the Monin-Obukhov formula.

Yearly meteorological files conforming to PVWatts standard inputs were created and a batch processing script was used to run simulations and recombine the output into cohesive time-series. Total cost of ownership for the solar plant is estimated at \$1000/kW.

Capacity factors for each location support this selection and are provided in Table

Table 5.1: Locations and 20 year average capacity factors for the two analyzed renewable resources, wind and solar. The locations analyzed in this research were selected based on average solar irradiation and wind speed data to ensure a mix of different resource profiles and high/low average availability. Regions were selected to ensure at least class III wind speeds were achieved, to verify that wind installations were at minimum feasible. Resource availability for each location, presented as capacity factors as calculated from WRF simulations using a Vestas 112 3 MW (wind) and a single-axis tracking, tilted photovoltaic panel (solar).

Location	Wind capacity factor	Solar capacity factor
Arizona	38.6% (low)	34.1% (high)
Iowa	52.3% (high)	25.5% (low)
Massachusetts	40.7% (low)	24.2% (low)
Texas	61.7% (high)	31.0% (high)

5.1. Additionally, combinations of wind and solar resources were analyzed in order to determine the best mix of renewable resources for each location. Solar and wind generation combinations were analyzed in 5% increments.

**Grid role selection.** Three output shapes were defined to roughly match the timing and shape of the typical demand profile<sup>81</sup>, depicted in Figure 5-1. The baseload profile is a constant output shape for every hour of the twenty year period. The intermediate shape is based on the bulk of variation in the typical load profile to cover the hours in which most residences, commercial, and industrial loads are operating, from 0800-2200 daily. The peaker profile covers the highest demand period of 1200-1800. Finally, a fourth shape, the bipeaker, was defined to cover the hours from 0800-1100 and 1800-2200. This shape makes use of wind or solar and storage to generate during the high ramp rate periods that occur before and after sunset<sup>28</sup>.

**Mathematical formulation for LCOSE minimization.** Cost optimization of wind and solar plus storage to meet a defined output shape was performed in two

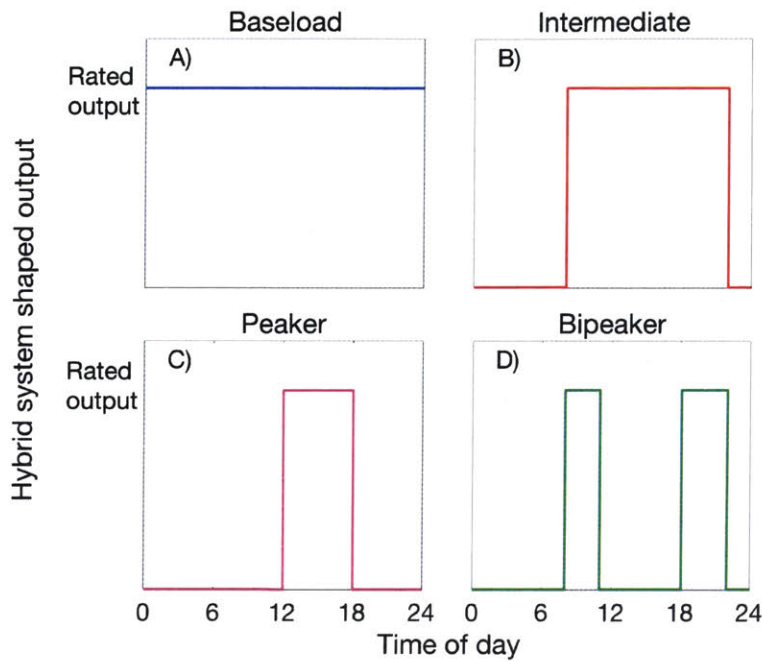


Figure 5-1: Examples of the pre-defined output shapes that solar or wind with storage are required to consistently produce for the twenty year period. Shapes were designed to match generation behavior as required by the typical load profile for residential, consumer, and industrial demand<sup>81</sup>. When stacked, the combinations of baseload, intermediate, and peaker or bipeaker, roughly match typical load profiles. For the analysis, the intermediate, peaker, and bipeaker have no output during non-operating periods. Parameters and ranges considered are listed in the Table 5.3.

steps, as depicted in Figure 5-2. For each resource mix and output shape combination all combinations of storage power capacity,  $\dot{E}_{\max}$ , and duration,  $h$ , and generation capacity were analyzed to produce a defined output shape subject to the constraints. Only combinations of generation and storage capacity able to consistently produce the output shape for twenty years are saved. For the analysis, a storage round-trip efficiency,  $\eta$ , of 75% was used for all locations. In the second step of the analysis the generation capacity and storage power and energy capacities which minimize total

Table 5.2: Locations analyzed in this research were selected to represent different resource profiles as determined by their average solar irradiation and wind speeds. To verify that wind installations were at minimum feasible, regions were selected to ensure at least class III wind speeds were achieved.

	Rich solar	Poor solar
Rich wind	Texas	Iowa
Latitude	34.714°	42.369°
Longitude	-102.124°	-95.443°
Poor wind	Arizona	Massachusetts
Latitude	32.294°	42.103°
Longitude	-110.099°	-71.811°

system cost are selected for each pair of storage power and energy capacity costs.

$$x(t)_{\text{generation}} - x(t)_{\text{charge}} + x(t)_{\text{discharge}} \geq \text{output shape} \quad (5.1)$$

$$x(t)_{\text{generation}} \geq \frac{\dot{E}_{\text{max}}}{\sqrt{\eta}} = x(t)_{\text{charge}} \quad (5.2)$$

$$x(t)_{\text{discharge}} \leq \dot{E}_{\text{max}}\sqrt{\eta} \quad (5.3)$$

$$0 \leq x(t)_{\text{charge}} - x(t)_{\text{discharge}} \leq \dot{E}_{\text{max}}h \quad (5.4)$$

$$C_{\text{system}} = \%_{\text{solar}}\text{solar}_{\text{gen}}C_{\text{solar}} + (1 - \%_{\text{solar}})\text{wind}_{\text{gen}}C_{\text{wind}} + \dot{E}_{\text{max}}C_{\text{storage}}^{\text{power}} + \dot{E}_{\text{max}}hC_{\text{storage}}^{\text{energy}} \quad (5.5)$$

**Sensitivity analysis.** Resource profiles differ substantially across locations providing an important basis for comparing output shapes across multiple resource profiles. Wind speed distributions are stronger during the night and early morning in Texas and Iowa. Solar profiles, while more similarly shaped, still demonstrate the impact of relative location within a timezone on the timing of solar ramping up and down. To

Table 5.3: Input parameters for the analysis

Solar total cost of ownership	\$1000/kW
Wind total cost of ownership	\$1500/kW
Storage power capacity overnight capital cost	\$0 - \$2000/kW
Storage energy capacity overnight capital cost	\$0 - \$250/kWh
Storage round-trip efficiency	75%
Storage power capacity	0.25 - 4 kW/kW <sub>gen</sub> *(total <sub>gen</sub> )
Storage duration	0 - 800h
Baseload hours	0000 - 2400
Intermediate hours	0800 - 2200
Peaker hours	1200 - 1800
Bipeaker hours	0800 - 1100 1800 - 2200
PV DC system losses	14.08%
PV DC-to-AC ratio	1.2
PV inverter nominal efficiency	96%
PV ground coverage ratio	0.4
Technology I costs	\$20/kWh, \$1000/kW
Technology II costs	\$150/kWh, \$700/kW

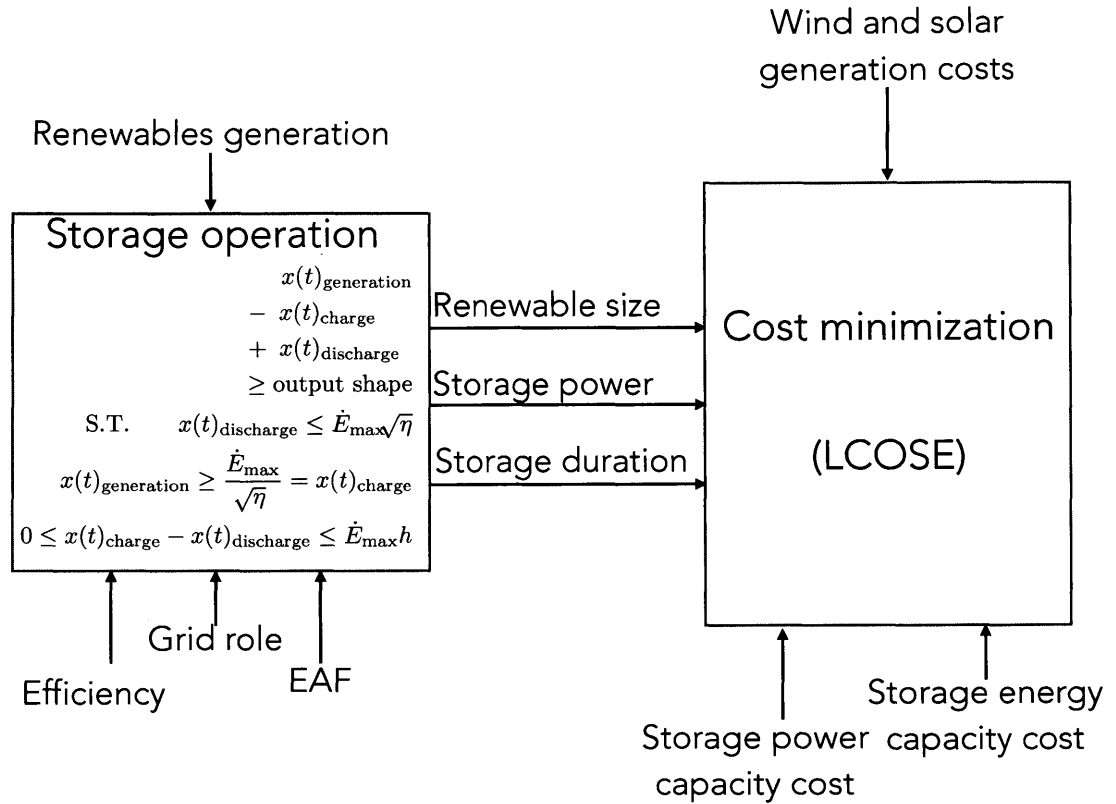


Figure 5-2: Block diagram of modeling methodology employed to analyze the role wind and solar with storage can have in long-term grid decarbonization. Where  $\dot{E}_{\text{max}}$  is the storage power capacity,  $h$  is the storage duration,  $\eta$  is storage round-trip efficiency, and  $x(t)$  gives the hourly renewables generation, storage charge, and storage discharge energy. The model first determines all combinations of storage and generation capacity which can meet the defined output shape given constraints of efficiency and Equivalent Availability Factor (EAF). For all considered combinations of storage power capacity and energy capacity costs, the model then selects the cost minimum combination of renewables and storage. Parameters and ranges considered are listed in the Table 5.3.

capture this impact, simulations were conducted for a range of shape commencement times and durations, demonstrating robustness in our general findings.

Sensitivity to a reduced efficiency of 65% and increased efficiency to 95% was assessed for all locations for wind and solar only profiles and for a range of resource

mixes for Arizona. Arizona was selected as a focus for the analysis over a range of resource mixes, since it showed the most diverse optimal resource mix in the original analysis. Lastly, sensitivity to the number of allowed failures were conducted by changing the EAF percentage. We allowed for an increasing number of ‘missed hours’ through the course of the 20 year period to determine the impact of relaxing contractual constraints.

### 5.3 Results

Our results are presented in three sub-sections. We first discuss results on the least-cost combinations of wind, solar, and storage installations to meet baseload, intermediate, and peak power output shapes (Figure 5-1). We then quantify cost targets for energy storage that would enable these plants to reach cost-competitiveness with traditional electricity sources. Finally, we discuss cost features of current and future energy storage technologies as compared to these targets.

**Cost-minimized wind, solar, and storage installations for baseload, intermediate, and peak power.** Here we examine how storage with wind and solar can be used to provide baseload, intermediate, and peak power outputs for twenty years across four locations representing different combinations of high and low resource availability (Table 5.1): Arizona, Iowa, Massachusetts, and Texas. In each location, we solve for cost minimizing combinations of wind, solar, and storage, while varying technology costs.

The costs of optimized systems are shown in Figure 5-3, for two different storage technology cost structures. Various factors affect the levelized cost of shaped energy (LCOSE, e.g. in \$/kWh), including the output shape, location, degree of

diversification across the solar and wind resource portfolio, and the technology costs. Across all locations and resources, the LCOSE rises in order of the following output shapes: peaker, bipeaker, intermediate, and baseload. In most locations, the least cost resource portfolio emphasizes wind over solar for all output shapes. The one exception is Arizona, which has more abundant sunshine. In Arizona, solar makes up greater than 50% of the portfolio, as measured by installed solar and wind generation capacity, for all output shapes. The least-cost portfolios result in LCOSE values that are lowest in Texas and highest in Massachusetts across all output shapes. Iowa and Arizona switch places as having the second and third lowest LCOSE values, depending on the output shape and storage technology cost.

Technology costs also have an impact on the cost-minimized system and LCOSE. As seen in Figures 5-4 and 5-3, the LCOSE rises with the cost of storage (and with the cost of solar or wind energy capacity), as expected. The cost structure of storage, namely the ratio of power capacity cost to energy capacity cost, also matters. As can be seen in Figure 5-4, technologies with lower energy capacity cost to power capacity cost ratios give lower LCOSE values (see, for example, Technology I in Figure 5-4). Technology I has a lower energy to power cost ratio (\$20/kWh and \$1000/kW), while Technology II has a higher energy to power cost ratio (\$150/kWh and \$700/kW). Examples of technologies with cost structures similar to Technology I are pumped hydro storage (PHS), compressed air energy storage (CAES), and potentially future flow battery technologies with low storage energy capacity costs<sup>63</sup>. Examples of Technology II might include future Li-ion batteries after further cost reduction, and possibly other closed battery technologies, flywheels, and supercapacitors<sup>91</sup>. The numerical results in Figures 5-4 and 5-3 are based on projected wind and solar overnight capital costs of \$1500/kW and \$1000/kW<sup>118</sup>.

For all output shapes, the installed generation capacity for wind and solar is

greater than the rated output required, to varying degrees that depend on the output shape and resource availability. For example, the installed generation capacity for a wind-storage plant in Texas supplying baseload is between 2 and 4 times the required baseload power output (Figure 5-5). For a solar and storage peaker in Texas, this factor is lower, ranging between 1.2 and 2.4 times, due to better matching of output shape and resource availability. Location also matters. Higher generation capacities are required in lower wind capacity-factor regions like Arizona or Massachusetts.

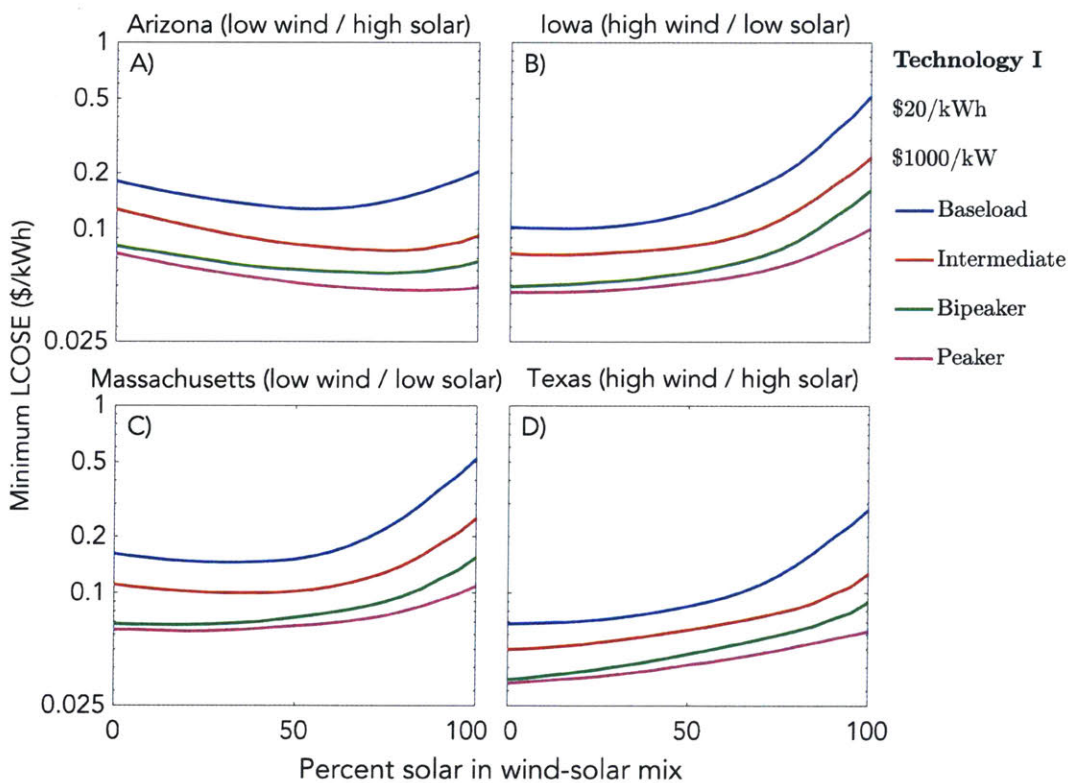


Figure 5-3: Levelized cost of shaped electricity (LCOSE, \$/kWh) for the four grid roles (denoted by color) across Arizona, Massachusetts, Iowa, and Texas for combinations of wind and solar. Total cost of ownership for wind (solar) is estimated as \$1500/kW (\$1000/kW). Wind is the preferred generation technology in most locations. Arizona is the exception, with low wind and high solar insolation.

Intra- and inter-year resource variabilities influence system characteristics and

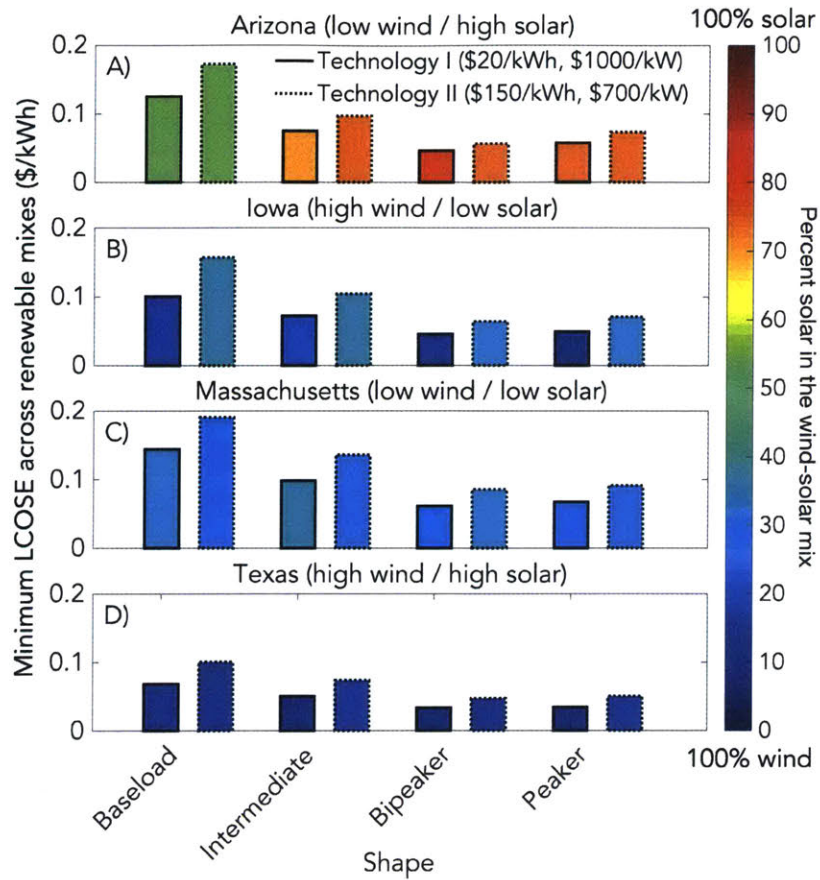


Figure 5-4: Minimum levelized cost of shaped electricity (LCOSE, \$/kWh) for the four grid roles (horizontal axis) and two different storage technologies (bar outline) across Arizona, Massachusetts, Iowa, and Texas. Bar shading denotes the optimal renewable resource generation mix. To highlight the different sensitivities of the renewables-storage system cost to storage energy costs we selected two technologies with high/low cost combinations: Technology I (solid bar outline, \$1000/kW and \$20/kWh) and Technology II (dotted bar outline, \$700/kW and \$150/kWh). Lower energy capacity costs yield lower LCOSE for all resource mixes despite the higher power capacity costs. Total cost of ownership for wind (solar) is estimated as \$1500/kW (\$1000/kW).

therefore the total plant cost. The impact of resource variability on the storage energy level is shown in the periods of deep discharge, in Figure 5-6. The intra-year solar seasonality between periods of higher resource availability (summer) and low resource availability (winter) requires a higher capacity storage system compared to

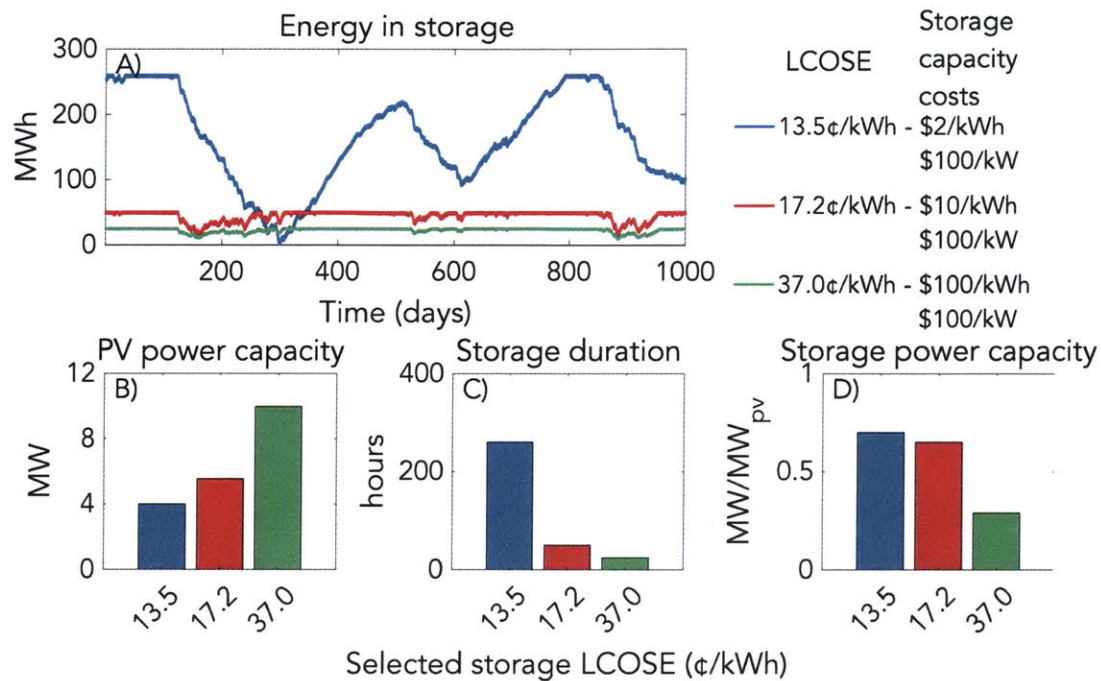


Figure 5-5: Storage operation and optimal sizing for a solar power plant relative to 1 MW baseload power in Texas. We optimize the solar power plant generation capacity, storage power capacity, and storage energy capacity for each pair of storage capacity costs and given generation costs. Solar total cost of ownership is estimated as \$1000/kW. Three different pairs of storage cost intensities are shown to demonstrate how minimizing the levelized cost of shaped energy (LCOSE) leads to different optimal combinations of renewables-storage system characteristics and operation. Solar generation capacity, storage energy capacity, and storage power capacity can all vary to meet the desired output shape. Panel A) depicts how storage operation changes for different storage sizes. As storage costs increase, the solar power plant size increases, B). As storage energy capacity costs increase, optimal storage duration decreases, C), as does the storage power capacity relative to the generation capacity, D).

a resource like wind that is more evenly distributed over time. (If we were also to allow rated output power to vary seasonally, for example producing higher output shapes in summer than winter, summer peaking electric grids would benefit from the higher resource availability.) For long-term planning, inter-year variability is critical, with renewables-storage sizing determined by the low resource years in the 20 year

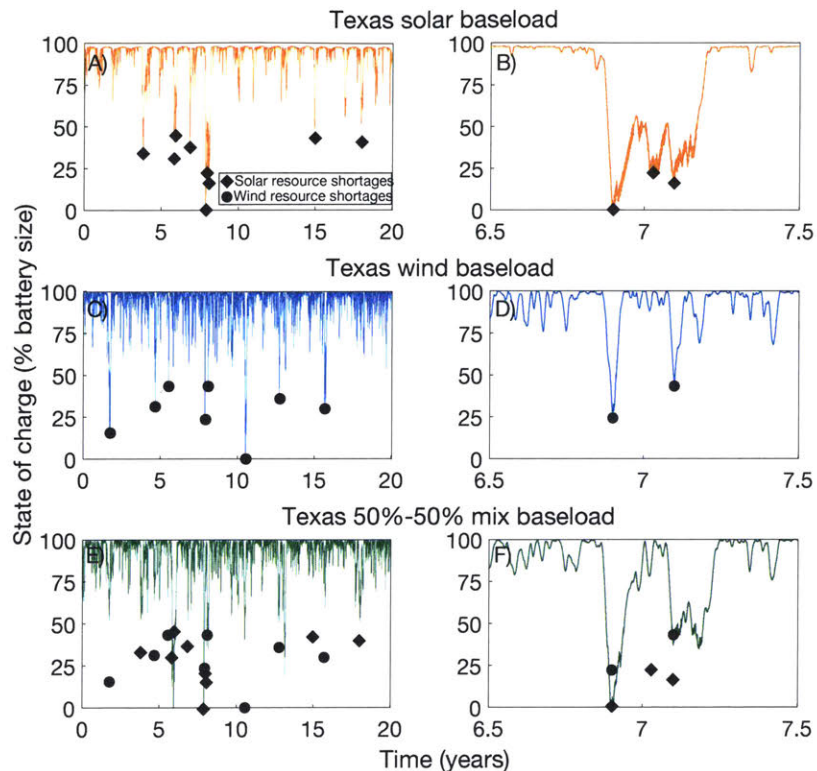


Figure 5-6: Storage state of charge (SOC) over 20 years for solar, wind, and a 50%-50% mix providing baseload power, panels A), C), E). Panels B), D), F) show detailed storage stage of charge for years 6 and 7. Storage SOC is the percentage of storage energy capacity available for discharge, a proxy for resource availability fluctuation through the analysis. Optimal storage size is determined by the number of events where the overall system cannot output the necessary power (SOC = 0%). Severe solar resource shortages are represented by diamonds, while wind resource shortages are represented by circles. In a 50%-50% mix, E) and F), storage is only fully drained when there is a simultaneous resource shortage of wind and solar (diamonds+circles). Using more than one renewable resource can increase system resiliency but remains sensitive to smaller shortages of both. For example, the 50-50 system is robust to the wind shortage in year 10, panels C) and E), but not to the wind/solar shortages shown in panels B), D) and F).

period.

Allowing for periods of unmet demand relative to the desired output shape during low resource periods can substantially reduce the storage power and energy capacity requirements and the LCOSE at which shaped electricity is supplied. A useful metric to quantify plant downtime is the equivalent availability factor (EAF), i.e. the

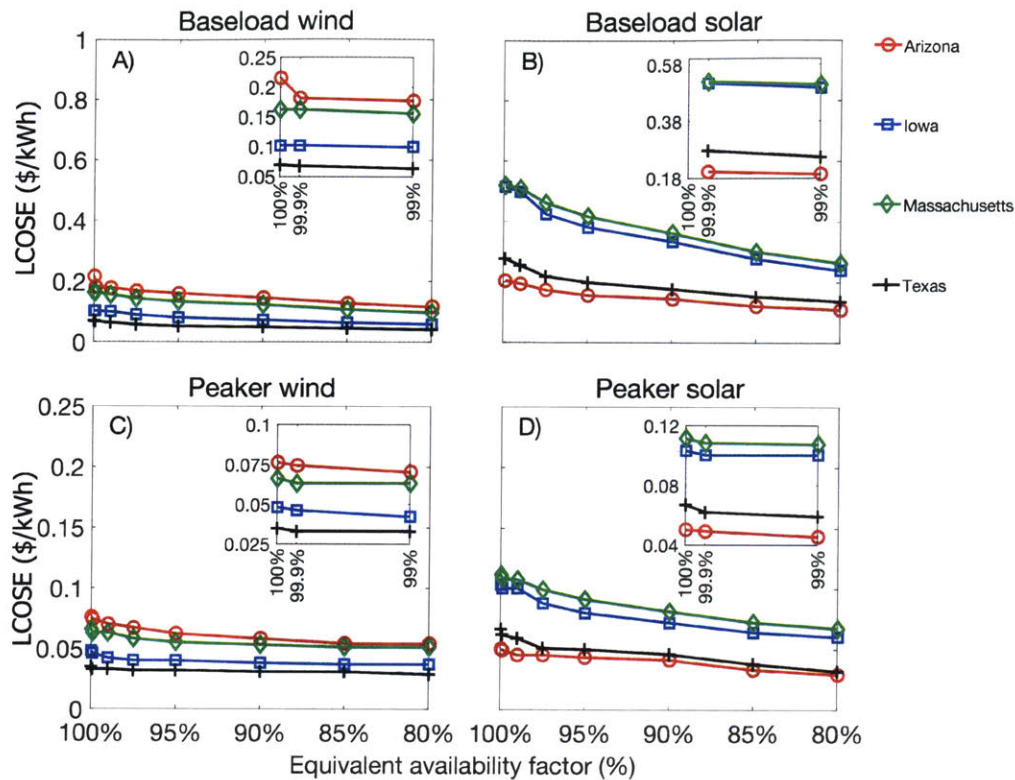


Figure 5-7: Levelized cost of shaped electricity (LCOSE, \$/kWh) plotted against equivalent availability factor (EAF) for baseload and peaker roles using only wind or solar across four locations. The storage technology modeled has low energy capacity costs but high power capacity costs (Technology I). The EAF can be interpreted as the time the power plant is forced to meet the role requirements. Lowering the EAF relaxes the grid requirements. Reducing EAF substantially lowers system LCOSE due to smaller storage requirements. EAF of around 85% are common in a combined cycle gas turbine, coal, and nuclear systems<sup>23</sup>. Lowering the EAF for renewable-storage systems to 85% from 100% achieves a nearly 50% reduction in LCOSE.

fraction of rated output that can be provided after all types of outage and deratings. Industry reference EAF values range between 83% for coal and 88% for gas turbines<sup>23,74</sup>. We present an EAF sensitivity analysis, changing renewables-storage plant availability between 100% and 80% in Figure 5-7. In Texas, for example, we observe a reduction in LCOSE of up to 44% for a solar peaker meeting the target output 90% vs. 100% of the time.

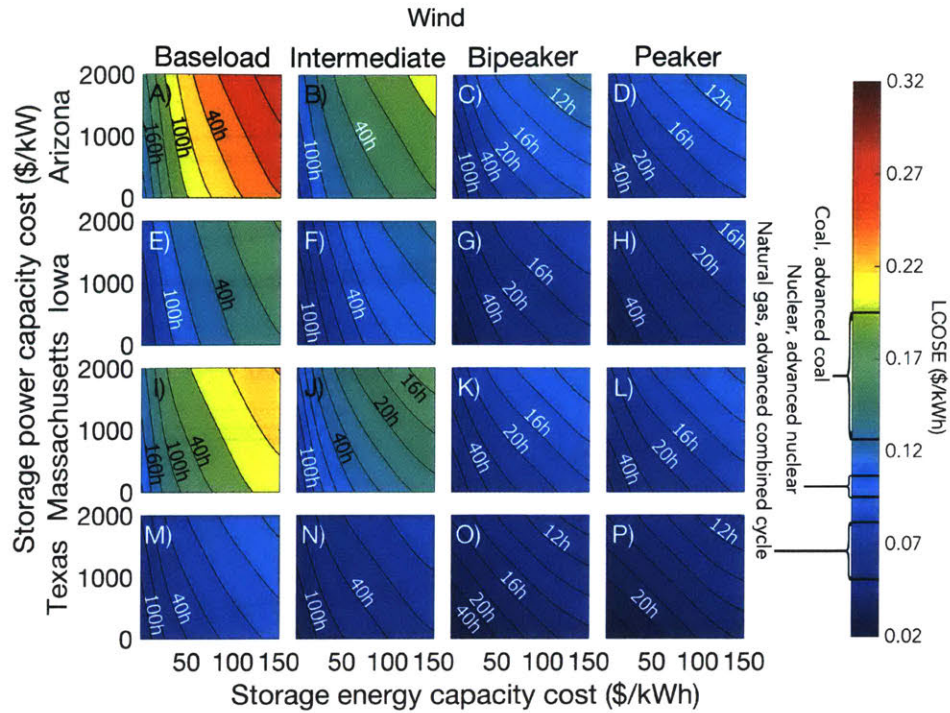


Figure 5-8: Levelized cost of shaped electricity (LCOSE, \$/kWh) for a wind and storage power plant producing baseload, intermediate and peak (bipeaker and peaker) power (columns left to right) for twenty years considering a range of storage energy and power capacity costs for Arizona, Iowa, Massachusetts, and Texas (rows top to bottom). Total cost of ownership for wind is estimated as \$1500/kW. Storage with energy capacity costs below \$50/kWh can make wind cost-competitive in Texas for all output shapes, and with peaker and bipeaker shapes in all locations. Wind capacity factor plays a large role in determining LCOSE, with the higher capacity factor locations having lower LCOSE. The optimal storage duration is given, and this duration is the number of hours that the optimally sized storage system could discharge at maximum power. The LCOE for other technologies are shown as brackets in the color axis, to compare against the LCOSE for renewables and storage, and consider the regional variation in LCOE for plants entering in service in 2022<sup>110</sup>.

**Cost and performance targets to reach cost-competitiveness.** Storage capacity costs are the single greatest impediment to significant growth in stationary storage, though other performance factors are also important<sup>12,68</sup>. At what storage costs do these systems become cost-competitive with other generation technologies? Here we determine cost targets for storage at which renewables-storage plants become

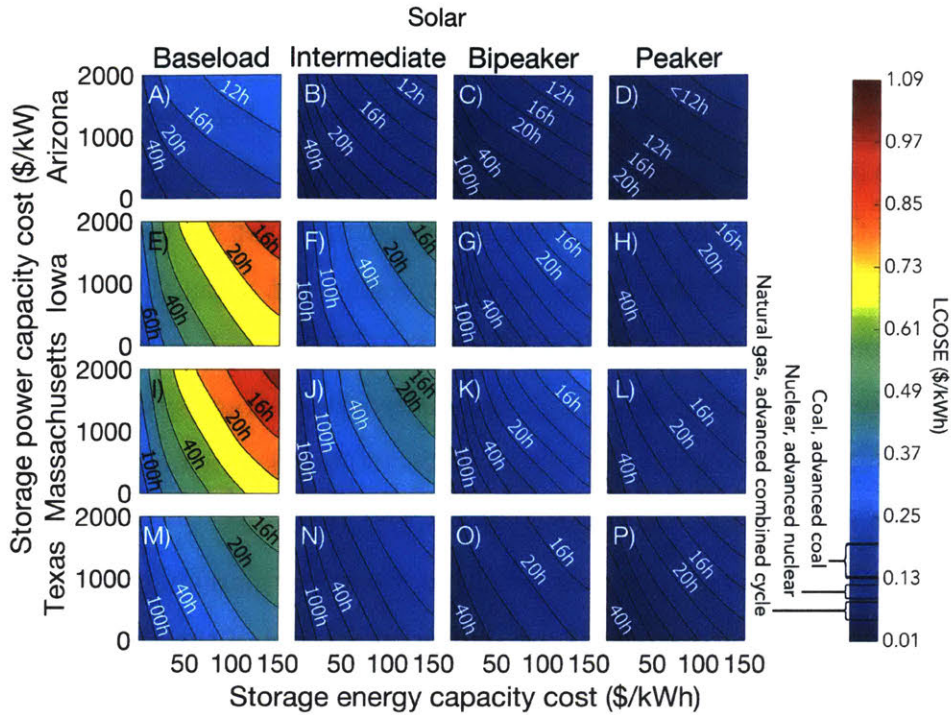


Figure 5-9: Levelized cost of shaped electricity (LCOSE, \$/kWh) for a solar and storage power plant producing baseload, intermediate and peak (bipeaker and peaker) power (columns left to right) for twenty years considering a range of storage energy and power capacity costs for Arizona, Iowa, Massachusetts, and Texas (rows top to bottom). Total cost of ownership for solar is estimated as \$1000/kW. Storage with energy capacity costs below \$50/kWh can make solar cost-competitive for peaker and bipeaker shapes in all locations, and intermediate shapes in Texas and Arizona. Storage energy capacity costs must fall to \$30/kWh to be cost-competitive with baseload in Texas. Solar capacity factor plays a large role in determining LCOSE, with the higher capacity factor locations having lower LCOSE. The optimal storage duration is given, and this duration is the number of hours that the optimally sized storage system could discharge at maximum power. The LCOE for other technologies are shown as brackets in the color axis, to compare against the LCOSE for renewables and storage, and consider the regional variation in LCOE estimated for plants entering in service in 2022<sup>110</sup>.

competitive with current generation technologies. Figures 5-8 and 5-9 compare the LCOSE of renewables and storage with the estimated LCOE of current generation technologies.

We find that renewables-storage systems can be competitive with conventional

generation technologies if storage energy capacity costs fall to \$10-50/kWh, especially in locations with high resource availability, assuming total costs of ownership of wind and solar plants of \$1500/kW and \$1000/kW respectively. The cost targets show high sensitivity to storage energy capacity costs and less sensitivity to storage power costs: The lowest LCOSE for the use contexts examined here can be reached when using storage technologies with low energy capacity costs, even when this is accompanied by a higher power capacity cost. The reason behind this finding is that the ratio of system energy to power capacity in the optimally sized storage systems for these use contexts corresponds to storage durations of 20-160 hours. Figures 5-8 and 5-9 show these storage durations as the slopes of iso-LCOSE contours.

For grid roles of shorter duration and better temporal matching with the resource availability, the storage cost targets are on the higher end of the \$10-50/kWh range. Across both solar and wind resources and all four locations, the baseload output shape requires the lowest storage costs in order to be competitive. However, for a location with abundant solar or wind resources (e.g. Arizona or Texas, respectively), storage energy capacity cost targets are higher, even for a baseload output shape.

**Evaluation of candidate storage technologies.** To meet the cost targets estimated in this paper, storage technologies should be able to achieve ultra-low energy capacity costs. Several mechanical and chemical storage systems may be suitable for achieving these target costs. Mechanical energy storage, such as PHS and CAES, tend to have low energy capacity costs where suitable topography or underground caverns are available, with energy capacity costs estimated at under \$50/kWh). PHS in particular has been proven to work for large scale installations over many decades<sup>79</sup>. However, both technologies also have geographical and environmental constraints that may inhibit further deployment. While mechanical storage is scal-

able to large size, its energy density is several hundredfold lower than electrochemical storage and thus can produce a large spatial footprint for above-ground systems. Electrochemical energy storage technologies face different limitations, including higher energy capacity costs<sup>12</sup> compared to PHS and CAES, which is exacerbated by degradation over time and the need for technology replacement. However, while every electrochemical technology degrades over time, those with exceptionally low energy costs may allow a full replacement of the chemicals with acceptable cost impact.

The ability to install an electrochemical storage system in many locations is one of the greatest advantages as compared to PHS and CAES. But what is the potential for cost decline? A recent bottom-up analysis compares the chemical cost of battery storage, defined as the cost of energy-storing compounds normalized by their stored energy, for 40 technologies developed over the past 60 years<sup>63</sup>. The chemical cost represents a floor for the cost for each battery technology, upon which additional materials, manufacturing, and other costs must be added to arrive at a system cost. Taking Li-ion batteries as an example, the analysis found that there are several distinct chemistries for which the range of chemical costs based on current materials prices is \$35-\$100/kWh. Under some assumptions these batteries could meet the energy capacity cost targets needed to provide electricity that is cost-competitive with traditional sources for peaker and intermediate plants, and even for baseload plants in particularly resource-rich locations.

Electrochemical batteries of lower energy capacity costs than Li-ion may also be possible, with several proposed aqueous electrochemical couples having an estimated chemical cost below \$10/kWh<sup>63</sup>. A low chemical cost does not always translate into low system cost, though. For example, the high temperature sodium-sulfur battery has a \$1-\$2/kWh chemical cost but system level energy capacity cost exceeding

\$500/kWh<sup>104</sup>. However, ambient temperature batteries that use highly abundant, low chemical-cost components in a low-cost architecture may achieve lower costs. Moreover, the long storage durations required, as well as the need to tune energy and power in order to optimize LCOSE in different locations and with different resources, would benefit from a flow battery architecture with significant economies of scale and modularity in energy and power capacity sizes. As with PHS and CAES and unlike Li-ion batteries, flow batteries have independently scalable energy and power. The energy capacity is determined by the sizing of the energy-storing medium, whether mechanical or chemical, and the power capacity by the sizing of the power generator, whether a turbine or an electrochemical stack. Nevertheless, not all flow battery chemistries have low energy cost; for example, the most widely studied variant, vanadium redox flow batteries, have  $\approx$  \$100/kWh energy capacity cost<sup>24</sup>. With continued research, costs may drop, however. For example, a recent example of a low energy capacity cost, projected to be \$10-\$20/kWh, with a power capacity cost of  $\approx$  \$1000/kW battery was described by Li et al.<sup>63</sup>. If these costs are achieved, they would fall within the target range estimated here for cost-competitiveness with combined cycle natural gas, coal, and nuclear generators across all locations and all grid roles evaluated in our study.

## 5.4 Conclusions

Future high renewables penetration scenarios will require supply and demand to be met at all times, and shaping renewables output to match traditional grid roles is one possible path to this end. Here we ask whether energy storage can cost-effectively help enable this, and what storage cost features are needed.

We find that ultra-low energy capacity costs are needed to cost-competitively fill

this role. The cost targets depend on the location and output shapes, since these systems require different storage sizes, but across all locations and outputs, costs would need to fall below \$50/kWh. Cost targets are lowest for baseload output profiles across all locations. Various approaches can be used to relax these cost targets. For example, reducing the EAF to 90% from 99.9%, cuts the LCOSE nearly in half, but unmet demand would need to be met by other sources. Increased transmission can be used to smooth the short-term variability of renewables through the geographical dispersion of generation. But the results of this study suggest that in low resource availability years, which may impact larger geographies, long duration storage would still be needed.

Some technologies offer lower energy capacity costs, such as PHS and CAES, but their application is geographically limited. Amongst currently available electrochemical storage technologies, the cost declines that have been projected in some studies would enable Li-ion batteries to meet cost targets for peaker and intermediate plants, and in some locations (with abundant wind) baseload plants. Whether materials resource constraints will limit deployment at terawatt hour scale, remain open questions for these and other electrochemical technologies. The analysis points to the importance of developing storage technologies that utilize ultra-abundant low-cost reactants (such as sulfur and sodium in aqueous media), and storage architectures with independent scaling of energy and power capacities (such as in flow batteries).



# Bibliography

- [1] Abbas A Akhil, Georgianne Huff, Aileen B Currier, Benjamin C Kaun, Dan M Rastler, Stella Bingqing Chen, Andrew L Cotter, Dale T Bradshaw, and William D Gauntlett. DOE / EPRI Electricity Storage Handbook in Collaboration with NRECA. *Sand2015-XXX*, (January), 2015.
- [2] Riccardo Amirante, Cassone E, Elia Distaso, and Paolo Tamburrano. Overview on recent developments in energy storage: Mechanical, electrochemical and hydrogen technologies. *Energy Conversion and Management*, 132:372–387, 2017.
- [3] Cristina L. Archer and Mark Z. Jacobson. Supplying Baseload Power and Reducing Transmission Requirements by Interconnecting Wind Farms. *Journal of Applied Meteorology and Climatology*, 46(11):1701–1717, Nov 2007.
- [4] M Armand and J.-M. Tarascon. Building better batteries. *Nature*, 451:652–7, Mar 2008.
- [5] John Baker. New technology and possible advances in energy storage. *Energy Policy*, 36(12):4368–4373, Dec 2008.
- [6] P. Balachandra and Vijay Chandru. Modelling electricity demand with representative load curves. *Energy*, 24(3):219–230, 1999.
- [7] R. J. Barthelmie and S. C. Pryor. Potential contribution of wind energy to climate change mitigation. *Nature Clim. Change*, 4(8):684–688, Oct 2014.
- [8] Islam Safak Bayram, Mohamed Abdallah, Ali Tajer, and Khalid A. Qaraqe. A Stochastic Sizing Approach for Sharing-Based Energy Storage Applications. *IEEE Transactions on Smart Grid*, 8(3):1075–1084, 2017.
- [9] Luís M. A. Bettencourt, Jessika E. Trancik, and Jasleen Kaur. Determinants of the pace of global innovation in energy technologies. *PLoS ONE*, 8(10):e67864, 10 2013.

- [10] M Bolinger and S Weaver. Utility-Scale Solar 2013: An Empirical Analysis of Project Cost, Performance, and Pricing Trends in the United States. Technical report, 2014.
- [11] Alexander Boogert and Cyriel de Jong. Gas Storage Valuation Using a Monte Carlo Method. Technical Report Dec, 2006.
- [12] William A. Braff, Joshua M. Mueller, and Jessika E. Trancik. Value of storage technologies for wind and solar energy. *Nature Climate Change*, 6:964–969, 2016.
- [13] California ISO Website. <http://www.caiso.com>, 2017.
- [14] Anya Castillo and Dennice F. Gayme. Grid-scale energy storage applications in renewable energy integration: A survey. *Energy Conversion and Management*, 87:885–894, 2014.
- [15] Edgardo D Castronuovo and João A Peças Lopes. Optimal operation and hydro storage sizing of a wind–hydro power plant. *International Journal of Electrical Power & Energy Systems*, 26(10):771–778, 2004.
- [16] Monika Chawla, Rajendra Naik, Rajni Burra, and Herman Wiegman. Utility energy storage life degradation estimation method. In *2010 IEEE Conference on Innovative Technologies for an Efficient and Reliable Electricity Supply*, pages 302–308, 2010.
- [17] Haisheng Chen, Thang Ngoc Cong, Wei Yang, Chunqing Tan, Yongliang Li, and Yulong Ding. Progress in electrical energy storage system: A critical review. *Progress in Natural Science*, 19(3):291–312, 2009.
- [18] S. X. Chen, H. B. Gooi, and M. Q. Wang. Sizing of Energy Storage Systems for Microgrids. *IEEE Transactions on Smart Grid*, 3(1):142–151, 2012.
- [19] Feng Cheng, S. Willard, J. Hawkins, B. Arellano, O. Lavrova, and A. Mammoli. Applying battery energy storage to enhance the benefits of photovoltaics. In *Energytech, 2012 IEEE*, pages 1–5, May 2012.
- [20] Satishkumar B. Chikkannanavar, Dawn M. Bernardi, and Lingyun Liu. A review of blended cathode materials for use in Li-ion batteries. *Journal of Power Sources*, 248:91–100, Feb 2014.

- [21] D. Connolly, H. Lund, P. Finn, B.V. Mathiesen, and M. Leahy. Practical operation strategies for pumped hydroelectric energy storage (PHES) utilising electricity price arbitrage. *Energy Policy*, 39(7):4189–4196, Jul 2011.
- [22] D. Connolly, H. Lund, B.V. Mathiesen, E. Pican, and M. Leahy. The technical and economic implications of integrating fluctuating renewable energy using energy storage. *Renewable Energy*, 43:47–60, Jul 2012.
- [23] G. Curley. Reliability Analysis of Power, Plant Unit Outage Problems. Technical report, Generation Consulting Services LLC, 2013.
- [24] Robert M. Darling, Kevin G. Gallagher, Jeffrey a. Kowalski, Seungbum Ha, and Fikile R. Brushett. Pathways to low-cost electrochemical energy storage: a comparison of aqueous and nonaqueous flow batteries. *Energy Environ. Sci.*, 7(11):3459–3477, 2014.
- [25] Bhaskarjyoti Das and Ashwani Kumar. A NLP approach to optimally size an energy storage system for proper utilization of renewable energy sources. *Procedia Computer Science*, 125:483–491, 2018.
- [26] Paul Denholm, Gerald L Kulcinski, and Tracey Holloway. Emissions and energy efficiency assessment of baseload wind energy systems. *Environmental science & technology*, 39(6):1903–1911, 2005.
- [27] Paul Denholm and Robert M. Margolis. Evaluating the limits of solar photovoltaics (PV) in traditional electric power systems. *Energy Policy*, 35(5):2852–2861, may 2007.
- [28] Paul Denholm, Matthew O’Connell, Gregory Brinkman, and Jennie Jorgenson. Overgeneration from Solar Energy in California: A Field Guide to the Duck Chart. Technical report, NREL - National Renewable Energy Laboratory, 2015.
- [29] Department of Energy Global Energy Storage Database. <http://www.energystorageexchange.org>, 2017.
- [30] Francisco Díaz-González, Andreas Sumper, Oriol Gomis-Bellmunt, and Roberto Villafáfila-Robles. A review of energy storage technologies for wind power applications. *Renewable and Sustainable Energy Reviews*, 16(4):2154–2171, May 2012.

- [31] K.C. Divya and Jacob Ostergaard. Battery energy storage technology for power systems—An overview. *Electric Power Systems Research*, 79(4):511–520, 2009.
- [32] Energinet Danish Electricity Website. <http://www.energinet.dk>, 2017.
- [33] Energy Reliability Council of Texas Website. <http://www.ercot.com>, 2017.
- [34] EPRI. EPRI-DOE Handbook of Energy Storage for Transmission and Distribution Applications. Technical Report 1001834, Palo Alto, CA, 2003.
- [35] Annette Evans, Vladimir Strezov, and Tim J. Evans. Assessment of utility energy storage options for increased renewable energy penetration. *Renewable and Sustainable Energy Reviews*, 16(6):4141–4147, 2012.
- [36] Jim Eyer, J.J. Iannucci, and G.P. Corey. Energy Storage Benefits and Market Analysis Handbook, A Study for the DOE Energy Storage Systems Program. *Sandia National Laboratories*, 2004.
- [37] Frank A. Felder and Ruthanne Haut. Balancing alternatives and avoiding false dichotomies to make informed U.S. electricity policy. *Policy Sciences*, 41:165–180, 2008.
- [38] Yi Feng, Lei Jun Shao, Bang Ling Zhang, Meng Jie Wu, Yu Pei Shao, Qiang Qiang Liao, Guo Ding Zhou, and Bo Sun. Technical and Economic Analysis on Grid-Connected Wind Farm Based on Hybrid Energy Storage System for Active Distribution Network. *Applied Mechanics and Materials*, 672-674:274–279, Oct 2014.
- [39] Helder Lopes Ferreira, Raquel Garde, Gianluca Fulli, Wil Kling, and Joao Pecas Lopes. Characterisation of electrical energy storage technologies. *Energy*, 53:288–298, 2013.
- [40] Emily Fertig and Jay Apt. Economics of compressed air energy storage to integrate wind power: A case study in ERCOT. *Energy Policy*, 39(5):2330–2342, May 2011.
- [41] F.C. Figueiredo, Flynn, P.C., and E.A. Cabral. The economics of energy storage in 14 deregulated power markets. *Energy Studies Review*, 14(2):2, 2006.
- [42] Carolyn Fischer and Richard G. Newell. Environmental and technology policies for climate mitigation. *Journal of Environmental Economics and Management*, 55:142–162, 2008.

- [43] Charles Forsberg. Hybrid systems to address seasonal mismatches between electricity production and demand in nuclear renewable electrical grids. *Energy Policy*, 62:333–341, 2013.
- [44] Frank Graves, Thomas Jenkin, and Dean Murphy. Opportunities for Electricity Storage in Deregulating Markets. *The Electricity Journal*, 12(8):46–56, 1999.
- [45] Jeffery B. Greenblatt, Samir Succar, David C. Denkenberger, Robert H. Williams, and Robert H. Socolow. Baseload wind energy: modeling the competition between gas turbines and compressed air energy storage for supplemental generation. *Energy Policy*, 35(3):1474–1492, 2007.
- [46] Mehreen Gul, Yash Kotak, and Tariq Muneer. *Review on recent trend of solar photovoltaic technology*, volume 34. 2016.
- [47] Xian He, Erik Delarue, William D’haeseleer, and Jean-Michel Glachant. A novel business model for aggregating the values of electricity storage. *Energy Policy*, 39(3):1575–1585, mar 2011.
- [48] Lion Hirth. The market value of variable renewables, The effect of solar wind power variability on their relative price. *Energy Economics*, 38:218–236, 2013.
- [49] Eric Hittinger, J. F. Whitacre, and Jay Apt. Compensating for wind variability using co-located natural gas generation and energy storage. *Energy Systems*, 1:417–439, Aug 2010.
- [50] Eric Hittinger, J F Whitacre, and Jay Apt. What properties of grid energy storage are most valuable? *Journal of Power Sources*, 206:436–449, 2012.
- [51] Samuel C. Huntington, Pablo Rodilla, Ignacio Herrero, and Carlos Batlle. Revisiting support policies for RES-E adulthood: Towards market compatible schemes. *Energy Policy*, 104(August 2016):474–483, 2017.
- [52] H Ibrahim, A Ilinca, and J Perron. Energy storage systems - Characteristics and comparisons. *Renewable and Sustainable Energy Reviews*, 12(5):1221–1250, 2008.
- [53] IRENA. Renewable Power Generation Costs in 2014. Technical report, 2015.
- [54] ISO New England Website. <http://www.iso-ne.com>, 2017.
- [55] Mark Z. Jacobson. Review of solutions to global warming, air pollution, and energy security. *Energy Environ. Sci.*, 2:148–173, 2009.

- [56] O. A. Jaramillo, M. A. Borja, and J. M. Huacuz. Using hydropower to complement wind energy: A hybrid system to provide firm power. *Renewable Energy*, 29(11):1887–1909, 2004.
- [57] J K Kaldellis, D Zafirakis, and K Kavadias. Techno-economic comparison of energy storage systems for island autonomous electrical networks. *Renewable and Sustainable Energy Reviews*, 13:378–392, 2009.
- [58] Makoto Kamibayashi, David K. Nichols, and Taku Oshima. Development update of the NAS battery. In *IEEE/PES Transmission and Distribution Conference and Exhibition*, volume 3, pages 1664–1668. IEEE, 2002.
- [59] Georgios Karmiris and Tomas Tengnér. Control Method Evaluation for Battery Energy Storage System utilized in Renewable Smoothing. In *IEEE Conference of the Industrial Electronics Society*, pages 1566–1570, 2013.
- [60] Goksin Kavlak, James M. McNerney, and Jessika E. Trancik. Evaluating the causes of photovoltaics cost reduction. *Energy Policy*, In review:xx–xx, 2017.
- [61] T. Kousksou, P. Bruel, A. Jamil, T. El Rhafiki, and Y. Zeraouli. Energy storage: Applications and challenges. *Solar Energy Materials and Solar Cells*, 120:59–80, 2014.
- [62] Chun-Hua Li, Xin-Jian Zhu, Guang-Yi Cao, Sheng Sui, and Ming-Ruo Hu. Dynamic modeling and sizing optimization of stand-alone photovoltaic power systems using hybrid energy storage technology. *Renewable Energy*, 34(3):815–826, 2009.
- [63] Zheng Li, Menghsuan Sam Pan, Liang Su, Ping Chun Tsai, Andres F. Badel, Joseph M. Valle, Stephanie L. Eiler, Kai Xiang, Fikile R. Brushett, and Yet Ming Chiang. Air-Breathing Aqueous Sulfur Flow Battery for Ultralow-Cost Long-Duration Electrical Storage. *Joule*, 1(2):306–327, 2017.
- [64] Yun Liu, Chi Keung Woo, and Jay Zarnikau. Wind generation’s effect on the ex post variable profit of compressed air energy storage: Evidence from Texas. *Journal of Energy Storage*, 9:25–39, 2017.
- [65] James Mason, Vasilis Fthenakis, Ken Zweibel, Tom Hansen, and Thomas Nikolakakis. Coupling PV and CAES power plants to transform intermittent PV electricity into a dispatchable electricity source. *Progress in Photovoltaics: Research and Applications*, 16(8):649–668, 2008.

- [66] Ben Mehta. CAES Geology. *EPRI Journal*, 17(7):38–41, 1992.
- [67] Nelson J. H. Johnston J. Mileva, A. and D. M. Kammen. SunShot solar power reduces costs and uncertainty in future low-carbon electricity systems. *Environmental science & technology*, 47:9063–9070, 2014.
- [68] Andrew Mills and Ryan Wiser. Changes in the Economic Value of Variable Generation at High Penetration Levels: A Pilot Case Study of California. (Jun):1–111, 2012.
- [69] Joshua M. Mueller, Gonçalo D. Pereira, Marco Ferrara, Yet-Ming Chiang, and Jessika E. Trancik. Energy storage requirements for shaping renewable energy toward grid decarbonization. *In preparation*, 2018.
- [70] Joshua M. Mueller and Jessika E. Trancik. Determinants of the value of storage for wind and solar energy. *In preparation*.
- [71] Joshua M. Mueller and Jessika E. Trancik. Impact of forecasting uncertainty on the value of storage for renewable energy arbitrage. *In preparation*.
- [72] National Solar Radiation Database. <http://rredc.nrel.gov/solar>, 2017.
- [73] GF Nemet. Beyond the learning curve: factors influencing cost reductions in photovoltaics. *Energy Policy*, 34:3218–3232, 2006.
- [74] NERC. North American Electric Reliability Corporation, Equivalent Availability Factor, 2017.
- [75] NREL. National Renewable Energy Laboratory, <http://www.nrel.gov/>, 2017.
- [76] Manasseh Obi, S. M. Jensen, Jennifer B. Ferris, and Robert B. Bass. Calculation of levelized costs of electricity for various electrical energy storage systems. *Renewable and Sustainable Energy Reviews*, 67:908–920, 2017.
- [77] Ryoichi Okuyama and Eiichi Nomura. Relationship between the total energy efficiency of a sodium-sulfur battery system and the heat dissipation of the battery case. *Journal of Power Sources*, 77(2):164–169, Feb 1999.
- [78] Curtis M. Oldenburg and Lehua Pan. Porous Media Compressed-Air Energy Storage (PM-CAES): Theory and Simulation of the Coupled Wellbore-Reservoir System. *Transport in Porous Media*, 97:201–221, Jan 2013.

- [79] Task Committee on Pumped Storage of the Hydropower Committee of the Energy Division of ASCE. Compendium of Pumped Storage Plants in the United States. *American Society of Civil Engineers, New York, NY*, 1993.
- [80] Alexandre Oudalov, Daniel Chartouni, and Christian Ohler. Optimizing a battery energy storage system for primary frequency control. *IEEE Transactions on Power Systems*, 22(3):1259–1266, 2007.
- [81] M. Parvizimosaed, F. Farmani, and A. Anvari-Moghaddam. Optimal energy management of a micro-grid with renewable energy resources and demand response. *Journal of Renewable and Sustainable Energy*, 5(5), 2013.
- [82] Stephan Pfister, Dominik Saner, and Annette Koehler. The environmental relevance of freshwater consumption in global power production. *The International Journal of Life Cycle Assessment*, 16(6):580–591, 2011.
- [83] William F. Pickard, Amy Q. Shen, and Nicholas J. Hansing. Parking the power: Strategies and physical limitations for bulk energy storage in supply-demand matching on a grid whose input power is provided by intermittent sources. *Renewable and Sustainable Energy Reviews*, 13(8):1934–1945, 2009.
- [84] PJM Regional Transmission Operator Website. <http://www.pjm.com>, 2017.
- [85] AWS True Power. AWS True Power Renewable Resource Data, [www.awstruepower.com](http://www.awstruepower.com), 2017.
- [86] D Rastler. Electricity Energy Storage Technology Options: A White Paper Primer on Applications, Costs, and Benefits. Technical report, 2010.
- [87] S. Ould Amrouche, D. Rekioua B, T. Rekioua B, and S. Bacha. Overview of energy storage in renewable energy systems. *Hydrogen Energy Publications LLC.*, 41:20914 –20927, 2016.
- [88] Hossein Safaei, David W. Keith, and Ronald J. Hugo. Compressed air energy storage (CAES) with compressors distributed at heat loads to enable waste heat utilization. *Applied Energy*, 103:165–179, Mar 2013.
- [89] Bikash Kumar Sahu, Moonmoon Hiloidhari, and D C Baruah. Global trend in wind power with special focus on the top five wind power producing countries Global trend in wind power with special focus on the top five wind power producing countries. 19:348–359, Mar 2013.

- [90] R Schmalensee, V Bulovic, R Armstrong, C Batlle, P Brown, and J Deutch. The Future of Solar Energy; An Interdisciplinary MIT Study. Technical report, 2015.
- [91] O. Schmidt, A. Hawkes, A. Gambhir, and I. Staffell. The future cost of electrical energy storage based on experience rates. *Nature Energy*, 2:17110, 2017.
- [92] Susan M Schoenung and William V Hassenzahl. Long- vs . Short-Term Energy Storage Technologies Analysis A Life-Cycle Cost Study A Study for the DOE Energy Storage Systems Program. *Power Quality*, SAND2011-2(April), 2003.
- [93] Bruno Scrosati, Jusef Hassoun, and Yang-Kook Sun. Lithium-ion batteries. A look into the future. *Energy & Environmental Science*, 4(9):3287–3295, 2011.
- [94] Nicola Secomandi. Optimal Commodity Trading with a Capacitated Storage Asset. *Management Science*, 56(3):449–467, 2010.
- [95] Matthew. R. Shaner, Steven. J. Davis, Nathan. S. Lewis, and Ken Caldeira. Geophysical constraints on the reliability of solar and wind power in the United States. *Energy & Environmental Science*, Advance Article 2018.
- [96] Ramteen Sioshansi. Increasing the value of wind with energy storage. *Energy Journal*, 32(2):1–29, 2011.
- [97] Ramteen Sioshansi, Paul Denholm, and Thomas Jenkin. A comparative analysis of the value of pure and hybrid electricity storage. *Energy Economics*, 33(1):56–66, Jan 2011.
- [98] Ramteen Sioshansi, Paul Denholm, and Thomas Jenkin. Market and Policy Barriers to Deployment of Energy Storage. *Economics of Energy & Environmental Policy*, 1(2):1–14, Apr 2012.
- [99] Ramteen Sioshansi, Paul Denholm, Thomas Jenkin, and Jurgen Weiss. Estimating the value of electricity storage in PJM: Arbitrage and some welfare effects. *Energy Economics*, 31(2):269–277, 2009.
- [100] A A Solomon, Daniel M Kammen, and D Callaway. Investigating the impact of wind – solar complementarities on energy storage requirement and the corresponding supply reliability criteria. *Applied Energy*, 168:130–145, 2016.

- [101] A.A. Solomon, Daniel M. Kammen, and D. Callaway. The role of large-scale energy storage design and dispatch in the power grid: A study of very high grid penetration of variable renewable resources. *Applied Energy*, 134:75–89, Dec 2014.
- [102] Iain Staffell. Wind Turbine Power Curves, [www.academia.edu](http://www.academia.edu), 2017.
- [103] B. L. Stoll, T. A. Smith, and M. R. Deinert. Potential for rooftop photovoltaics in tokyo to replace nuclear capacity. *Environ. Res. Lett.*, 8:014042(9pp), 2013.
- [104] Sandhya Sundararagavan and Erin Baker. Evaluating energy storage technologies for wind power integration. *Solar Energy*, 86(9):2707–2717, 2012.
- [105] Jessika E. Trancik. Scale and innovation in the energy sector: a focus on photovoltaics and nuclear fission. *Environmental Research Letters*, 1(1):014009, 2006.
- [106] Jessika E. Trancik. Renewable energy: Back the renewables boom. *Nature*, 507:300–302, 2014.
- [107] Jessika E. Trancik, Patrick R. Brown, Joel Jean, Goksin Kavlak, Magdalena M. Klemun, Morgan R. Edwards, James McNerney, Marco Miotti, Joshua M. Mueller, and Zachary A. Needell. Technology improvement and emissions reductions as mutually reinforcing efforts. Technical report, Massachusetts Institute of Technology, 2015.
- [108] Jessika E. Trancik, Michael T. Chang, Christina Karapataki, and Leah C. Stokes. Effectiveness of a segmental approach to climate policy. *Environmental Science & Technology*, 48(1):27–35, 2014.
- [109] Jessika E. Trancik and D. Cross-Call. Energy technologies evaluated against climate targets using a cost and carbon trade-off curve. *Environmental Science & Technology*, 47:6673–6680, 2013.
- [110] U.S. Energy Information Administration. Levelized Cost and Levelized Avoided Cost of New Generation Resources in the Annual Energy Outlook 2017. Technical report, U.S. Energy Information Administration, 2017.
- [111] Vestas. Vestas Turbine Power Curves, [www.vestas.com/V112](http://www.vestas.com/V112), 2017.
- [112] Vestas Website. <http://www.vestas.com>, 2017.

- [113] Rahul Walawalkar, Jay Apt, and Rick Mancini. Economics of electric energy storage for energy arbitrage and regulation in New York. *Energy Policy*, 35(4):2558–2568, 2007.
- [114] D. Weißbach, G. Ruprecht, A. Huke, K. Czerski, S. Gottlieb, and A. Hussein. Energy intensities, EROIs (energy returned on invested), and energy payback times of electricity generating power plants. *Energy*, 52:210–221, 2013.
- [115] Daniel Weisser. A guide to life-cycle greenhouse gas (GHG) emissions from electric supply technologies. *Energy*, 32(9):1543–1559, September 2007.
- [116] Charlie Wilson, Arnulf Grubler, Kelly S. Gallagher, and Gregory F. Nemet. Marginalization of end-use technologies in energy innovation for climate protection. *Nature Clim. Change*, 2(11):780–788, 11 2012.
- [117] R Wiser and M Bolinger. 2014 Wind Technologies Market Report. Technical report, U.S. DOE Energy Efficiency & Renewable Energy, 2015.
- [118] Ryan Wiser and Mark Bolinger. 2015 Wind technologies market report. Technical report, U.S. DOE Energy Efficiency & Renewable Energy, 2016.
- [119] World Bank GDP Deflator Website. <http://www.worldbank.org>, 2017.
- [120] XE Currency conversion. <http://www.xe.com>, 2017.
- [121] Shiwei Xia, K.W. Chan, Xiao Luo, Siqu Bu, Zhaohao Ding, and Bin Zhou. Optimal sizing of energy storage system and its cost-benefit analysis for power grid planning with intermittent wind generation. *Renewable Energy*, 2018.